A Biomechanical Analysis of

Growing Rods used in the Management of

Early Onset Scoliosis (EOS)

Masters of Engineering Thesis

Faculty of Built Environment & Engineering

Queensland University of Technology

Submitted by

Dr Mark Eric Quick (MBBS, BSc)

January 2014

Principal Supervisor: Professor Mark Pearcy

Associate Supervisor: A/Prof Clayton Adam

Abstract

Managing spinal deformities in young children is challenging, particularly early onset scoliosis (EOS). Current options include observation, bracing and surgery. Some children present with small non-progressive curves, which respond to non-operative treatment, such as bracing or casting whilst others in spite of non-operative intervention progress rapidly, and require early surgical intervention.

If left untreated, rapid scoliotic deformity in the skeletally immature may be associated with significant health risks including: pulmonary insufficiency from thoracic shortening which in turn inhibits both the growth of lung alveoli and pulmonary arterioles; altered abdominal organ development and possible cardiopulmonary failure. Any progressive spinal deformity whether it be congenital or idiopathic in origin particularly in early life presents significant health risks for the child and a challenge for the treating surgeon.

Surgical intervention is often required if EOS has been unresponsive to conservative treatment and curves may have rapidly progressed. Numerous surgical interventions exist including fusion and fusionless techniques. An emerging treatment option particularly for EOS is fusionless scoliosis surgery. Similar to bracing this surgical option potentially harnesses growth, motion and function of the spine along with correcting spinal deformity. Dual growing rods is one such fusionless treatment, which aims to modulate growth of the vertebrae. Acting like an internal brace they can correct

scoliotic curves, prevent lateral bending, potentially protect adjacent vertebrae from early degenerative changes and depending on construct type may also allow continued axial growth.

A recent new design of the growing rod, semi-constrained, designed by surgeons from the Paediatric Spine Research Group (Mater Hospital, Brisbane, QLD, Australia) and manufactured by Medtronic (Medtronic, Sofamor Danek, Memphis, TN) with Therapeutic Goods Administration (TGA) and Food and Drug Administration (FDA) approval has been used to manage patients with EOS with good spinal correction at post-operative follow up. Having first been described by Harrington in the 1960's, growing rods have been modified extensively. However the principle of distraction and maintenance of spinal motion and function still remain key to the efficacy of spinal growing rods.

The aim of this study was to ascertain if 'semi-constrained' growing rods would result in a more compliant construct than standard 'rigid' rods in axial rotation testing and hence provide a more physiological mechanical environment for the growing spine. Using in-vitro experiments, performed on immature multi-segment unit (MSU) porcine spines, the initial phase of this study was to develop a testing apparatus to enable MSU spine testing in axial rotation at a constant rate of rotation. Prior to directly comparing two different types of rods, two preliminary studies were performed. The first, investigated the test-retest repeatability of the of MSU spines through stiffness analysis during axial rotation, whilst the second assessed the

consistency of results with instrumented dual rigid rods. The main study directly compared two different types of rods: dual semi-constrained growing rods and dual rigid rods.

Testing was carried out using, a displacement (axial rotation) controlled test at a constant speed, to a set maximum moment of ±4Nm. During testing a three dimensional camera system was used to track motion at each vertebral level and the rod components. This enabled individual motion during axial rotation to be recorded for each vertebrae and included intervertebral rotations.

The results of this low-cycle in vitro biomechanical study provide a strong justification for further evaluation of semi-constrained growing rods. The semi-constrained growing rod maintained rotation similar to the un-instrumented spines, while the rigid rods showed significant reduction in axial rotation across all instrumented levels. Clinically the implications of this study are significant. The likely clinical effect of semi-constrained growing rods evaluated in this study is that they will allow growth via the telescopic rod components, while maintaining the axial rotation ability of the spine, which is more physiological.

Keywords

Fusionless scoliosis surgery

Early onset scoliosis

Spine biomechanics

Growth modulation

Growing rods

Porcine vertebrae

Moment controlled testing

Axial rotation

Contents

Terminology

MSU	Multi-segment Unit
EOS	Early onset scoliosis
AIS	Adolescent idiopathic scoliosis
PMMA	Polymethylmethacrylate
ROM	Range of movement
NZ	Neutral zone
UN-IN	Un-instrumented
GR	Growing rods

Statement of original Authorship

"The work contained in this thesis has not previously been submitted at this or any other higher education institution to meet the requirements for a higher qualification. To the best of my knowledge and belief this thesis contains no material previously published by anyone else except where reference to prior research is made."

Mark Eric Quick, January 2014.

Acknowledgments

To Professor Mark Pearcy I'm grateful for your support and guidance throughout my thesis. Despite your busy schedule and multiple academic roles both at QUT and as head research co-ordinator of the Paediatric Spine Research Group (PSRG) you were always approachable and interested in assisting with the progress of my research. Thank you for teaching me about the tribulations of university research.

Although not physically present in Australia during the testing phase of my study I'm immensely grateful to A/Prof Clayton Adam. You assisted in the initial formulation of my research topic and at regular Skype interactions were interested in hearing about the studies progress. Thank you for your ideas and answers to the multitude of questions I asked regarding biomechanical spine testing.

To Caroline Grant I owe a huge thank you, not only for your patience with my constant barrage of questions but also your guidance in navigating the academic world of research. Your enthusiasm and willingness to teach has enabled me to achieve new goals and an appreciation to academic research.

Thank you to Dr Geoffrey Askin and Dr Robert Labrom, for the opportunity to be apart of an amazing and dynamic group. Your clinical expertise and encouragement as mentors has been invaluable during my development as a doctor.

Maree Izatt who is always available and willing to assist wherever possible. Thank you for providing information, pictures and advice I appreciated everything you did with a smile.

Lance Wilson, thank you for spending the time and ensuring I was safe and confident in using the biomechanical testing apparatus. I really appreciate the ideas you had at the initial design phase of my study ensuring a rigorous study was constructed.

A huge thank you goes to my fiancé Sophia, your love and support allows me to be the best person possible. Despite the rigors of juggling both clinical and academic workloads you always make me smile ☺

1 Clinical problem & hypotheses

Scoliosis is often described simply as a lateral curvature of the spine and for practical purposes curve progression is calculated using planar standing coronal radiographs (Figure 1.1) to calculate deformity parameters such as the Cobb angle and the rib vertebral angle difference (RVAD) [1, 2]. With the advancement of imaging techniques it is now understood that scoliosis is in fact a complex three-dimensional spinal deformity characterised by a deformation in the coronal, sagittal and transverse planes [3-5].

Figure 1.1. Posterior-anterior X-Ray of a scoliotic spine

Paediatric spinal deformities encompass a wide range of aetiologies including; congenital vertebral anomalies, neuromuscular conditions, connective tissue disorders, other syndromic presentations and unknown (idiopathic) causes. Idiopathic scoliosis is the most common paediatric spinal deformity with a higher predominance of female patients and of right sided

main thoracic curves [6]. Idiopathic scoliosis has been subdivided by the Scoliosis Research Society into three main groups; infantile (birth-3yo), juvenile (3-10yo) and adolescent (10yo to maturity) [7]. However the first five years of growth are peak years for spinal development with two thirds of a single adult vertebral height in the thoracic and lumbar vertebrae being achieved by the age of five, with further growth occurring during the adolescent growth spurt [8]. Steady vertebral growth has been demonstrated during the juvenile period and with this, a two subgroup division of scoliosis, early onset (0-5yo) and late onset (greater than 5yo) has also been described in the literature[9]. Children with early onset scoliosis (EOS), which encompasses infantile and juvenile categories account for on average 21% of all idiopathic scoliosis cases and the difference in prognosis and outcome with this patient cohort warrant consideration of EOS as a separate distinct subgroup to adolescent idiopathic scoliosis (AIS) [10,11].

The likelihood of curve progression is dependent on numerous factors including the patient's skeletal maturity, curve orientation and curve severity [12,13,14,15], such that curve progression is more likely in EOS patients with their significant growth potential [2]. Disruption in spinal growth can affect the thorax, abdomen and pelvis, but it is the close relationship between the thorax and spine that is of most importance in lung development. Progressive spinal deformity in EOS can result in, reduced lung growth and a condition known as thoracic insufficiency syndrome, whereby the thorax can not support lung growth and function [16]. Karol et al. [17] found that pulmonary function was significantly decreased in patients who underwent thoracic

spinal fusion before the age of nine and who required fusion of more than four segments of the thoracic spine. Traditionally, non-operative management for EOS with lateral spinal curves over 35 degrees has included casting, different types of orthoses (Figure 1.2) or a combination of the two [18].

Figure 1.2. Thoraco-lumbar orthosis (TLO)

However since the immature rib cage often deforms before any significant correction can be directed to the spine with the use of bracing or casting, poor results may be expected with their long-term use [18-20]. This is supported in several studies, which have shown curve progression despite non-operative treatment with different types of braces [21-25]. While bracing treatment will allow for thoracic growth, patient compliance is frequently poor particularly in warmer climates and there has been extensive literature on the adverse effects on personality development and self-esteem [26-28].

The best control of deformity in patients with EOS is provided by surgery and this is usually performed with spinal curves of a Cobb angle greater than 50 degrees [19]. Two classes of surgical procedure for EOS exist; those involving fusion, and fusionless techniques. Whilst spinal fusion achieves strong correction of the deformity, resulting in near normal physiological curves of the spine, it causes all potential growth to cease, leading to reduced vital lung capacity and altered organ development. It can also affect adjacent vertebrae, leading to future degenerative problems [17, 29, 30]. Rather than inhibiting spinal and chest growth by early arthrodesis, this clinical problem has been addressed with the use of fusionless or growth sparing procedures in EOS. Fusionless procedures have been divided by Skaggs [31] into distraction (tension based) or growth guiding procedures, with each aiming to harness the inherent growth of the spine in EOS and redirect it, so as to achieve maximum spinal length, optimal pulmonary function and to maintain spine motion.

Distraction based techniques include growing rods and vertical expandable prosthetic titanium ribs (VEPTR), whereas growth guiding techniques comprise vertebral staples, tethers, hemiepiphysodesis or vertebral wedge osteotomy [32]. Fusionless procedures preserve motion and function of the spine, but may also protect adjacent vertebrae from degenerative changes and spinal imbalances. Unlike external bracing, fusionless treatments are applied directly to the spine, eliminating patient compliance issues, however they are invasive procedures and carry surgical risks including, infection, instrument failures and neurological injuries. Depending on the type of

fusionless surgery, further procedures may be required and can include repeated lengthening and often a final fusion and stabilisation once maximal growth has been reached. Having first been described by Harrington in the 1960's, growing rods have been modified extensively. However the principle of distraction and maintenance of spinal motion and function still remain key to the use of spinal growing rods.

Despite its effective use in managing EOS prior to final fusion, as noted in the documented data series of patients who have undergone surgical management at the Mater Hospital (Brisbane, QLD), little is known about the biomechanics of the semi-constrained growing rod. There have been no studies to date explaining the biomechanics of this newer type of growing rod. This thesis aims to investigate two types of rods used to manage EOS, including the newer semi-constrained growing rod, through axial rotation testing on an immature porcine spine model. The constraint of vertebral motion, due to rod instrumentation, will be explored by measuring the intervertebral rotations across all levels of the tested spine, using a motion tracking system. It is assumed that the semi-constrained growing rods, which enable growth guidance and rotation in its construct, are more physiological in function, during corrective management of patients with EOS than conventional rigid rods. Hence, the overall aim of this in-vitro study is to ascertain the extent to which semi-constrained growing rods reduce rotational constraint on the spine, compared with standard "constrained / rigid" rods and thus provide a more physiological environment for the growing spine.

The specific objectives of the thesis are to:

1. Develop an apparatus to enable in-vitro testing of multi-segment spine specimens, in a bi-axial testing machine (Instron), by applying an axial rotation displacement, to a set maximum moment, without constraining the axis of rotation.

2. Compare the stiffness, in axial rotation of an un-instrumented multi-segment spine with two different multi-segment unit (MSU) constructs, consisting of either dual semi-constrained growing rods or dual standard "constrained / rigid" rods.

3. Analyse and quantify the intervertebral rotations of each level in the instrumented constructs, compared with the un-instrumented spine, through the use of a 3D motion tracking system (Optotrak).

4. Assess relative rotations of the growing rod components.

The hypothesis for the thesis are:

1. Instrumentation with dual semi-constrained growing rods will allow an even distribution of axial rotation across the instrumented levels similar to an un-instrumented spine.

2. That semi-constrained growing rods will result in a more compliant construct than rigid rods in axial rotation.

3. That dual rigid rods will significantly reduce the axial rotation allowed within the instrumented levels and therefore the overall ROM compared to semi-constrained growing rods.

2 Background & literature review

This section sets outlines initially the etiology of scoliosis and broadly explores the fusionless growing rod options previously used and currently available to manage EOS. What is clear to see from the literature is that, limited information is available regarding the newer semi-constrained growing rod, in particular the biomechanics of this fusionless growing rod. The aspect of growth guidance and stimulation from fusionless growing rods is accounted for in the review below, as is the justification of specimen choice, fixation and test parameters.

2.1 Vertebral anomaly and etiology of scoliosis

Although the cause of idiopathic scoliosis remains unknown, several theories have been proposed and studied including genetic, hormonal, biomechanical, spinal growth as well as central nervous system theories. Previous research has demonstrated a genetic component in the development of scoliosis with increased incidence in families with monozygotic twins which have a documented 73% to 92% prevalence of scoliosis compared to families with dizygotic twins with a 36% to 63% prevalence rate [33, 34].

Endocrine factors have also been explored as a possible link to developing scoliosis. An observational study by Machida et al., [35] supported a theory that melatonin deficiency following pineal gland destruction in chickens

induced the formation of scoliosis whereas melatonin supplementation prevented the formation of scoliosis [35, 36]. This however has not been supported in more recent clinical trials investigating the serum and urinary melatonin levels in patients with AIS [37]. A resistance in melatonin receptor function has instead been proposed with some promising research findings into dysfunctional signalling however the exact mechanism by which melatonin is related to causing scoliosis is still unknown [37].

The likelihood of curve progression in scoliosis has also been attributed to rapid growth during development [38, 39]. Unlike infantile scoliosis where curves normally resolve spontaneously, juvenile idiopathic scoliosis (JIS) resembles more closely AIS with rapid curve progression and scoliosis deformity. This is thought to be due to a contribution of biomechanical factors and anatomical abnormalities, which include vertebral wedging and disproportionate spinal growth [40-44]. This abnormal growth and curve progression could be attributed to the Hueter-Volkman principle, which states that growth is retarded with compressive forces whilst accelerated with distractive forces. Once established as a 'vicious feedback cycle' of pathologic strong pressures applied to one side of the vertebral end plates, the result is asymmetrical growth. This principle formulated by Stokes et al. [41, 43, 45] would account for the progressive deformity observed in scoliosis and is further discussed below.

Both spinal cord and central nervous system processing abnormalities such as syringomyelia, Chiari or cervicothoracic syrinx malformation have also

been postulated as possible causes of scoliosis [46, 47]. The support for theories of a central nervous system abnormality is further substantiated with dysfunction in postural balance and proprioception being observed in patients with scoliosis [48-51].

There has been a significant amount of research into understanding the etiology of scoliosis. However it seems fair to say that the cause of scoliosis may not be explained by a single entity.

Management of scoliotic deformities in young children with skeletally immature spines is challenging particularly in EOS, which presents earlier, progresses more rapidly and can result in more serious organ complications. In-vitro spine research is important, particularly biomechanical spine analysis as it improves the understanding of intervertebral kinematics and enables preclinical evaluation of new spinal implants and the efficacy of surgical procedures.

2.2 Growing rod instrumentation for EOS

2.2.1 Harrington rods

Harrington described the first type of fusionless surgery for young children with scoliosis in 1962. He developed a system in which posterior correction with; either a distraction rod, compressive rod or both, could be applied to a scoliotic spine posteriorly to correct abnormal curvature [52]. A distraction rod was placed across the concavity of a curve and secured by transverse process hooks (Figure 2.1). The early paper by Marchetti and Faldini [53] reported good curve correction in a cohort of 14 patients with EOS using a Harrington distraction rod and principle. However the technique initially described failed because of several reasons including spontaneous partial fusion or soft tissue scarring from large surgical exposures at initial rod instrumentation, early rod design breakages and because of hook dislodgement.

The Harrington rod system was later modified by Moe et al. [10] who emphasised limited soft tissue, ligamentous and periosteal dissection and devised a method for inserting the rods subcutaneously rather than disrupting the submuscular/periosteal layers. The Moe modified Harrington rods were thicker, contained a smooth central region allow the rod to slide through subcutaneous tissue unlike the threaded or fluted original Harrington rods. Planned planned lengthenings of the construct at regular intervals were also required. A cohort of twenty patients presented by Moe et al. [54] treated at one scoliosis centre indication that curves greater than 60 degrees that did not respond to conservative bracing, responded well to single rod

instrumentation. Patients who had on average 6-7 months between lenegthenings showed also the best maintenance of curve correction. Although many patients required unplanned surgery due to implant complications, patients achieved 84% of expected growth within the instrumented spinal segment [54]. There are however, few long-term studies available to evaluate the outcome of using a single Moe modified Harrington rod.

A.   B.
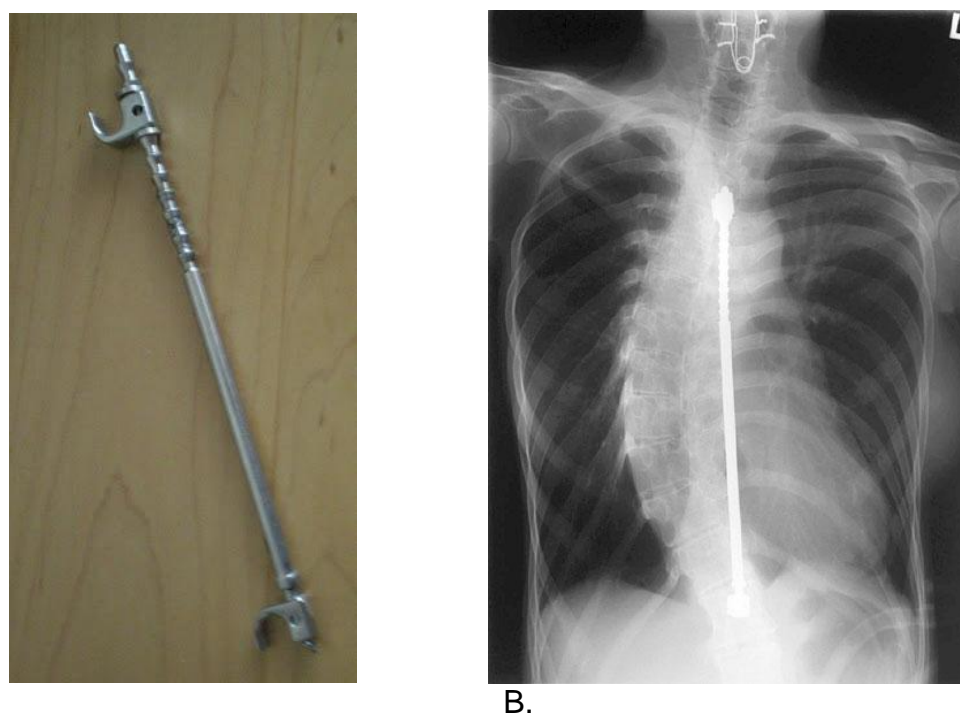
Figure 2.1. A) Harrington distraction rod with transverse process hooks on either end. B) Posterior-anterior radiograph showing instrumented Harrington rod on the concave side of a scoliotic curve.

A study by Klemme et al. [19] reported on a group of sixty-seven children, over a period of twenty-one years, who underwent single rod fusionless spinal surgery with incremental distraction prior to final fusion. The children in this study were also made to wear an external orthotic brace full-time prior to final fusion. Over a mean treatment period of 3.1yrs prior to final fusion, the instrumented but unfused spinal segments averaged 3.1cm of measured growth or 82% of predicted growth for age with a 47% improvement in

scoliotic curve correction from pre-operative values [19]. Despite these outcomes however, 33% of the study population in Klemme et al.'s [19] paper, showed progression instead of improvement in scoliotic curves. Other papers have also reflected mixed outcomes with the use of a single growing rod including significantly more unplanned surgeries, rod breakage and hook dislodgement [19, 54-56].

Using a single rod has also proved difficult at the time of initial surgery particularly in scoliotic spines, which have decreased flexibility. A study by Acaroglu et al. [29] of twelve patients, showed a significant increase in rotational abnormality in using a single growing rod despite controlling for curve deformity in the coronal plane. Questions have also been raised in several papers regarding rod placement in fusionless EOS surgery [29, 55, 56]. Subcutaneous rod instrumentation as described and used in previous scoliosis surgical procedures has been shown in the retrospective study by Bess et al., [56] to have increased wound complications and significantly more unplanned surgical procedures. More likely due to the prominence of the implant compared to submuscular rod placement which would be more protected [56]. Further refinement of the growing rod and improved surgical techniques has been made since first being devised by Harrington [56-58].

2.2.2 Constrained growing rods and tandem connectors

Further progress in rod design and instrumentation came with research by Akbarnia et al. [57] in which dual ISOLA (Depuy Spine, Raynham, MA, USA) growing rods with solid sub-periosteal proximal and distal foundations

spanning two to three levels and using either a combination of hooks or screws were used in managing EOS (Figure 2.2) [57]. However, the number and location of anchors were dependent on several factors including curve type, location and patient age. Two rods for each side were contoured for sagittal alignment, passed either submuscularly or subcutaneously and the expansion mechanism connecting the dual-rod construct was moved from the end of the rod, as in previous surgical techniques and rod designs by Harrington [52], to a more central position with tandem connectors for added stability (Figure 2.2).

A.   B.   C.   D.
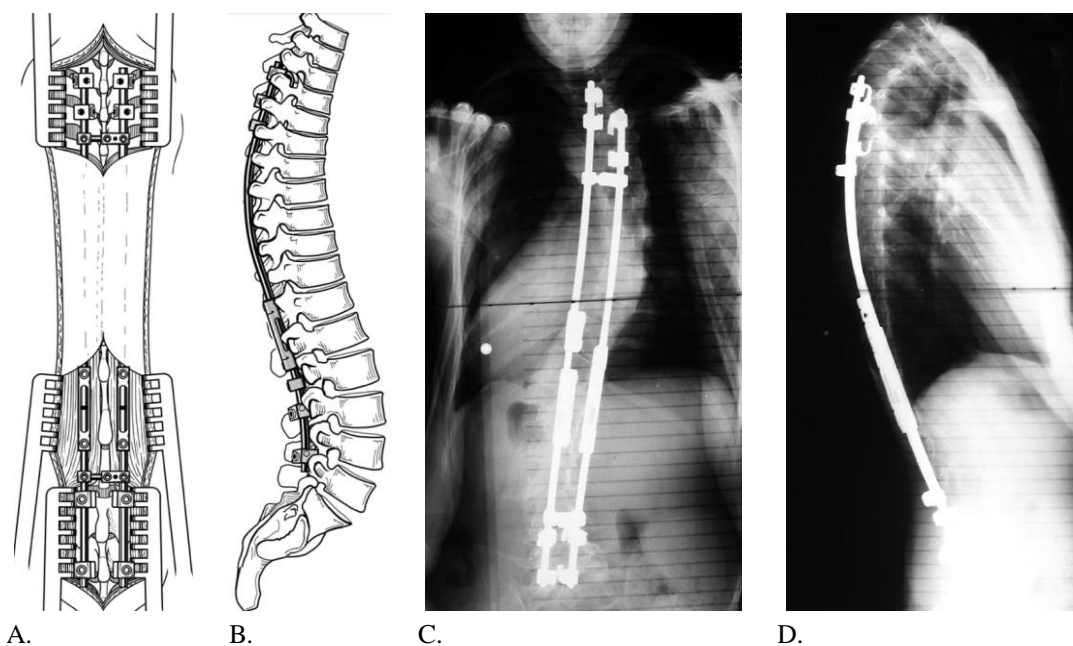
Figure 2.2. A and B) Dual rod instrumentation with ISOLA growing rods shown in schematic orientation. C and D) Posterior-anterior and lateral radiographs [57]. From Ovid, DOI: 10.1097/01.brs.0000175190.08134.73.

An external orthosis (TLSO brace) was used for patients in Akbarnia et al.'s [57] study, for four to six months following initial rod insertion and then discontinued. The study series consisted of twenty-three patients divided into three groups based on age (Group 1 from 0-5yrs N=10, Group 2 from 5-

10yrs N=12 and Group 3 one 12yrs N=1) who were followed up for a minimum of two years (average 4.75yrs, range 2.0-9.3yrs). All participants underwent planned six month lengthening procedures, with a total of seven patients being followed until final fusion. All patients significantly improved their preoperative deformity, with a mean scoliosis improvement from 82 degrees to 38 degrees (53% improvement) in Cobb angle after initial surgery and measured a mean Cobb angle of 36 degrees at either last follow up or post final fusion (54% improvement). The group of participants also averaged 1.21cm.year^{-1} growth in the T1-S1 segment [57]. This study and along with several others have supported the use of dual growing rods rather than single rods for managing EOS prior to final fusion, both at initial corrective surgery and in maintaining correction at follow up examinations [57, 59, 60].

2.2.3 Shilla growth guidance system

Another type of fuisonless growing rod for managing EOS is the Shilla (Medtronic, Memphis, TN, USA) growth guidance system. Like all fusionless surgical options in managing EOS it allows for continued spinal growth. It has been tested in several in-vitro studies including an unpublished internal test report by Medtronic (Memphis, TN, USA) demonstrating the high tolerance of the Shilla implant withstanding one million cycles without failure and only reporting metallic wear debris as the only consequence of multiple repeated cycles (Medtronic, internal test report, TR04-331, 2006). However the number of cycles before wear debris is noted is not revealed. The Shilla growing rod is a growth guidance system with the apex of scoliotic curves

being corrected, fused and fixed to dual growing rods. At the ends of the construct polyaxial Shilla screws, which capture the rod but don't constrain it are secured in the pedicles and allow the growing rod to slide along its length with increased rod length below and above the fixation point (Figure 2.3).

Although previously described and compared in the literature, the only published study to date utilising the Shilla system is a recent caprine animal study by McCarthy et al. [61] which showed that the construct does allow vertebral column growth. Moderate to high wear debris was noted on subjective analysis at the unconstrained instrumentation levels (Shilla screws Figure 2.3 A) but this did not cause any structural failures [61]. As an alternative fusionless system for managing EOS which does not require the usual scheduled lengthenings as in previous described growing rods, the Shilla system still requires further research to test its efficacy.
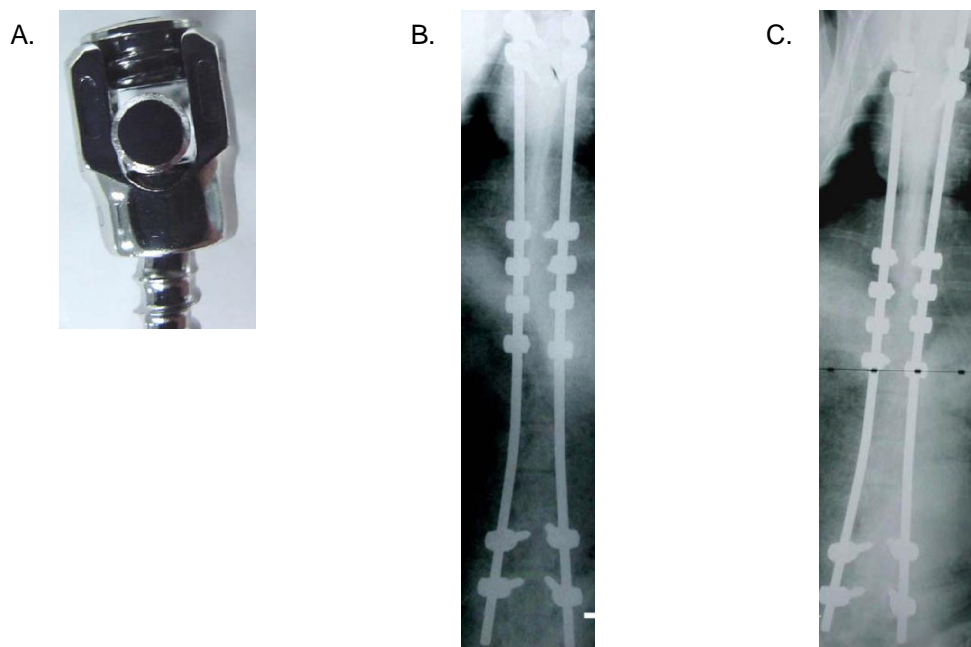
Figure 2.3. A) Shilla polyaxial screws which capture the rod but do not constrain it during growth at the cephalad. Posterior-anterior radiographs from the study by McCarthy et al. [61] showing the Shilla growing rods immediately after insertion (B) and at 6 months (C) with growth guidance having occurred as shown by a shortened distal distance between the non constraining polyaxial screws and the caudal rod ends [61]. ProQuest: http://dx.doi.org.ezp01.library.qut.edu.au/10.1007/s11999-009-1028-y

2.2.4 Luque trolley

Similar to the Shilla guidance system the Luque trolley is another self-guiding growing rod technique. Described first by Luque and Cardoso in 1977 [62] it was later modified by them to include two L or U shaped rods fixed to the spine using sublaminar wires. Because the rods were able to slide through the sublaminar wires, lengthening procedures were thought to be unnecessary, as was the use of any external support such as a brace post operatively [62]. The Luque trolley offers a more rigid fixation particular with dual rod construct than traditional Harrington rods. However, because of high failure rates including, rod breakages, numerous difficult revision surgeries due to fibrosis around the wires, spontaneous fusion rates at instrumentation levels (ranging from 4-100% in documented cases) and poor spinal growth, the use of the Luque trolley, as initially described by Luque and Cardoso [62] was abandoned [63, 64].

Recent research by Ouellet [65] reviewed five patients, who underwent EOS surgery with a modified (modern) Luque trolley and followed them up for a minimum of 2years. The construct consisted of inserting apical gliding sublaminar wires, using a muscle sparing technique, in combination with proximal and distal fixed anchors (Figure 2.4). This construct achieved 60% of Cobb angle correction (with initial 60 degree cobb angles being reduced and maintained at around 21 degrees), with four of the five patients obtaining 0.75cm.year^{-1} of spinal growth and achieving 90% of their expected growth across the instrumented levels of vertebrae. As a novel approach to managing EOS the modernised Luque trolley described by Ouellet does

show potential as a fusionless surgical option in managing EOS, particularly in terms of removing the need for repetitive lengthening procedures [61]. Further research into the use of self-lengthening techniques such as the Luque trolley is required in order to evaluate the effectiveness and efficacy of this procedure.
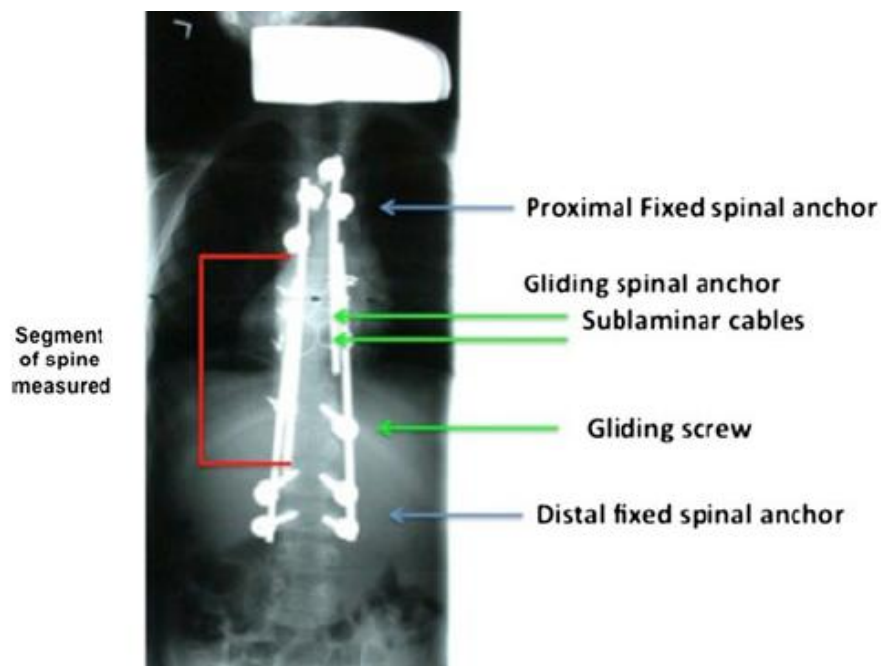
Figure 2.4. Posterior-anterior radiograph showing a modern Luque trolley construct consisting of four proximal and distal fixation screws with sublaminar cables across the thoracic spine and a guiding screw [65]**. ProQuest:http://dx.doi.org.ezp01.library.qut.edu.au/10.1007/s11999-011-1783-4**

2.2.5 Semi constrained growing rods

A recent new design of growing rod, devised by surgeons from the Paediatric Research Group (Mater Hospital, Brisbane, QLD, Australia) and manufactured by Medtronic (Medtronic, Sofamor Danek, Memphis, TN, USA) with Thearapeutic Goods Administration (TGA) and Food and Drug Administration (FDA) approval has been used to manage patients with EOS with good post operative results through to final fusion at patient maturity.

Known as a semi-constrained growing rod this system utilises a similar submuscular placement, fixation method and distraction technique to hold the rods in place, as with standard "constrained / rigid" rods. It differs in design however, with interconnecting male and female components, which rotate on each other and with the sleeve acting as a guide during growth. A locking washer/hinge prevents loss of growth at the top of the sleeve component and is locked off at the new gained height during lengthening procedures. The semi-constrained growing rod however, does not prevent the need for regular lengthenings, unlike the Shilla or modern Luque trolley designs.

Similar in telescopic design to the rod described and biomechanically tested by Wilke et al. [66], this semi-constrained growing rod does not require extensive stripping of tissue or inter-spinous drilling for fixation during instrumentation nor does it utilise sliding polyethylene coils for guidance as in other growth sparing constructs. It instead relies on adequate overlap of the telescoping portions (male and female components) of the rod and adequate fixation at the ends of the construct. This construct also aims to prevent spontaneous vertebral fusion by inserting the rods using a subcutaneous technique and thus preserving soft tissues and bony periosteum.
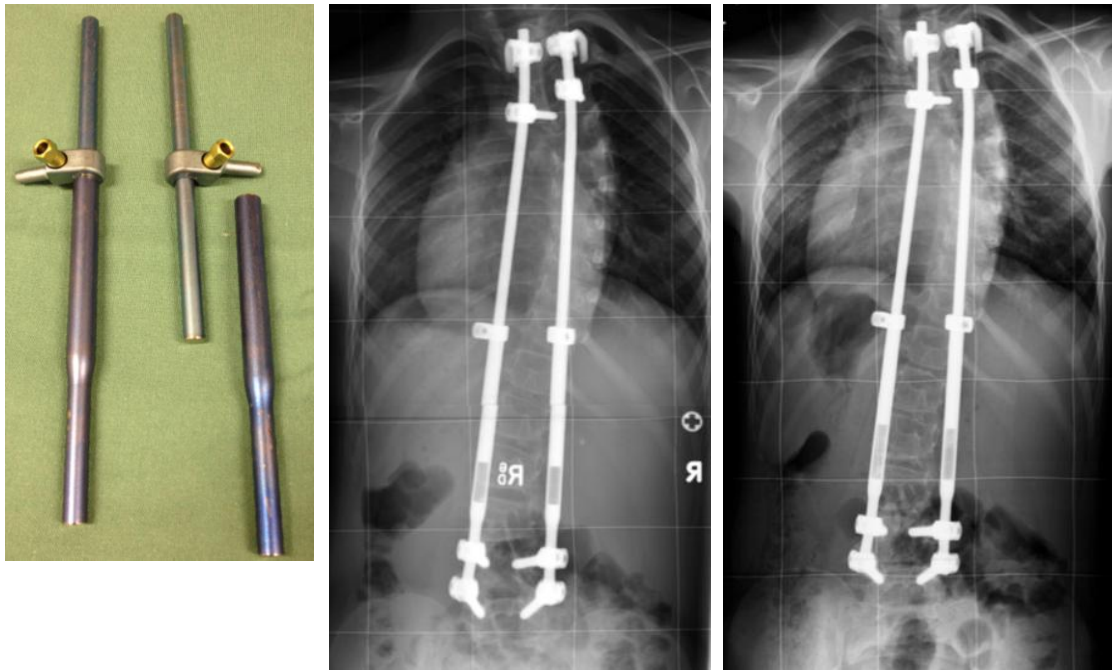
A.   B.   C.

Figure 2.5. A) Semi-constrained growing rods with restriction clamp. B and C) Two Posterior-anterior radiographs from the same patient taken 1yr apart showing a combination of pedicle screws and hook configurations with the length gained post a lengthening procedure at the telescopic sleeve.

It is believed that the telescopic sleeve of semi-constrained growing rods aid in guiding growth, whilst also allowing some rotation, which is more physiological in function than rigid rods. This is thought to be of particular importance during the corrective growth management of patients with EOS. Having first been described by Harrington in the 1960s, growing rods have been modified extensively. However, the principle of distraction and maintenance of spinal motion and function still remains key to the concept of growing rods and fusionless techniques in managing EOS.

Figure 2.6. Schematic diagram showing the different types of growing rods including several fusionless (self lengthening) constructs.
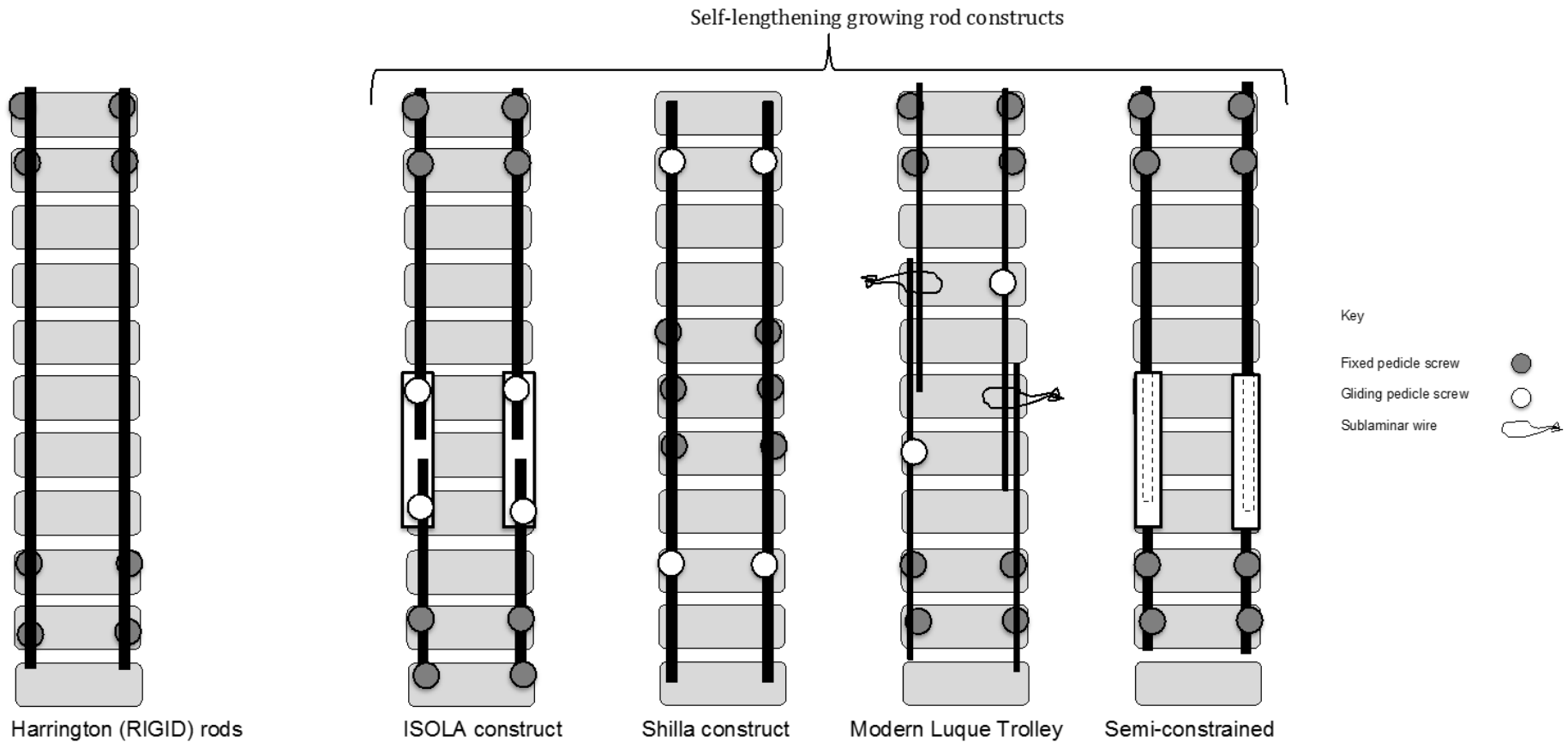
2.3 Distraction and lengthening procedures

As mentioned previously, the use of dual distraction based growing rods requires periodic lengthenings. This is in order to maintain correction of scoliotic curves and to keep up with spinal growth in the developing child. Normal growth patterns can't be expected in EOS. This is because unlike normal straight spinal segments, scoliotic segments can differ in flexibility and orientation, due to varying etiologies and growth potentials.

At birth the T1-S1 interval measures 19cm and by maturity, it measures 45cm in an average male and 42cm in an average female [8]. Normal growth rate slows significantly between the ages of 5 to 10 years to a rate of 1.2cm.year^{-1} after the initial growth spurt. It is during this time period that most patients undergo initial instrumentation for managing EOS [57, 58, 67]. In several dual growing rod studies treating EOS, the measured growth rate between T1-S1 has been similar to that of normal spinal growth, with documented values ranging from 1.01 to 1.84cm.year^{-1}. The factors attributing to this, equal or in some studies, surpassed growth potential include; more frequent lengthenings, the large correction achieved during initial instrumentation, length achieved at the time of distraction, the force applied to distract the rods during lengthening procedures and the effect of distraction on the immature spine which are all discussed further below.

More frequent lengthening procedures of ≤ 6-month intervals between lengthenings in a study by Akbarina et al. [58], revealed a statistically larger growth rate. A rate of 1.84cm.year^{-1} in the T1-S1 segment was recorded, compared to 1.02cm.year^{-1} in patients who were lengthened less frequently at >6 month intervals. The influence that spinal distraction can have on overall spinal height and rate of increased height will be explored further below. There was also a statistically significant correction in Cobb angle from pre-initial to post final fusion, in the group lengthened more frequently compared to patients lengthened less regularly [58]. The potential for increased risk of complications with more frequent surgeries was not evident in the study by Akbarina et al. however, only a small series of 13 patients was analysed [58].

Despite increased growth being achieved with more frequent lengthenings a study by Sankar et al. [67] showed the effect of diminishing returns with repeated growing rod lengthenings in a study of 38 patients which were followed up for a minimum of 2 years. The mean T1-S1 gain, at initial instrumentation and lengthening was 1.04cm, which decreasing significantly at each preceding distraction/lengthening procedure, with a mean gain of only 0.41cm by the seventh lengthening procedure. The decrease in T1-S1 gain was also noted over time, if the interval period between lengthenings was controlled for. These results may guide a surgeon in not expecting large distractions at repeated lengthenings and may also influence when lengthenings should stop. Regardless of a diminishing gain at each lengthening procedure, there was still a positive increase in length being

noted, which supports the growth guidance effect of this fusionless technique for managing EOS.

The gradual stiffening of the instrumented spines noted in the study by Sankar et al. [67] can also be inferred from research by Noordeen et al. [68], which showed that distraction forces significantly increased after repeated lengthenings of a single submuscular growing rod construct, with a side to side connector, used to manage a broad spectrum of scoliotic etiologies. By the 5th lengthening procedure, the distraction force had almost doubled to a force of a 368N, which was also significantly higher when compared to the distraction force recorded at the previous lengthening. Measured forces were also significantly higher in patients who had undergone apical fusion at the initial instrumentation compared to those who had no apical fusion. With this increase in force required to distract the growing rod, the mean length acquired halved in value by the 5th lengthening procedure to an average gained length of 8mm or less. In this study the main increase in length achieved through serial distraction and lengthening procedures was shown to occur during the first three to four distractions after initial fusionless surgery [68]. Several studies have shown that the majority of scoliotic correction in the coronal plane deformity known as the Cobb angle is predominately achieved during the first instrumentation of growing rods [58, 59, 67]. Maintaining curve correction with growing rods following the initial instrumentation encourages spinal growth, with small additional improvements in alignment after each subsequent lengthening procedure, prior to final fusion.

The reporting of spinal growth in the literature is not standardised, making it difficult to compare the achieved growth between differing constructs. However the documented marked growth inhibition in the conventional Luque and Shilla constructs is more likely associated with the hemi-epiphysiodesis (loss of growth on one half of the vertebral end plate) or spinal fusion across the fixation points of the spine (Figure 2.6) [61, 64]. As such the studies by Pratt et al. [64] and McCarthy et al. [61] with epiphysodesis achieved only 32% of expected growth and an additional growth of 12% respectively.   The complication rate of the newer Luque trolley is similar to other fusionless technqiues although compared to the conventional Luque trolley it has fewer documented implant failures requiring fewer revision surgeries. However concerns with design still exist with the modern construct.

2.4 Growth stimulation or preservation

Several research papers have supported the preservation of spinal growth, during EOS instrumentation after regular routine lengthenings prior to final fusion. What is interesting is that distraction of physes has been shown to also stimulate faster growth. This effect has been known for numerous years as a result of prior appendicular skeletal studies of patients with angular deformities and limb length differences [69-72]. Based on the findings of Stokes et al. [45] mentioned below it is likely that a similar effect is achieved within the axial skeleton. Known as the Hueter-Volkmann principle, can this relationship between distractive forces exerted on growing vertebral physes and increased growth vertically, not only preserve growth but stimulate it as well?

A study by Stokes et al. [45] instrumented the tails of rats with external fixation apparatuses and applied either a distractive or compressive force. When loaded with distraction the tails of rats grew faster compared to un-instrumented vertebrae, whilst a compressive force cause growth to cease [45]. The principal of growth modulation through the Hueter-Volkmann law has also been explored in a goat model by Braun et al. [73], where scoliosis was experimentally introduced through concave rib tethering. This resulted in cessation of growth on the tethered side. Growth rate in an immature pig study by Yilmaz et al. [69] using spinal growing rods under distraction was shown to continue at a higher rate within distracted instrumented levels, than compared to superior vertebral levels under no distraction. Although this difference was not significant different when comparing the two groups, this

experimental model concluded that growth can be stimulated by elongating the vertebral column under distraction.

Growth stimulation within instrumented vertebral levels under distraction, has also been shown in a retrospective paediatric case series by Olgun et al. [74]. Where by growth was greater in the instrumented levels, than compared to lower un-instrumented lumbar levels following regular 6 month lengthenings with follow up over an average of 49 months. The instrumented levels included thoracic and lumbar vertebrae with at least one lumbar vertebra outside the construct to compare growth with. A significantly different height was achieved in the instrumented levels undergoing distraction, when compared to the lumbar vertebrae directly outside this. An even more striking difference would have been shown, if the growth rates for thoracic and lumbar vertebrae were accounted for separately [74]. Further research assessing the height achieved across all vertebrae within an instrumented spine, whether under distraction or tensile force, needs to be performed and not just with the vertebrae adjacent to fixation points.

2.5 Biomechanical testing of growing rods

The concept of surgically instrumenting progressive scoliotic curves in patients with EOS is not new having outlined several early surgical constructs which have been modified and re-developed as with the new semi-constrained growing rods. Despite dual rods showing superior curve control and maintenance in curve correction in retrospective studies [57-60], little is known about the biomechanical consequence of growing rod insertion particularly the immature spine as in EOS. Several papers have looked at the biomechanical characteristics of the human spine in order to understand complex dynamic loading conditions the spine is exposed to during activities, with the first being Panjabi et al. [75] in 1976 where thoracic spine segments were found to be more flexible in flexion than in extension. *In-vivo* studies have provided useful information, but have shortcomings in regard to the accuracy in measuring loads or applied forces, whereas *in-vitro* experiments allow tighter controls on variables and can be used to validate new implants and surgical procedures [76]. There have been a few research studies investigating the biomechanics of growing rods used to manage EOS curves [66, 77], however no study to the author's knowledge has investigated the spinal biomechanics of the semi-constrained growing rod construct to date.

2.5.1 Porcine spines as an animal model for testing

There is extremely limited availability of fresh frozen human cadaveric spines especially from the younger population. Of the available human spines, they usually vary in age, existence of degenerative changes, geometry and thus biomechanical properties. This makes it difficult to not only test but also

compare vertebral levels to a younger population. Because of these factors, the use of animal models in biomechanical research is widely accepted as an appropriate substitute to cadaveric human specimens, particularly in regard to reducing costs, with easier availability and because of similarity across species, depending on what is being investigated. There are however, several factors to consider when deciding upon which animal model to choose, particularly when taking into account the differences in morphology and function with human spines. These differences must be recognized when designing experimental parameters and also during data interpretation.

Extensive spine biomechanics research has already been done with a variety of animal models, including sheep, goat, calf and pig [76, 78-81]. The immature porcine spine has been noted in several papers to be the best analogy to the human spine. Two papers by Busscher et al. [78, 82] are the only papers that directly compare the porcine spine anatomically and biomechanically with human spines. They also use a similar setup and test protocol, unlike other studies which use known human literature in order to compare with porcine study results [78, 82]. The complete porcine spine has 7 cervical, on average 15 thoracic and 6 lumbar vertebrae [83] unlike human spines which have 7, 12, and 5 vertebral levels respectively. Other papers including one by McLain et al. [84] compared a specific lumbar vertebrae (L4) across varying animal species, including the pig, and a paper by Dath et al. [85] compared the entire porcine lumbar vertebrae with known human lumbar anatomical measurements. Similarities were found across several anatomical areas including vertebral body height, shape of end plates, spinal canal and pedicle

size, when compared with a large series of anthropometric measurements, documented in the Hamman-Todd collection at the Cleveland Museum of Natural History [86]. In terms of bone turnover, the porcine spine also undergoes trabecular and cortical remodelling, which is similar to humans [87]. Although higher trabecular density and bone mass has been recorded in porcine spines than compared to human spines [88].

Unlike human spines where the zygapophysial joint facet orientation changes below the thoracolumbar junction, this change occurs in the lower thoracic region of porcine spines [82]. Biomechanically with similar geometry and orientation of zygapophysial-facets the lower thoracic region of porcine spines is comparable to the lumbar spine in humans [82]. The similar geometry between porcine quadrupeds and bipedal human spines indicate that they are loaded in a similar way. This has been further substantiated and supported through research by Busscher et al. [82] and others [89-91], in which the biomechanical properties of the two species are comparable. Analysis of CT scans, have also showed comparable results with regard to intervertebral disc heights in relation to the vertebral body, across both human and porcine spines [82].

Vertebral body and end plate measurements in porcine spines are taller and narrower than compared to human spines, which are short and broader. Another important aspect in this current study is the instrumentation of the vertebral pedicles. Several papers have shown that porcine spine pedicles are similar in widths and heights to human pedicles [78, 84, 92, 93] (Table 2.1).

The paper by Dath et al. [85] analysed older porcine cadavers, compared to McLain et al. [84] and Busscher et al. [78] and this would account for the larger values in pedicle height and width being obtained. If these larger values were accounted for, the use of immature porcine spines of less than 60kg total body weight would be an appropriate animal model to use. Analysis of data presented in the table below (Table 2.1) also supports the use of 5.5mm diameter multi-axial pedicle screws (Medtronic, Memphis, TN, USA) chosen for this study.

Porcine spines are also readily available from local abattoirs, they show good homogeneity across similar body weight specimens and from the studies mentioned above are a good representation of the human spine [82]. With similar metabolic, anatomical, and biomechanical parameters the porcine spine could be used as a representative of the human spine in experimental spinal implant testing. These aspects support the choice of porcine spines for the current biomechanical study.

Table 2.1. Comparative results of anatomical measurements of porcine and human pedicle width and height.

Author	Busscher et al. (2010) [78]		Dath et al. (2007) [85]		McLain et al. (2002) [84]	Bozkus et al. (2005) [94]	
Study type	Direct comparison of entire human and porcine vertebrae		Anatomical measurements of porcine lumbar vertebrae only (L1-L6) compared to collated literature of human lumbar measurements [93]		Comparison of L4 vertebrae morphology across several animal models including porcine to humans	Comparison between porcine and human thoracic vertebrae only. Split up results into right and left sides (right side state below)	
No.	6 Human & 6 Porcine		6 Porcine		2 Porcine, 7 Human L4	10 Porcine & 10 Human	
Age	H: (mean 72yo, av 55-84yo) P: (4month old, 40kg)		18-24month old 60-80kg		H: (62-75yo, 55-85kg) P: (immature 55-65kg)	P: (6 month old, 30kg) H: (mean 66yo, av 57-81yo)	
Pedicle Width (PedW)	Comparable in low thoracic and lumbar between both (p<0.05) 8 mm in low thoracic and lumbar	Porcine (mm) L1 – 12.6 L2 – 12.2	Human (mm) L1 – 8.0 L2 – 7.80		22% narrower than matched human pedicles 7mm compared to 9mm.	Porcine (mm) T9 – 6.8 T10 – 6.5 T11 – 7.1 T12 – 7.6 T13 – 7.6 T14 – 8.1 T15 – 8.6	Human (mm) T9 – 7.6 T10 – 8.3 T11 – 8.8 T12 – 8.8
Pedicle Height (PedH)	Comparable between both except for lower thoracic where porcine vertebrae was significantly larger 12-16mm in low thoracic and lumbar for porcine spines	Porcine (mm) L1 – 21.4 L2 – 22.2	Human (mm) L1 – 15.9 L2 – 15.0		Not measured	Porcine (mm) T9 – 15.6 T10 – 15.5 T11 – 16.7 T12 – 16.1 T13 – 16.4 T14 – 17.9 T15 – 19.0	Human (mm) T9 – 13.9 T10 – 14.7 T11 – 16.9 T12 – 16.5

2.5.2 Freeze-thawing of specimens prior to testing

During mechanical testing of a biological specimen, the preservation of *in-vivo* properties is important. It is often assumed that the mechanical properties of a fresh frozen specimen will be reflective of this. However, multiple freeze-thaw cycles are often required particular in staged specimen preparation and testing. This is the case for the current thesis work. Therefore understanding the effect that multiple freeze-thaw cycles have on biological specimens is important, particularly the biomechanical properties, which have been noted to change even after a single freeze-thaw cycle [95].

The spine is a close integration of bony and ligamentous structures supported by hydrated intervetebral discs and synovial joints. The tissue-water content of the intervetebral disc is one important factor, which can affect the results of biomechanical spine research. Following freezing, porcine spine discs have been noted to increase in water permeability [96]. Increased intervertebral disc height has been shown to cause changes in stiffness, with an overall increase in stiffness, reduced range of movement and stretch on surrounding ligaments and support structures. By exposing the spine during testing to the outside atmosphere there is movement of water through the collagen matrix within the intervetebral disc, such that a loss of fluid is experienced. A moment-angular displacement study by Hongo et al. [95] found that the neutral zone (NZ) size and slope of the moment-angular displacement graph changed after the first freeze-thaw cycle of porcine spines. Such that the NZ decreased in size and increased in slope, however the results did not alter with as many as two subsequent freeze-

thaw cycles [95]. This study supports the use of porcine spines in research, where multiple freeze-thaw cycles of more than one and less than three are required, with stable biomechanical results being obtained.

Numerous methods have been used in an attempt to maintain constant water content and thus intervertebral disc height during testing, including testing in humidified environment chambers kept at body temperature. This is however hard to replicate, particularly when instrumentation and measuring devices need to be attached and monitored during biomechanical testing. A simpler and easier option used in several previous biomechanical studies involves wrapping the motion segments being tested in saline soaked gauzes to reduce moisture evaporation and ensure a moist environment is maintained during testing [82, 97]. Research by Wilke et al. [81] showed that a more stable range of movement is recorded with moist specimens than compared to air exposed or constantly irrigated specimens.

It has also been shown in research by Thompson et al. [98], where spines were immediately frozen (at minus 20 degrees Celsius) once removed from the body did not require a compressive preload, prior to testing, in order to return the intervertebral disc to its original in-vivo height.

2.5.3 Constant rate of rotation to a set maximum moment

As previously mentioned, *in-vitro* studies provide a more objective assessment of surgical implants. They also allow variables, such as the loading applied to the spine-implant construct to be more precisely controlled. *In-vitro* testing of the spine can be undertaken using either moment or displacement controlled testing; each has its own advantages and disadvantages.

During moment-controlled testing the primary motion axis is controlled in order to apply a known moment, while (some or all) other axes are allowed to 'float' in order to prevent the generation of non-physiological reaction forces. This allows a specimen to move freely in response to an external load. By adjusting the desired set moment to be reached during testing, one can measure the resultant displacement achieved [75, 99, 100]. Regardless of the spinal instrumentation used, this approach applies constant loading across all individual levels of a specimen. If large displacements are required to reach a set maximum moment, specimen damage may occur making it difficult to compare specimens. Some critics of this type of testing, point out that during moment testing, the specimen is likely to rotate around a different centre of rotation after each intervention (spinal implant is applied. This changes the forces acting on joints and surrounding structures and also makes comparison between implants difficult.

In displacement/rotation-controlled testing, rotational or displacement motions are controlled for and the resultant moment measured. This allows

the centre of rotation to be defined with uniform displacement with greater reliability when making comparisons of the affect following spinal implant application. But this may not be reflective of physiological motion, because of the complex muscular control of movement [101].

There will continue to be debate about which biomechanical method is best suited to analyse spinal implants. At present setting a maximum moment during testing seems to be the accepted standard protocol [76, 81, 102, 103]. Constrained moment controlled testing ensures each specimen experiences a constant rate (degrees per second), about the primary axis to a set maximum moment. This prevents the possibility of test speed changing to reach the set maximum moment. A variety of systems have been used to apply pure moments during testing and include cable driven systems [104-108] and suspended weights [109]. More recently spine testers have been refined with more sophisticated torque motors and the use of six-axis testing machines [82, 100, 110]. This thesis used a displacement controlled test at a constant rate to a set maximum moment.

2.5.4 Fixation methods

The type, location and configuration of anchors in securing growing rod constructs are just as important as implant design and overall function. The superior and inferior foundations that provide anchor points for dual growing rod constructs can incorporate a wide variety of either, laminar hooks, mono or poly axial screws or a hybrid design of both, which can also include transverse cross links between rods. There has been several reports in the literature of implant failure, at the bone-implant interface, in growing rod constructs [19, 56, 111-113]. These studies have often only tested a single implant construct and not compared them biomechanically against other implant constructs.

A study by Mahar et al. [114], compared four different anchor constructs by testing the biomechanics of each. The screw only constructs were significantly stronger than hook-hook and screw-hook constructs with cross-links. The addition of a cross link in a screw-screw construct demonstrated the greatest failure load, but this was not statistically significant when compared against a screw-screw only construct. Although useful in guiding the choice of anchor selection, the study by Mahar et al. tested failure in a posterior loading direction only, whereas a more realistic future study should test pullout strength during an arc of rotation or torsional forces in long cyclic loading tests. The choice of construct also depends on surgeon preference, bone density, anatomical dimensions and bone quality, as well as construct design.

Research by Skaggs et al.[115], presented at the International congress on EOS with growing rods in Toronto 2010, comparing the direct complication rates between hook and screw anchors. The research group found fewer complications with a screw anchor construct (2.4% complications from a study of 896 pedicle screws), compared to using hooks (6.9% complication rate in N=867 hooks studied) [115]. There were no documented vascular or neurological injuries directly related to using a hook or a screw fixation method to secure growing rods.

Other retrospective studies have supported the use of pedicle screws compared with hook or hybrid constructs [116, 117]. Advantages include superior fixation, stability at the bone-implant interface, correction of coronal plane deformity and reduced neurological problems. This is particularly evident at final fusion when multiple levels are instrumented with pedicle screws allowing superior coronal, sagittal and transverse plane correction and alignment. Complications directly related to the use of pedicle screws will be discussed further below. Pedicle screws use the largest area of bone contact, connecting the pedicle to the vertebral body, thus forming a strong anchor for fixation. This is important particular when large corrective forces are often required when translating and derotating the deformed scoliotic spine.

The design of pedicle screws has improved over the past decade with advances in understanding of spinal biomechanics. A wide variety of screws are available including; mono-axial, uniaxial, multi-axial and more recently

6DOF (multiple degrees of freedom) [118]. Limited research data is available on the newer 6DOF pedicle screw and therefore was not considered for use in the current thesis as screw fixation. One can easily see on inspection that greater freedom in screw head orientation and assistance in seating of the rod into the screw head saddle would be achieved with a multi-axial screw than compared to a mono-axial screw (Figure 2.7). It would be difficult to control for any malalignment between the rod and screw head with mono-axial screws. With the potential of additional stresses on the bone-screw interface, movement of the screw in the bone and eventual loosening of the vertebral fixation. With more degrees of freedom, multi-axial screws can facilitate better rod-screw seating reducing high stresses at the bone screw interface and provide a more superior form of fixation than compared to mono-axial screws.

A.   B.   C.
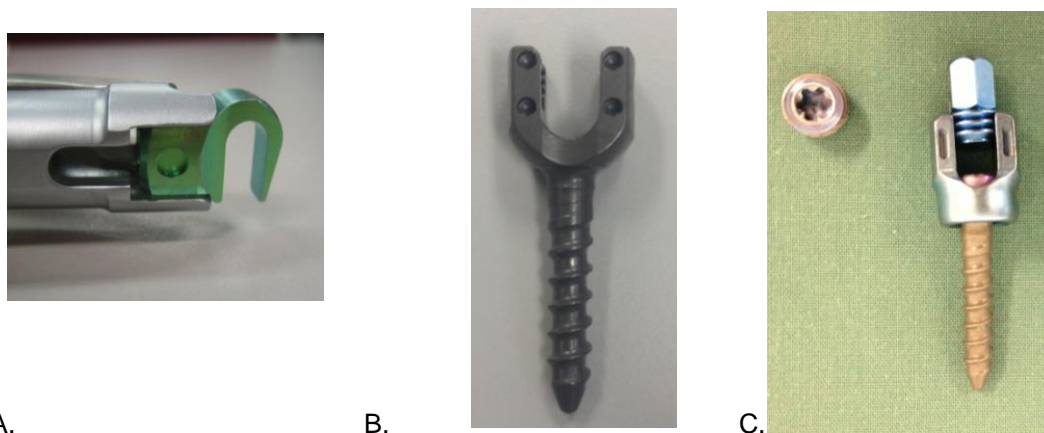
Figure 2.7. A) Laminar hook construct. B) Mono-axial screw. C) Multiaxial screw and set screw, component of the set screw once "break-off" has occurred (left of the image).

A retrospective study by Kuklo et al.[119], on the management of AIS with posterior pedicle screw fixation, supports the use of pedicle screws over segmental hooks, because they provide better deformity correction in the coronal and sagittal planes. The study compared an age and curve matched

cohort of 35 patients; 15 of who underwent mono-axial screw fixation and 20 multi-axial screw constructs. The group was followed up for a minimum of 2yrs with comparison of pre-operative and post-operative radiographs being used to assess correctional capacity of screw construct. Of note was that mono-axial screws showed greater derotational and restoration of thoracic symmetry than compared to multi-axial screws. Although a curve matched cohort was used, this was a final fusion study in managing adolescent scoliosis and clinically it may be difficult to seat mono-axial screws particularly if the rod-screw position is not closely aligned at the time of curve correction. Multi-axial screws allow the head to pivot and rotate in all directions and are more forgiving during seating of spinal rods. The head is locked onto the threaded body once the setscrew is tightened, eliminating this motion.

A computer biomechanical model from ten patients with AIS having undergone spinal correction was constructed in a paper by Wang et al. [118] and used to analyse four types of pedicle screw constructs, either; mono, uni, multi-axial or 6DOF. Simulation of surgical instrumentation using a different pedicle screw construct was then tested at 15 different screw placement variations and the forces at the bone-screw interface recorded. On average, mono-axial screws recorded the highest screw-bone load measuring 229N, compared to multi-axial screws, which recorded 141N. This reduction in load can be attributed to the pivoting and rotation allowed as described above. Allowing wider freedom in screw insertion orientation, the study by Wang et al. [118] supports the use of multi-axial screws in large and

stiff spinal deformities. A young child's spine is inherently flexible, however in those with EOS large curves often need to be managed surgically. The use of multi-axial screws with the ability to orientate the head in different directions and capture the rod more securely during correction is supported in several studies mentioned above [118, 119] and is the fixation of choice used in this study.

2.6 Complications of growing rods

Dual growing rod techniques have demonstrated superior deformity correction, maintenance correction and allowed continued growth, which equals or surpasses predicted growth compared to single-rods [57-60]. However, complications are expected with the complexity of managing EOS and have been reported to range from 20% to 48% [56-59].

The documented complications during the management of EOS with fusionless growing rods (either single or dual rod techniques) include; wound infections both deep and superficial, implant complications with hook or screw dislodgement, screw breakage, rod fracture or prominent implants, alignment complications, neurological complications both during and post surgical procedures and other medical complications such as pulmonary problems post instrumentation [31, 56, 57, 59, 67, 113].

A study by Klemme et al. [19] reported an overall complication rate of 40% (or 0.6 per patient) in a series of 67 patients who underwent posterior instrumentation with either Harrington rods, modified Moe rods or a paediatric Cottrell-Dubousset system design, all types of fusionless surgery for scoliosis. They noted 33 rod or anchor failures, 3 cases of prominent implants requiring removal, 3 deep wound infections and 1 death [19]. A later retrospective study by Akbarina et al. [57] reported 13 complications in 11 of the 23 patients who underwent only dual growing rod surgery to manage EOS having been followed up for a minimum of 2 years.

In fusionless scoliosis surgery, a common complication is rod fracture with long vertebral segments being spanned without fusion, for extended periods prior to final fusion. Rod fractures were first documented by Moe et al. [10, 54] with 6 reported rod fractures in four patients and later followed up with a series of 20 patients, where 5 instances of rod fractures were documented. Moe et al. proposed the use of thicker Moe-modified Harrington rods as a more superior rod, since fractures occurred less than in thinner-threaded Harrington rods. This was refuted by Klemme et al. [19] in a study mentioned above finding longer survival times/fewer rod breakages for Harrington rods than compared to Moe-modified Harrington rods.

Compared to earlier research by Kilemme et al. [19] and Akbarina et al. [57], a recent research paper by Bess et al. [56] encompasses a broader cohort of EOS patients who underwent growing rod surgery and categorizes complications. Of the 140 patients in the study 81 (58%) had a minimum of one complication with significantly more patients ($p<0.05$) having unplanned surgical procedures for single compared to dual growing rods. This equated to 19 unplanned surgeries in 71 patients with a single rod compared to 7 of the 69 patients with dual rods [56]. Only 10% of patients (9 of the 88) with submuscular rod placement had wound complications, a likely explanation being the increased soft-tissue coverage compared to subcutaneous insertion, where 13 of the 51 patients (25%) had tissue compromise. It was thought with subcutaneous rod insertion (as in earlier rod designs) that auto-fusion would be reduced by not exposing the subperiosteal layer of a child's spine. However in the study by Bess et al. the greatest rate of unplanned

surgery was in those patients who had a single growing rod placed subcutaneously. Single growing rods have recorded higher fracture rates than compared to dual rods [59, 113], with repeat fractures occurring more in patients with single rods [113]. The most common fracture locations as noted in a study by Yang et al. [113] were superior and inferior to the tandem connector, followed by the thoracolumbar junction and then areas adjacent to the cephalad or caudal anchors. Although not statistically significant, rod fractures occurred least in constructs made entirely of screws. With more rod fractures occurring in hybrid constructs of hooks and screws and greatest number occurring in constructs entirely of hooks.

Although documented complication rates of 20% for growing rods, have been reported by Bess et al. [56], not all complications require a separate surgical procedure and can often be rectified at the next planned surgical procedure, such as distraction/lengthening. Managing EOS often requires a long duration of treatment and multiple procedures, including repeated surgical lengthening at frequent intervals. With each additional surgical procedure beyond the initial instrumentation Bess et al. [56] showed that there was a 24% increased risk of a complications occurring. It was postulated in the study by Bess et al. that by controlling the patients' age at the time of initial implantation and the number of procedures during treatment, the use of dual growing rods and placement via a sub-muscular insertion can reduce the risks of complication [56].

If initial EOS surgery could be postponed, Bess et al. [56] showed the likelihood of an adverse complication would decrease by 13% each year. Younger children with less developed organs and functional capacity as well as reduced soft tissue thickness are placed at higher risk of implant complication, particularly the younger they are at initial surgery. More surgical procedures would be required in those children with EOS requiring intervention at an earlier age as well, which places them at additional risk of complications. However the issues outlined in the study by Bess et al., need to be individualized for each patient, since progressive curves in EOS may need early intervention.

Although there has been extensive research regarding the use of pedicle screws for the treatment of adult and adolescent spinal deformities, few studies have examined complication rates of pedicle screws in paediatric spinal deformities. Two recent studies have looked at patients younger than 10 years of age, instrumented with pedicle screws, to manage various spinal deformities and disorders. A study by Harimaya et al. [120] evaluating the accuracy of pedicle screw insertion, with anterior-posterior and lateral radiographs, recorded no intra-operative or short term pedicle screw related complications, from 88 patients treated with 948 pedicle screws. This cohort consisted of 15 patients with idiopathic EOS. Of the 88 patients instrumented only 0.4% of long term complications (>2 years follow up) were related to screw insertion, namely due to screw pullout and prominence of proximal thoracic pedicle screw. Of the 948 pedicle screws inserted, only 8 were mal-positioned (0.84%), as reported by analysing plain radiographs and

using a standardized recording technique. Although not the gold standard in verifying screw position, (which is CT), plain radiographs limit the exposure of radiation to paediatric patients.

A recent study published this year by Baghdadi et al. [116], compared the rates of screw related complications including mal-positioning between children younger than 10 years of age and a matched control greater than 10 years. Instead of a heterogonous group of paediatric patients with spinal deformities as in Harimaya et al.'s study, a case-control design was used to match younger and older population groups. Although, limited by small patient numbers, the study by Baghdadi et al. found 3 of the 265 screws (1%) inserted in 33 patients 10 years or younger, were revised intra-operatively based on radiographic findings during surgery, whereas 13 out of 488 screws (2.7%) were revised intra-operatively in a matched cohort of 66 patients older than 10. There was no post-operative revision surgery in either matched group. Another interesting finding (without matching for diagnosis because of limited postoperative CT scanning), was that rates of severe (>4mm) mal-positioning were similar in each cohort, whereas moderately mal-positioned screws (2-4mm breech) were more common in the young cohort (21.5% compared to 13.4%). This study adds to the support of pedicle screws in managing young children with spinal deformities as an accurate and safe technique.

The management of EOS often presents challenges and difficulties for the treating surgeon. Each patient's treatment should be individualised. However, the use of growing rods to manage EOS, a fusionless procedure, which preserves spinal growth, has become increasingly popular. Several growing rods and fixation methods already exist as outlined in the literature review above, with dual growing rods, submuscular rod placement and anchoring of rods with pedicle screws, showing reduced complications and unplanned returns to theatre. While already clinically implemented with promising results, there is no published literature on the newer semi-constrained growing rod. This study aimed to identify and evaluate the biomechanics of the semi-constrained growing rod through *in-vitro* experiments, in direct comparison to the standard rigid rod, with the main aims having previously been outlined above.

3 Methodology & Materials

This chapter describes the experimental apparatus and test parameters used to investigate the biomechanics of semi-constrained growing rods, compared to rigid rods. The three main methodology sections follow the thesis objectives.

3.1 Apparatus development for in-vitro spine testing

3.1.1 Growing rod choice

Two different types of instrumented rods used to manage EOS were chosen, for direct biomechanical comparison in this thesis. A recent new design of growing rod, know as a semi-constrained growing rod (Medtronic, Sofamor, Danek, Memphis, TN, USA), with interconnecting male and female components (telescopic sleeve), enabling axial rotation on each other (Figure 2.5), was directly compared against standard 'constrained / rigid' rods. Although already surgically instrumented, biomechanical understanding of this growing rod was sort in the current thesis.

### 3.1.2 Specimen choice, preparation and mounting

Immature porcine spines served as the experimental model for this thesis. They have been shown in several research papers already outlined above, to be a valid model for the paediatric human spine [82, 84, 89-91]. Spines from English Large White pigs were obtained from a local abattoir, and ranged in age from 16 to 22 weeks with a weight range of 40-60kg and a mixture of sexes. They were sectioned to include the vertebral column from T4-L2 with

intact musculature and ligaments and at least 3 cm of ribs on each side. Each specimen underwent a pre-test computed tomography – CT scan with a Siemens Flash 128 slice scanner (Siemens, Munich, Bavaria, Germany), set at 2mm slices with an in slice resolution of 0.3mm, so as to exclude any anatomical anomalies. Each tested spine showed no radiological evidence of any bony pathology. Prior to potting, the specimens were stored at the testing facility in sealed plastic bags, at minus 20 degrees Celsius and when required were thawed for 12-17 hours in a 4 degree Celsius fridge. If further thawing was necessary each spine was left at room temperature for a further 1-2 hours.

Once thawed for the first time, each spine was then dissected to make up a multi-segment unit (MSU) consisting of 7 vertebrae and 6 intervertebral discs from thoracic vertebrae 10 through to 15 and the first lumbar vertebrae (T10-15 and L1). To represent the most commonly instrumented levels in human scoliosis corrective surgery, the thoracolumbar region was chosen. Non-ligamentous soft tissues were removed leaving the vertebral bodies, discs, zygaphphysial joints and ligamentous structures along with leaving 3cm of ribs either side. This preserved the biomechanically important costovertebral and costotransverse joints [121].

Through pilot studies a MSU spine, consisting of 7 vertebrae, was chosen as the most appropriate length to accommodate a modified semi-constrained growing rod, which was shortened. Levels one and seven of the MSU spine were left un-instrumented. Although the testing machine could accommodate

longer constructs, it was decided that a 7 level construct was adequate to investigate the chosen rods in this thesis. The minimum testing length of the shortened semi-constrained growing, which included adequate telescopic sleeve overlap (Figure 2.5 and Figure 3.1) consisted of 5 vertebral levels or between levels two to six of the MSU spine. This overlap was positioned and sized to achieve similar proportions to the ones instrumented in paediatric patients
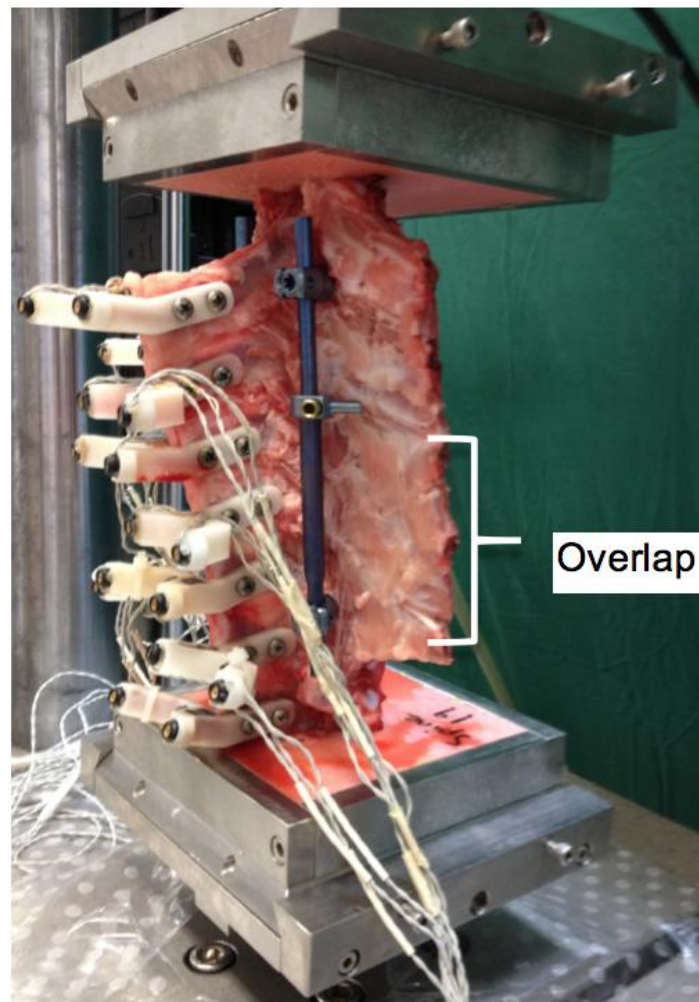
Figure 3.1. Semi-constrained growing rod inserted and mounted within the Instron machine with adequate overlap of the sleeve component.

The zygapophysial joints were localised and exposed at the second and sixth vertebra levels of the MSU. Two 4.5mm x 25mm multi-axial screws (Medtronic CD Horizon ® Legacy ™, Sofamor, Danek, Memphis, TN, USA) (Figure 3.2) were inserted into the pedicles and the vertebral bodies at these levels using standard instruments and procedure by a single operator. The choice of multi-axial screw size was supported from literature mentioned above, with the shorter 25mm length being chosen, so as to not penetrate through the anterior part of the vertebral bodies. These multi-axial screws formed the superior and inferior fixation points for each 5.5mm diameter titanium alloy (titanium, aluminium and vanadium) semi-constrained growing rods or rigid rods during testing, with break-off setscrews securing the rods.

Figure 3.2. Medtronic 4.5 x 25mm CD Horizon ® Legacy ™ multi-axial screws with break-off set screw not yet broken off.

Each MSU was then embedded into stainless steel (S-316) cups using polymethylmethacrylate (PMMA, bone cement). The specimens were potted such that the centre of the vertebral body lined up with the centre of the stainless steel cups and all spinal articulating parts, including zygagpophysial joints (articulation between the superior and inferior facets) being kept free (Figure 3.6). To ensure adequate fixation of the vertebrae in the specimen

cups, 3 stainless steel wood screws (7x25mm), were screwed into the top endplate of the upper vertebrae and bottom endplate of the lower vertebrae, to a maximal depth of 15mm (Figure 3.3). During preparation the spines were wrapped in normal saline soaked gauzes each 15 minutes. Following potting each specimen was removed from the stainless steel cups and stored in sealed plastic bags, labelled and re-frozen at minus 20 degrees Celsius for at least 48hours prior to re-thawing using the same technique as mentioned above.

Figure 3.3. Wood screw fixation in the superior endplate of the porcine vertebrae.

3.1.3 Displacement controlled testing to a set maximum moment

A single operator for all experimental setups was used to ensure consistency with test protocol. Specimens were tested in a custom built dynamic spine testing apparatus (Figure 3.5), mounted in an Instron MTS 8874 biaxial testing machine (Instron, Norwood, MA, USA) (0.1 degree accuracy in rotation, refer to error analysis in the results section). Displacement

controlled (axial rotation) tests were conducted at a constant speed up to a set maximum moment. The dynamic testing apparatus consisted of mounting plates, which could accommodate the potting cups. The most superior plate was secured to the rotational axis of the Instron load cell and the inferior plate was mounted on an x-y plate, which enabled translation in the x and y planes but not rotation. This allowed the specimen to find its own axis of rotation, during biomechanical testing. Prior to mounting and testing the un-instrumented MSU specimens, rigid markers for Optotrak (Optotrak 3020, Northern Digital Inc, Waterloo, ON, USA) data acquisition, were attached to each of the spinous processes, 7 in total, (Figure 3.6). With separate rigid markers being kept aside to be attached to the rod construct during testing, which is explained further below. Prior to mounting the test apparatus the Instron machine zeroed.

Utilising the Instron system described above, continuous pure axial rotations, were applied at a constant rotation rate (initially at 10deg.s^{-1} for one of the tests but lowered to 8deg.s^{-1} for each following test) about the primary axis, to a set maximum moment of ±4Nm. The constant rotation rate was lowered so that the Instron machine would not lag in data acquisition, which was noted to occur at the faster rate. Several pilot studies were performed in order to obtain the non-destructive moment during axial rotation testing. Pilot studies also defined the number of pre-conditioning cycles required, so that consistent and repeatable data for rotational displacement and calculated stiffness could be obtained. A non-destructive set maximum moment of ±4Nm was chosen from pilot studies showing consistent displacement,

moment and resultant stiffness curves after 5 cycles of continuous testing. It was observed that the first of five cycles (hysteresis plots of moment versus axial rotation) would often differ slightly prior to settling with subsequent cycles. The first cycle is often known as a pre-conditioning cycle. All tests were performed as five fully reversed continuous cycles of pure non-destructive axial rotation, with left prior to right axial rotation, with no change in sequence order (Figure 3.4). The 5th cycle was chosen as the cycle to be analysed as no further changes in biomechanical parameters was recorded (Figure 3.7).
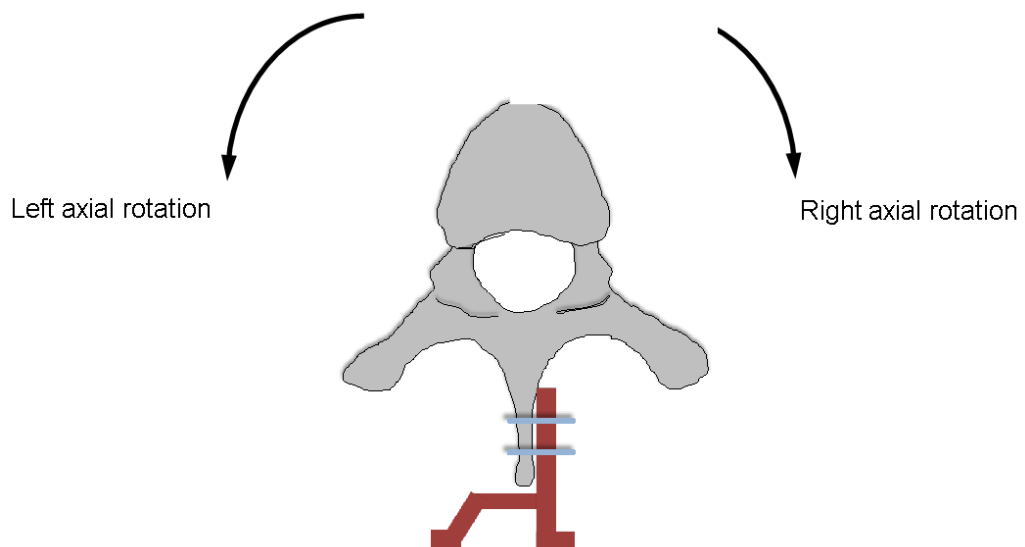
Figure 3.4. A schematic superior axial view of a vertebra showing the orientation of left and right axial rotations controlled by the Instron machine.

During axial rotation testing the z-axis (known as position) of the biaxial testing machine was fixed (Figure 3.15). This holding of position meant that there was no translation along the z-axis. It also ensured the same configuration of joints, with similar zygagpophysial overlap and length being maintained prior to axial rotation. Although fixing the z-axis could introduce potential forces, it prevented any difficulties the Instron machine may have had in controlling this axis. The forces generated by fixing the z-axis are

displayed in the results section below and explored in the discussion. All tests were carried out at room temperature, similar to other studies [78, 107]. No compressive axial preloads were applied prior to testing, as specimens were frozen post removal from the body, ensuring disc heights remained as closely representative to heights *in-vivo*, as supported by previous research [98, 107]. Also it was thought that the long 7 level MSU spine model, would be quite unstable in axial compression prior to testing. To allow for any viscoelastic recovery there was 5 minutes of rest between each test.
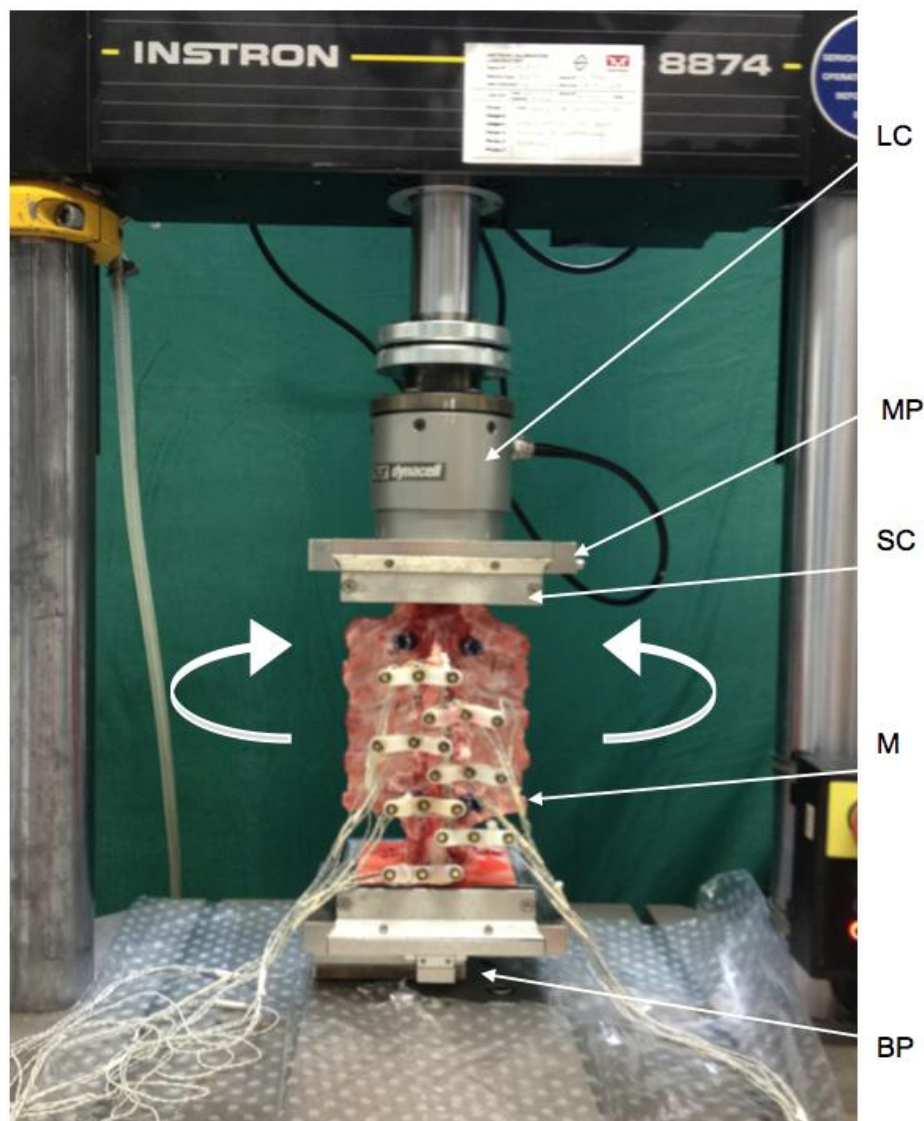
Figure 3.5. Test setup for the application of continuous ±4Nm under constant strain rate in axial rotation to an uninstrumented MSU. Biaxial load cell (LC). Stainless steel cup (SC). Mounting plate (MP) LED markers (M). X-Y ball bearing plate (BP).
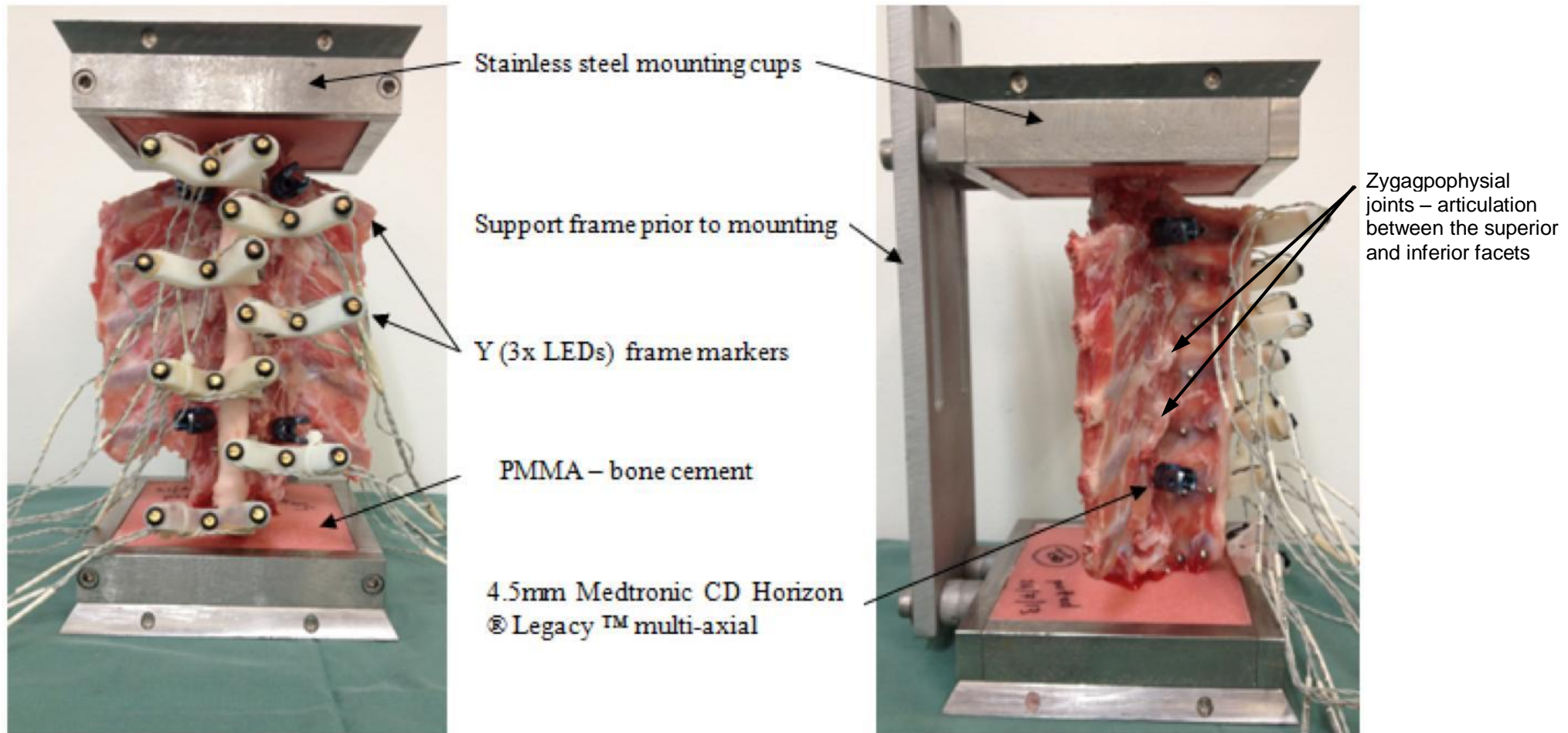
Figure 3.6. MSU specimen potted with polymethylmethacrylate & mounted with Y-frame Optotrak markers at each spinous process level shown in frontal and lateral views. Medtronic multi-axial screws already secured at levels 2 and 6 of the MSU spine construct.

Axial rotation (deg) through 5 cycles of testing
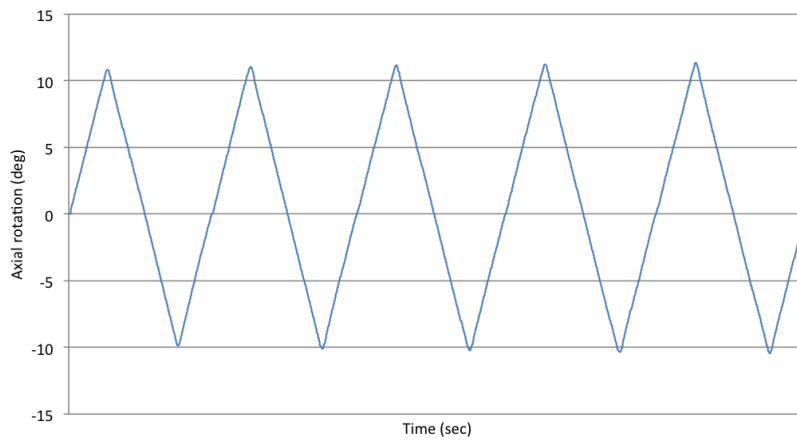
Moment (Nm) through 5 cycles of testing
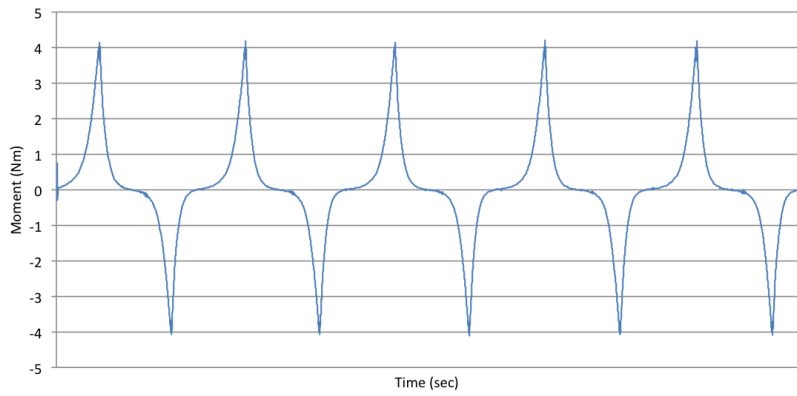
5 cycles of axial rotation at 8deg.s^{-1} to ±4Nm
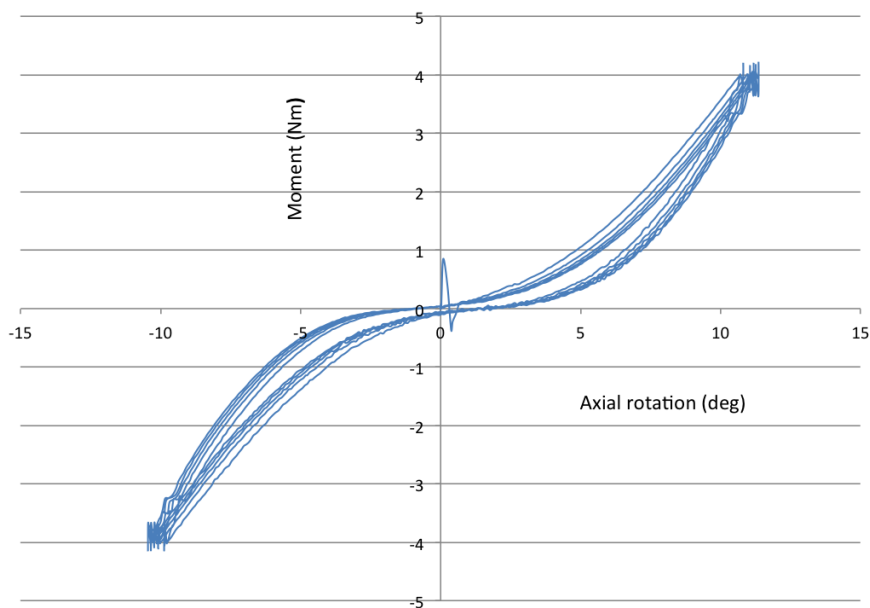
Figure 3.7. Representative raw data. Un-instrumented MSU porcine spines through 5 cycles of testing with stable consistent results.

3.2 Investigating the biomechanical parameters (stiffness and ROM) of two different rod constructs

Three studies were carried out, with the initial two being preliminary studies used to assess consistency of results and test protocol. The first study analysed three un-instrumented 7 level MSU specimens, in continuous axial rotation of 5 cycles each, with all cycles being recorded, but only the 5th cycle being analysed. This was done in order to assess the (test-retest) repeatability of the specimens. A second preliminary study tested a single specimen with dual rigid growing rods, in the sequence shown below. Using the same set up described previously, the third study consisted of 6 separate MSU porcine spines tested in a specific order (Table 3.1Table 3.2).

Table 3.1. Repeatability of dual rigid growing rods at a constant 8deg.s^{-1} to a maximum moment of ±4Nm on a single specimen. Each test comprised 5 continuous cycles each.

TEST	1	2	3	4	5	6	7
SEQUENCE	UN-IN	RIGID	RIGID	RIGID	RIGID	RIGID	UN-IN

Table 3.2. Dual Growing rod analysis in axial rotation at a constant 8deg.s^{-1} to maximum moment of ±4Nm for each specimen tested. Each test comprised 5 continuous cycles with 5min of rest prior to starting the next test with the same specimen.

SPECIMEN	Test – 1	Test – 2	Test – 3	Test – 4	Test – 5
1	UN - IN	GR	UN - IN	RIGID	UN - IN
2	UN - IN	RIGID	UN - IN	GR	UN - IN
3	UN - IN	GR	UN - IN	RIGID	UN - IN
4	UN - IN	RIGID	UN - IN	GR	UN - IN
5	UN - IN	GR	UN - IN	RIGID	UN - IN
6	UN - IN	RIGID	UN - IN	GR	UN - IN

(UN-IN; un-instrumented. RIGID; dual rigid rods. GR; dual semi-constrained growing rods)

Five pairs of 5.5mm diameter titanium alloy semi-constrained growing rods, (Medtronic CD Horizon ®, Sofamor, Danek, Memphis, TN, USA) were cut to appropriate testing size (explained above with regard to the 7 level MSU spine model). Each edge was de-burred to prevent any possible jamming or wear of the components (Figure 3.8). When analysed post testing there was no wear debris noted at the overlap (telescopic sleeve component) of the semi-constrained growing rods and it was decided that one set of these rods would be re-used, so that there was 6 test specimens in the third and final study. Six 5.5mm diameter titanium alloy (titanium, aluminium and vanadium) dual rigid rods were also prepared.

Once each specimen was mounted in the bi-axial testing machine (Instron), testing followed the protocol outlined above (Table 3.2). 4.5mm set screws (Medtronic CD Horizon ® Legacy ™) had a break-off torque limiting aspect built into them (Figure 2.7). They were initially inserted and secured the rod being tested. The set screws were then tightened, using a self-retaining break-off driver and counter torque spanner (Figure 3.9). The torque required to cause "Break off" by the break-off driver (Medtronic, Sofamor, Danek, Memphis, TN, USA) was measured at 13.2Nm (± 0.2Nm), (this was only done four times because of the limited supply of setscrews). Setscrews were reused and reinserted with a torque limiting driver (Medtronic, Sofamor, Danek, Memphis, TN, USA), set at 13.2Nm, calibrated by Medtronic and used surgically.

Figure 3.8. Semi-constrained 5.5mm diameter titanium growing rods (Medtronic, Sofamor, Danek, Memphis, TN, USA). De-burred edge of the sleeve component shown (left).

Figure 3.9. Medtronic self-retaining break off driver and counter torque spanner (left) and torque limiting spanner (right), (Medtronic, Sofamor, Danek, Memphis, TN, USA).

Because of different acquisition rates between the Instron set at 100Hz and the Optotrak at 69Hz (a set acquisition rate limited by the number of co-planar LED markers used to be explained further below) each data set was analysed separately and at no stage was the data synchronised. This was a decision at the initial stages of study design however data has been stored for reanalysed post synchronising at a later date. Using the Instron software, moment and axial rotation data was recorded for each test and saved in Excel format (Excel, Microsoft, Redmond, WA, USA).

Using the 5th cycle from each test moment versus axial rotation curves were generated and biomechanical parameters calculated from excel data. The neutral zone (NZ) was calculated first using a similar technique in studies by Wilke et al.[81, 110] and repeated by Clarke et al. [97]. The neutral zone was calculated as the range of movement where the loading curves during left and right axial rotation, crossed the x-axis at 0Nm moment (between the positive and negative loading cycles on the 0Nm axis). A centralised point was then calculated, by halving the neutral zone. The maximum range of axial displacement (ROM) in both left (positive) and right (negative) displacements was then calculated form this central point out to the set maximum moment of between ±4Nm. Stiffness (Nm.deg^{-1}) was also calculated from hysteresis plots from the 5th cycle, from each test sequence. The set maximum moment of ±4Nm was not included in stiffness calculations because the Instron data created slight fluctuations and irregularities during cycle turn around as shown in (Figure 3.10). The data points between + 2 to +3Nm and -2 to -3Nm (or 60-80% of the maximum applied moment in each

loading direction) were chosen in order to obtain consistent stiffness measures. This region was beyond the neutral zone, initial increase and exponential rise in the slope of the graph during the loading phase of each cycle. The linear gradient of the moment – axial rotation curve between +2 to +3Nm and -2 and -3Nm was calculated with an accepted r^2 value of >0.95 for each test (Figure 3.10). The chosen rotational speed and data acquisition rate gave a data point every 0.08 degrees ensuring adequate angular resolution. After checking for normality for each of the dual semi-constrained growing rod and dual rigid rod tests, paired t-tests were used to analyse total ROM and stiffness with a significance level of P<0.05 being considered statistically significant.
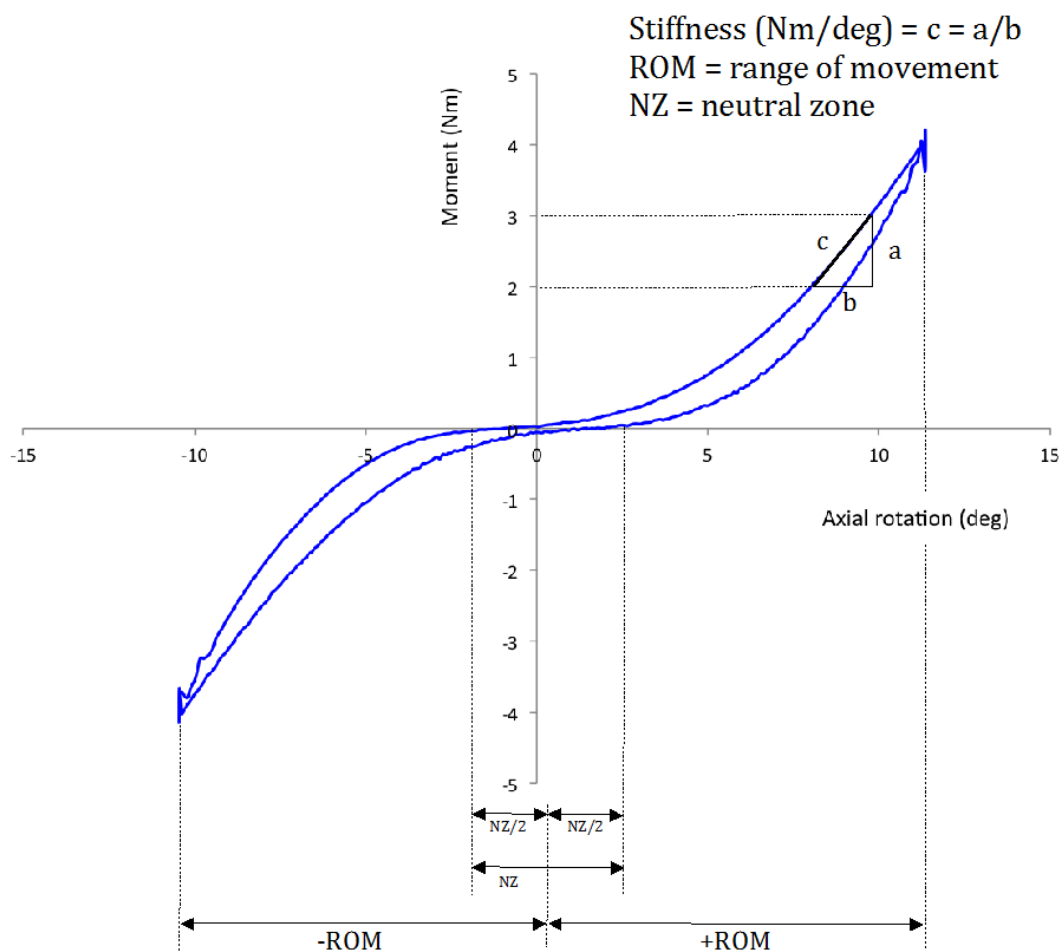
Figure 3.10. Typical moment versus axial rotation curve (5th cycle) with continuous left to right axial rotation. Definitions of parameters are labelled (Stiffness, ROM, NZ). Positive moment indicates left axial rotation and negative moment indicates right axial rotation.

3.3 Optotrak configuration and analysis of intervertebral rotations

Axial rotation of each specimen was captured using a 3D motion tracking system Optotrak [122, 123]. This system contained an array of 3 cameras in vertical orientation (Figure 3.11), operated within the recommended 1.5m minimum distances from the test apparatus mounted in the Instron machine. This configuration provided real time data acquisition. Room access was restricted during testing, so as to prevent possible vibrations or blocking of the camera field. Prior to testing Instron mounted MSU specimens, a global co-ordinate system was set up using a 6-marker digitizer (Figure 3.12) on the test apparatus. Its origin was at the most superior corner of the mounting plate (Figure 3.5 above) and enabled x-y-z orientated data acquisition. A single co-ordinate was also digitised, using the 6-marker digitiser, taken from the central part of each anterior vertebral body at each level (7 in total) prior to testing. This was done so as to define an anatomical landmark, from which to validate vertebrae and create a local co-ordinate system for each vertebral level (Figure 3.13).

Data was simultaneously collected from rigid Y-frame marker attached to each spinous process (Figure 3.14). Rigid body markers were also attached to the rod components, in the configuration shown below (Figure 3.15 – A and B). Each marker contained 3 LED's (not co-linear) in order to define a plane for each marker during either semi-constrained or rigid rod testing. Data was stored using Optotrak Analog Data Acquisition Unit (ODAU) and

support software, (NDI First Principles, Northern Digital Inc, Waterloo, ON, USA). Using the local co-ordinate system with respect to the global one, Optotrak data was processed with a custom designed MATLAB program (2013a, MathWorks Inc., Natick, MA, USA). This program was developed for specific analysis of Optotrak data through High Performance Computing and Research Support, which is apart of the QUT information technology services.

The intervertebral rotations of each level, with respect to the level beneath, were calculated with this MATLAB program using standard 3D vector analysis. Rotation occurring between the semi-constrained growing rod components was also calculated. To compare the total intervertebral ROM of the two dual rod constructs, Optotrak results were normalised to the average of the un-instrumented tests. Statistical significance was assessed using two tailed t-tests with significance when $P<0.05$.
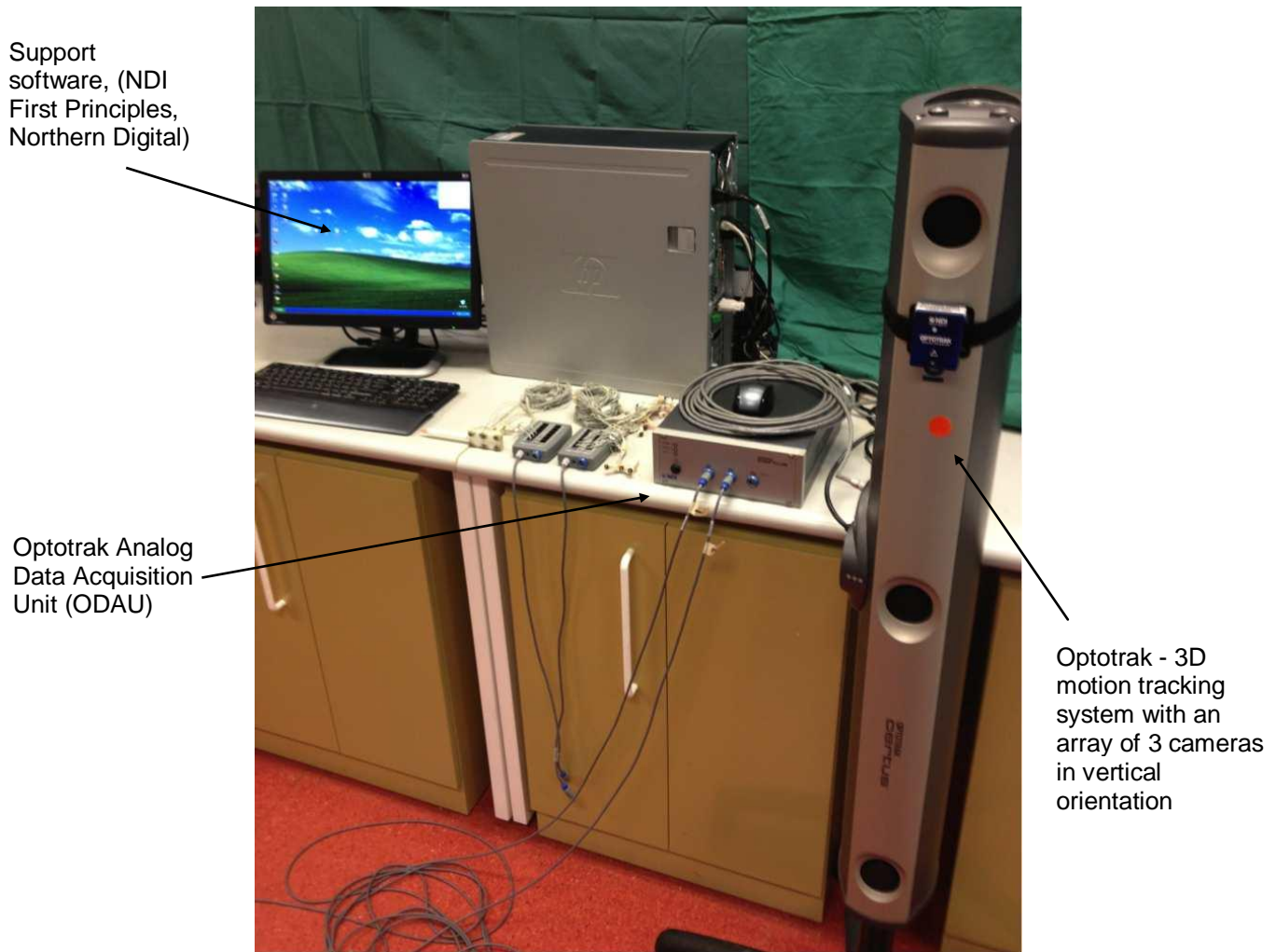
Figure 3.11. Optotrak 3020 series 1 array of 3 cameras (right) with data acquisition unit (ODAU) and marker strober units (central) all connected with NDI First Principles software.

Support software, (NDI First Principles, Northern Digital)

Optotrak Analog Data Acquisition Unit (ODAU)

Optotrak - 3D motion tracking system with an array of 3 cameras in vertical orientation

6-marker digitiser

Rigid marker Y-frames

Optotrak marker console
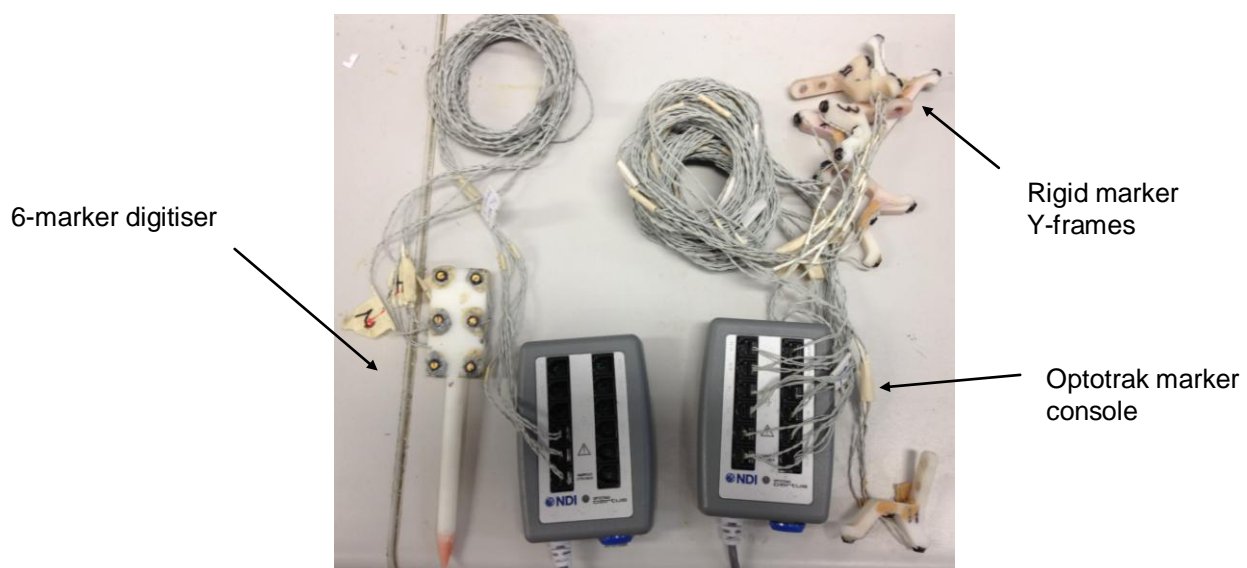
Figure 3.12. Digitiser (6-marker) used to capture local co-ordinate system prior to testing (left) and marker strobe console which could accommodate up to 24 markers and several Y frame digital markers attached (right).
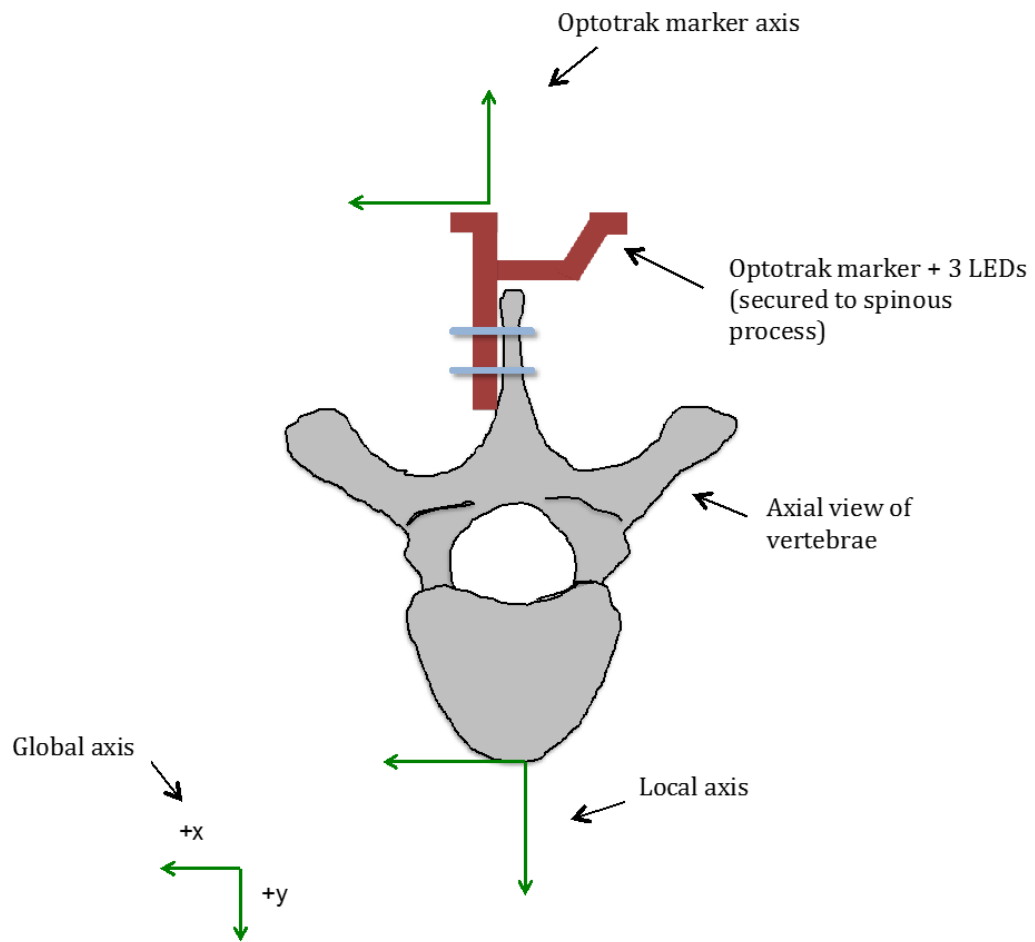
Figure 3.13. Diagrammatic representation of the local co-ordinate system created from digitised Optotrak points from the anterior of each vertebral body. Additional points in +x and +y orientation were created from the digitised Optotrak co-ordinates in line with the global axis as shown above.

Figure 3.14. Optotrak rigid body markers (3x LEDs) for attachment to the spinous processes (left) and each of the semi-constrained or a single rigid rod component (right).
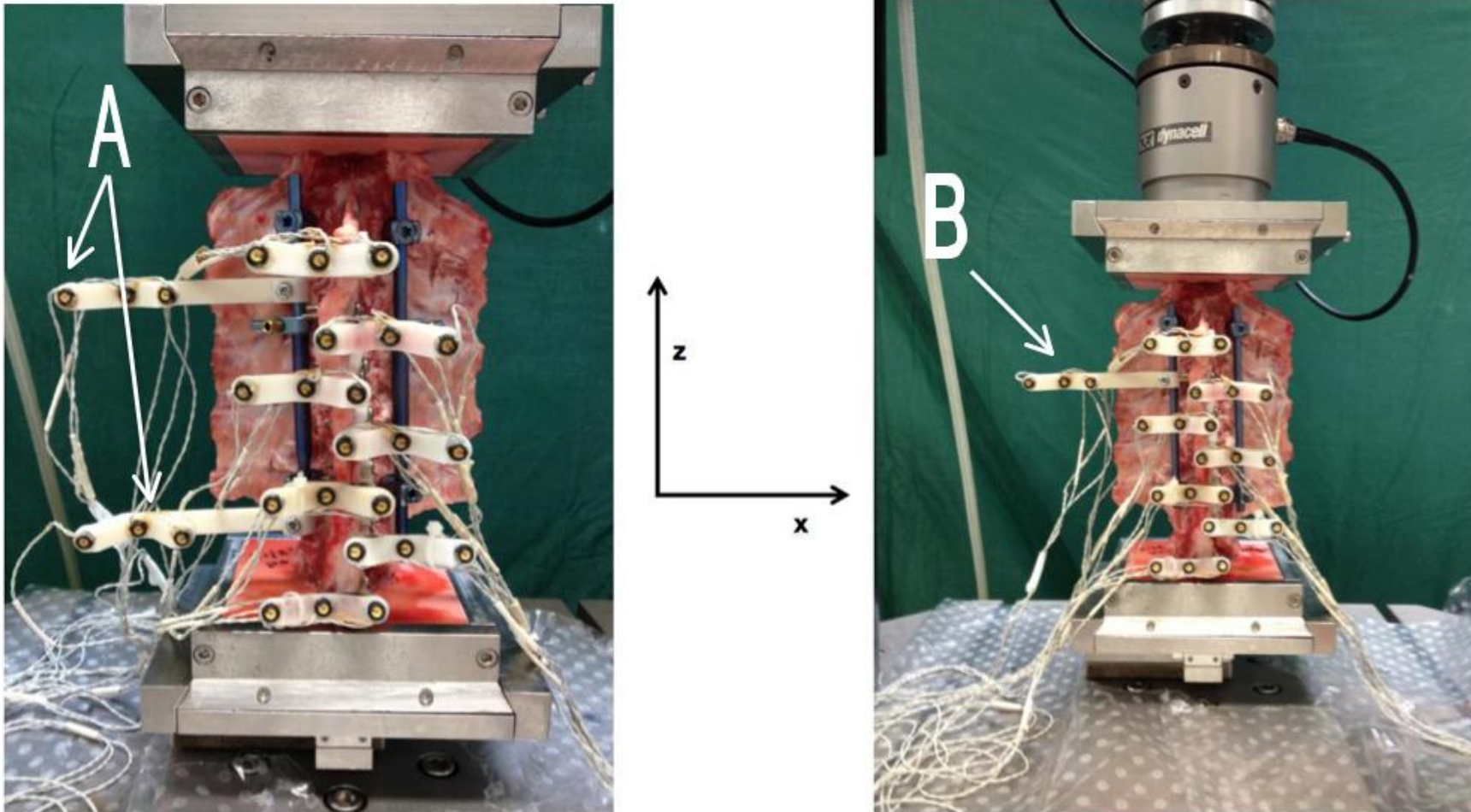
Figure 3.15. Two Optotrak marker frames attached onto each component of the semi-constrained growing rod (left – A arrows). A single Optotrak marker frame attached onto one of the rigid rods (right – B arrow).

After testing, each specimen was refrozen at minus 20 degrees Celsius with the multi-axial screws in-situ. Each specimen then underwent computer tomography (Siemens, Flash 128 slice scanner, set at 2mm slice spacing). A metal reduction sequence was carried out in order to assess the accuracy of screw placement within the pedicles, since adverse screw placement could affect the biomechanical test results. CT scans revealed no adverse screw placement (Appendix 1). Shown below are radiographs and axial computer tomography (CT) images from one of the tested specimens (Figure 3.16).
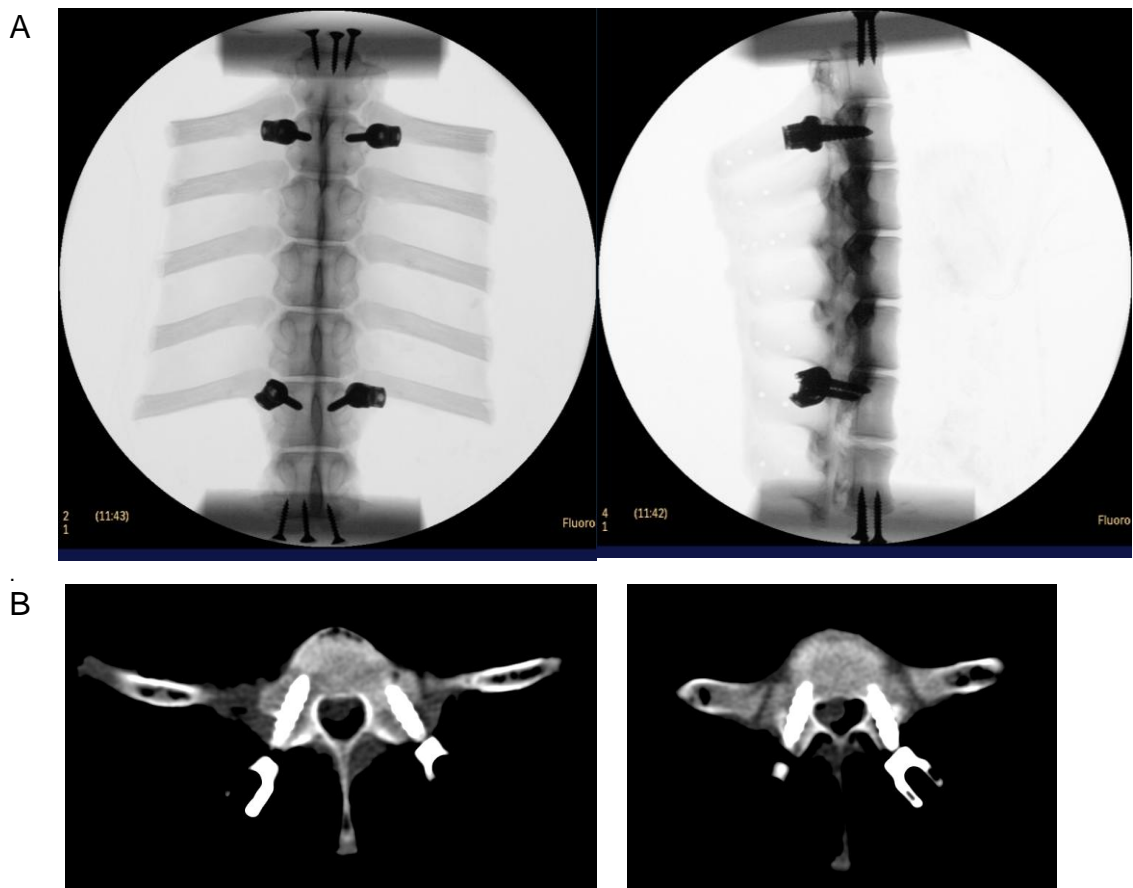
Figure 3.16. A) Anterior-posterior and Lateral views of a MSU porcine spine embedded in PMMA with support wood screws and multi-axial screws at spinal levels 2 and 6. B) CT of inserted multi-axial screws at level 2 (left) and 6 (right) of the MSU specimen respectively.

3.4 Error analysis

Error within each individual measurement was calculated including displacement (axial rotation), torque and stiffness from Instron data as well as error within the Optotrak marker position accuracy. Independent accuracies are reported for each channel within the Instron load cell below from the Instron manual [124].

The size of error was particularly relevant as only small moments (±4Nm) were applied to the test specimens. The largest recorded value for axial rotation during testing was taken as the most extreme value and using the set moment of ±4Nm, errors were calculated with rounding to significant figures specified for each measurement. The resulting measurement errors were assessed against the calculated standard deviations (SD) for all test sequences (Appendix 2).

3.4 Error analysis

4 Results

4.1 Investigating the biomechanical parameters of two different rod constructs

4.1.1 Repeatability of un-instrumented MSU spine testing

The first preliminary study consisted of investigating the repeatability of three un-instrumented 7 level MSU spines, tested 5 times each. The total ROM and NZ size for each un-instrumented MSU spine, during axial rotation at 8deg.s^{-1} to the set maximum moment of ±4Nm, is shown below (Figure 4.1), with calculated values displayed in table form in the appendix (Appendix 3). The average recorded maximum moment during testing, was 4.14Nm (range 4.028 to 4.308Nm). Although there was variation in how quickly the Instron changed from once it reach ±4Nm, the set maximum moment of ±4Nm was taken as the maximum value for assessing axial rotation (deg) and used throughout the thesis data analysis. Variability between specimens is noted, however small standard deviations are recorded when repeatedly testing the same specimen. Similar patterns were found for the NZ.
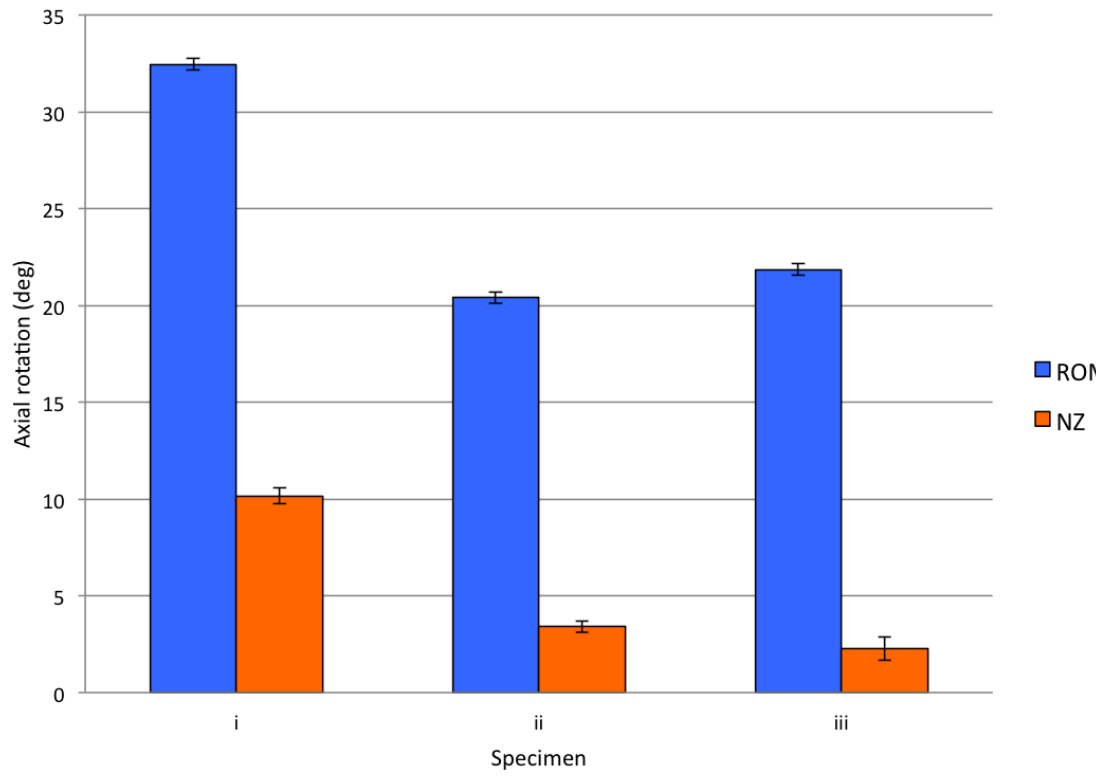
Figure 4.1. Total ROM and NZ size of three un-instrumented MSU porcine spines during the 5th cycle of five repeated test sequences in axial rotation at a constant 8deg.s[-1] tested to a set maximum moment of ±4Nm (±SD).

4.1.2 Repeatability of dual rigid rod testing

The second preliminary study assessed the repeatability of rigid rods (RIGID) in a single specimen. With similar results for the five repeated tests of rigid rods, the moment versus axial rotation curves below only displays one the five dual rigid rod tests (Figure 4.2). The entire study is displayed in the appendix (Appendix 4). In both left and right axial rotation, as shown in Figure 4.3, dual rigid rods resulted in reduced ROM across all tests, left 13.81 ±0.33 deg and right 11.89 ±0.33 deg (mean, ±SD respectively) compared to un-instrumented tests either done pre implant attachment (left 15.32 deg and right 13.33 deg) or post implant removal (left 16.44 and right 13.72 deg) (Figure 4.3). Figure 4.4 represents the stiffness (Nm/deg) of the porcine MSU spine with repeated cycles of dual rigid rods. There was a 5.3% change in Total ROM from the 7th to the 1st un-instrumented tests. Dual rigid rods produced stiffer results in both left and right axial rotation, 0.509 ± 0.003 Nm.deg^{-1} and 0.585 ±0.006 Nm.deg^{-1} respectively.
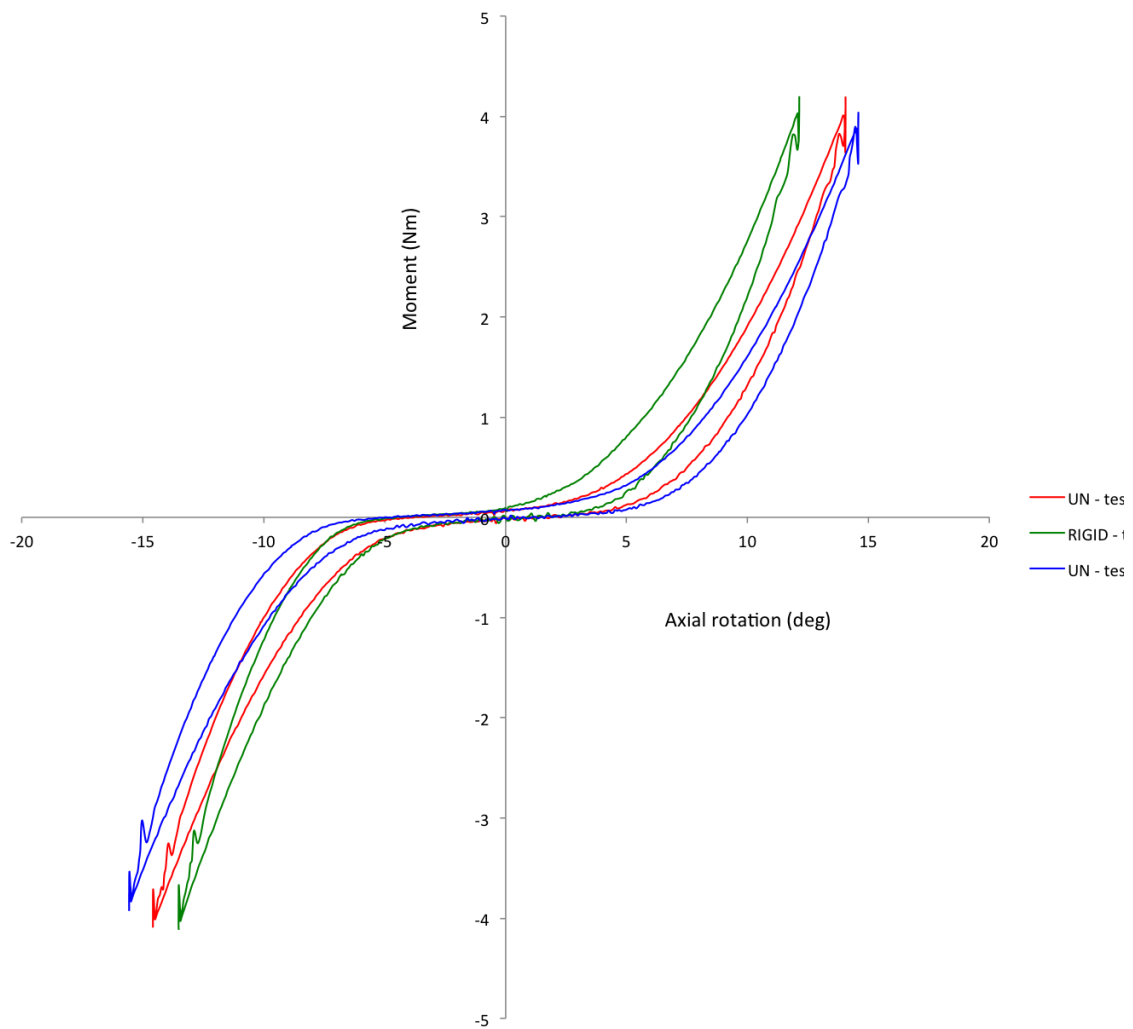
Figure 4.2. Repeated dual rigid rod analysis. The 2nd rigid rod test (test 3) is displayed against the pre and post un-instrumented moment versus axial rotation curves.
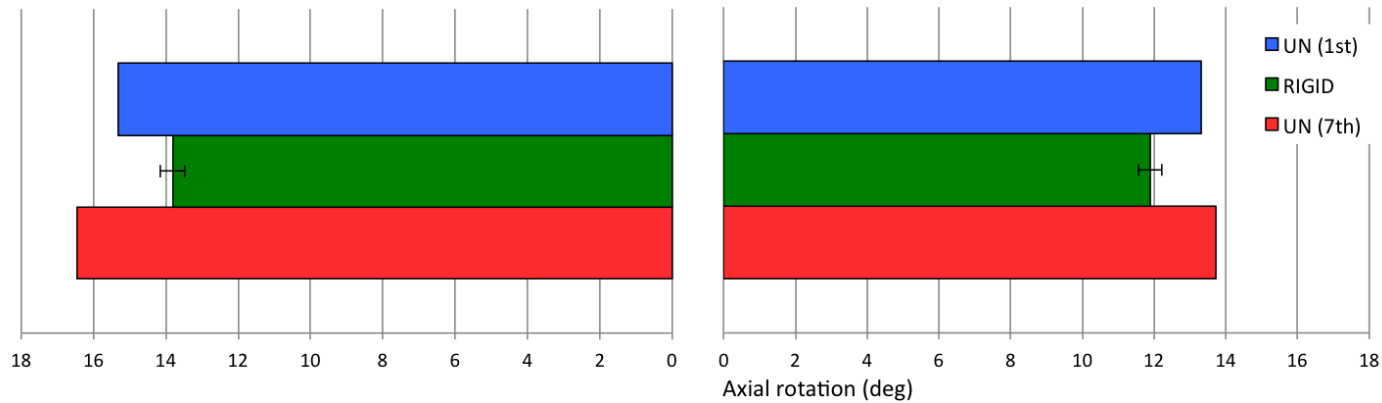
Figure 4.3. Axial rotation (deg) following five repeated tests comprising of five cycles each with dual rigid rods secured at levels 2 and 6 within the 7 level MSU spine, between pre and post un-instrumented tests.
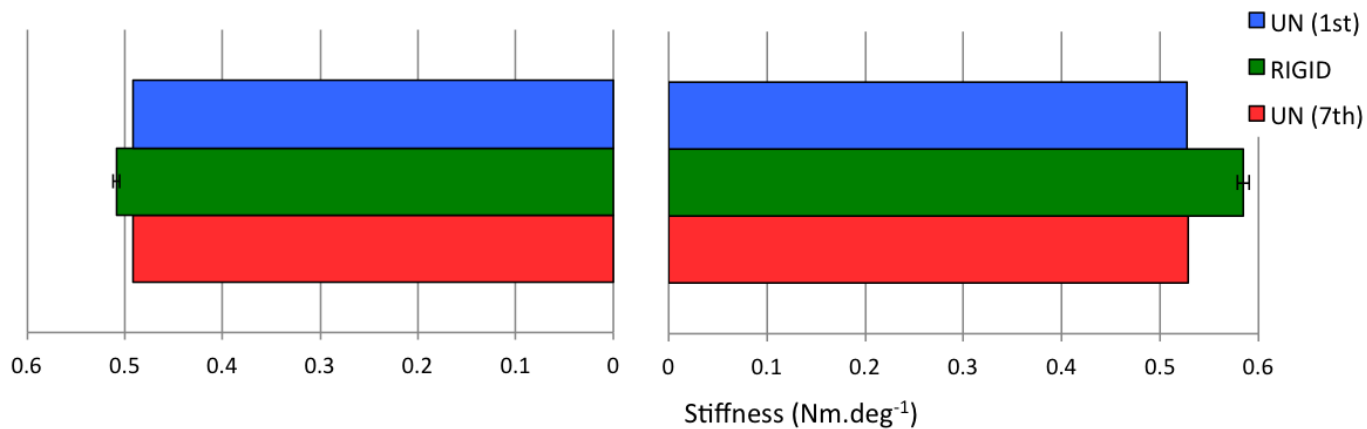
(UN; un-instrumented, RIGID; dual rigid growing rods)

Figure 4.4. Stiffness (Nm.deg^{-1}) recorded following five repeated tests comprising of five cycles each with dual rigid rods secured at levels 2 and 6 within the 7 level MSU spine, between pre and post un-instrumented tests. Left and right axial rotations displayed as left and right graphs.

4.1.3 Dual rod comparison in the biaxial testing machine

The total ROM and NZ size for each of the 6 specimens tested in axial rotation (Table 3.2), with either dual semi-constrained growing rods (GR) tested prior to dual rigid rods or vice-versa are displayed in Figure 4.5. Calculated left and right axial-rotation stiffness, for the six (7-level) specimens, are shown in Figure 4.6. The ROM and stiffness values are for the entire 7-level MSU spine, which contains un-instrumented segments (at level 1 and 7) even when instrumented with the tested rods (which are secured at levels 2 and 6 by multi-axial screws). The maximal change in total ROM differences between test 5 to test 1 (Table 3.2) of un-instrumented testing, was 6.7%.

The largest ROM and NZ was recorded in Specimen 4, however an abnormal moment versus axial rotation curve for semi-constrained growing rods during the third test was obtained (refer to Table 3.2 and Figure 4.7).

Normalising the ROM and stiffness results from each rod (semi-constrained and rigid) against the mean un-instrumented ROM and stiffness values for the same six specimens gave the graphs shown in Figure 4.8 and Figure 4.9 respectively. Paired t-test analysis showed significant differences between the two types of rods tested, irrespective of sequence order. Rigid rods significantly reducing the total ROM compared to semi-constrained growing rods ($p<0.05$) and resulted in a significantly stiffer spine for both left and right axial rotation loading directions ($p<0.05$).

4.1.4 Axial (z-axis) constraining forces during axial rotation loading

As stated in the Methods section during apparatus development for in-vitro spine testing, the z-axis of the Instron testing machine was fixed (constrained) during all tests. The measured loads during un-instrumented testing reached 70N whilst 70N and 110N were recorded during semi-constrained growing rods and rigid rods respectively. As an example the recorded load of Specimen 1 during the first un-instrumented test is displayed in the Appendix (Appendix 5). These values were tensile in nature, meaning that during axial rotation the specimen was trying to contract. Although small there was some asymmetry recorded in load between left and right rotations.
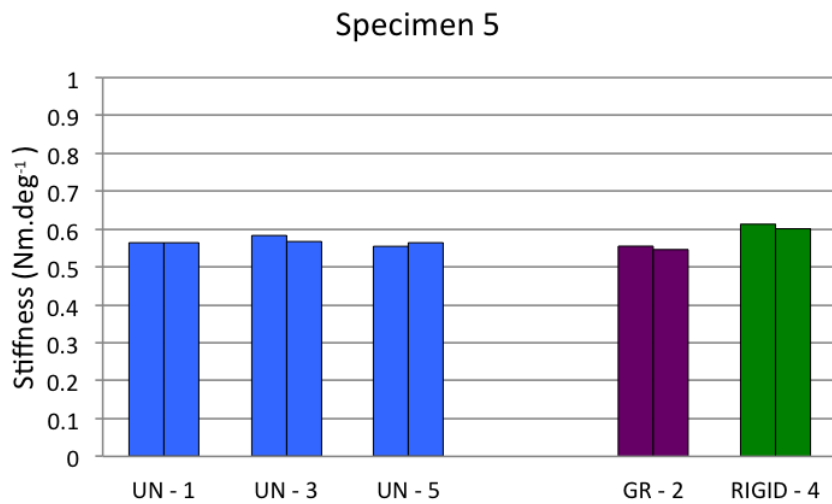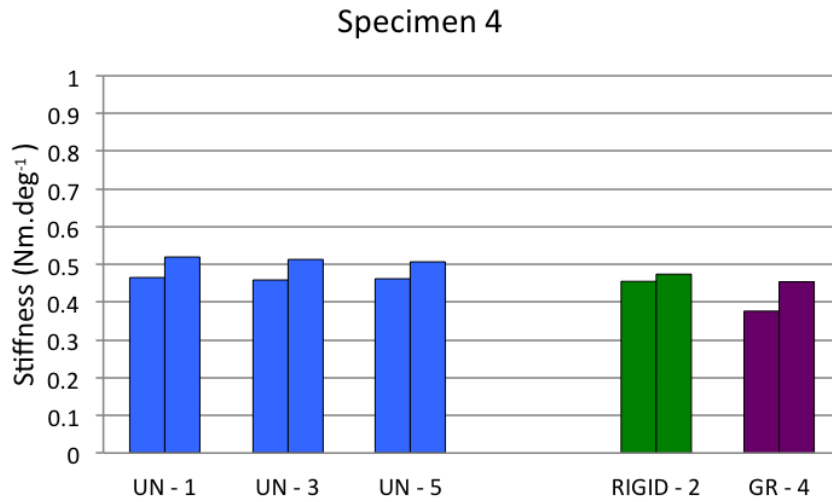
Specimen 1
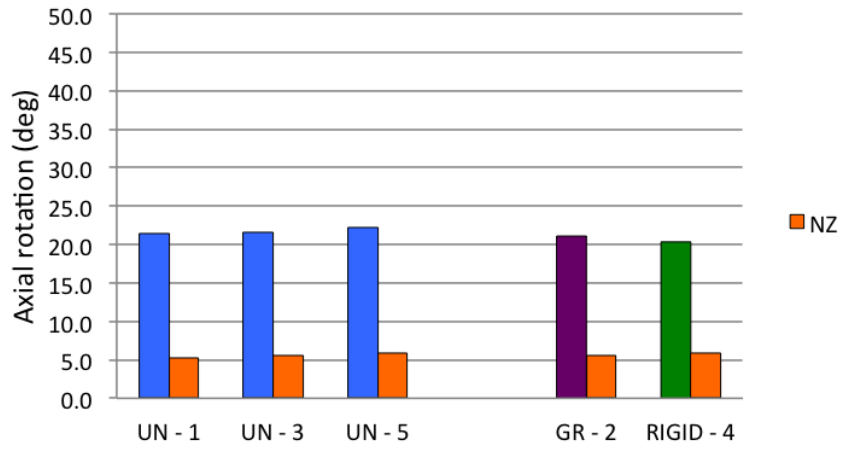
Specimen 2
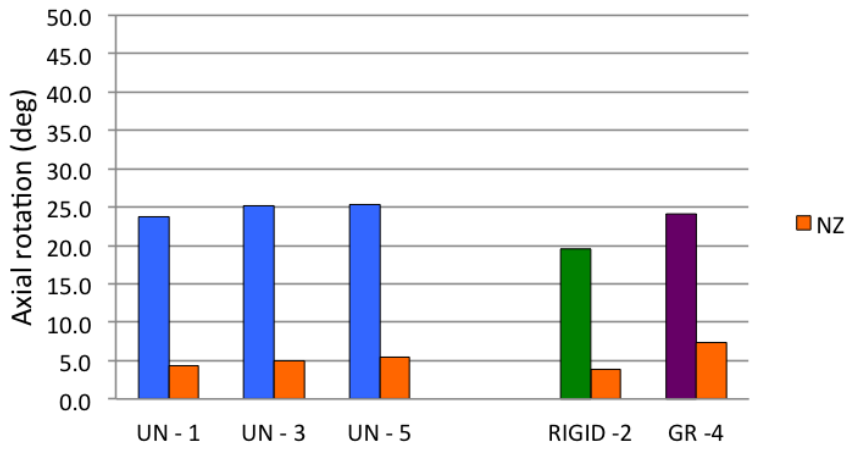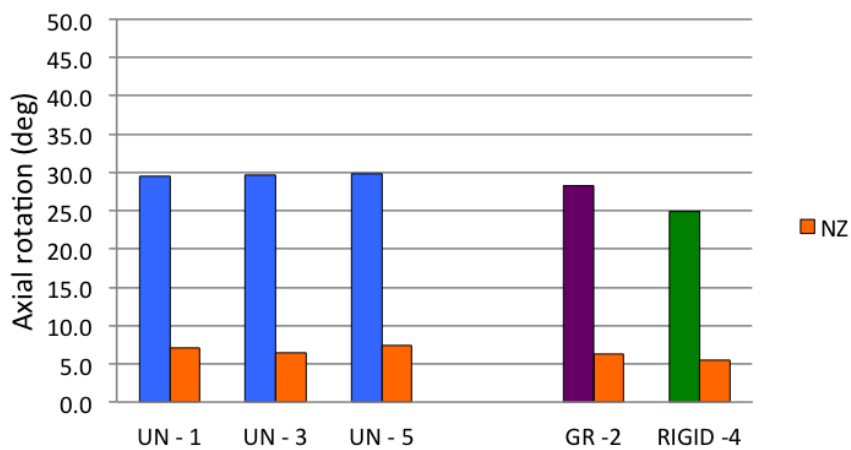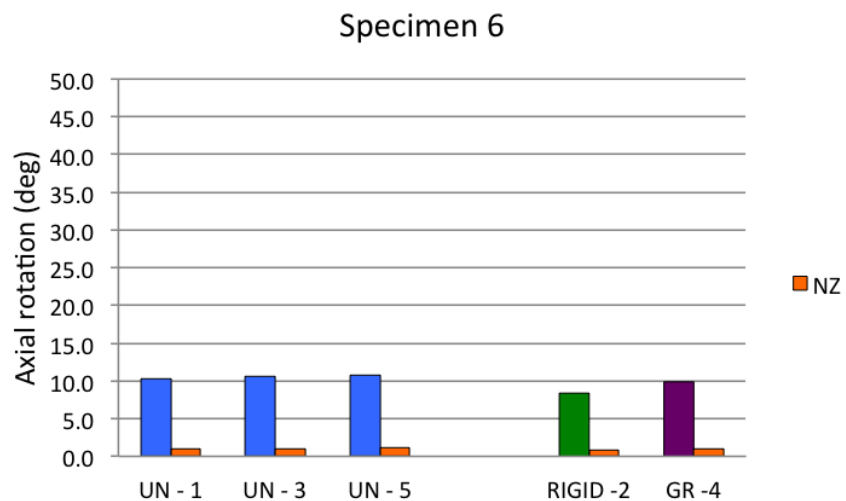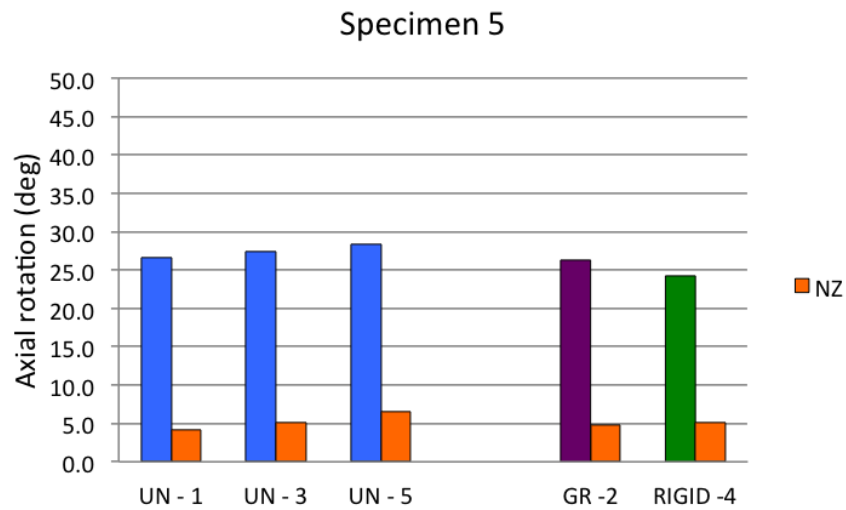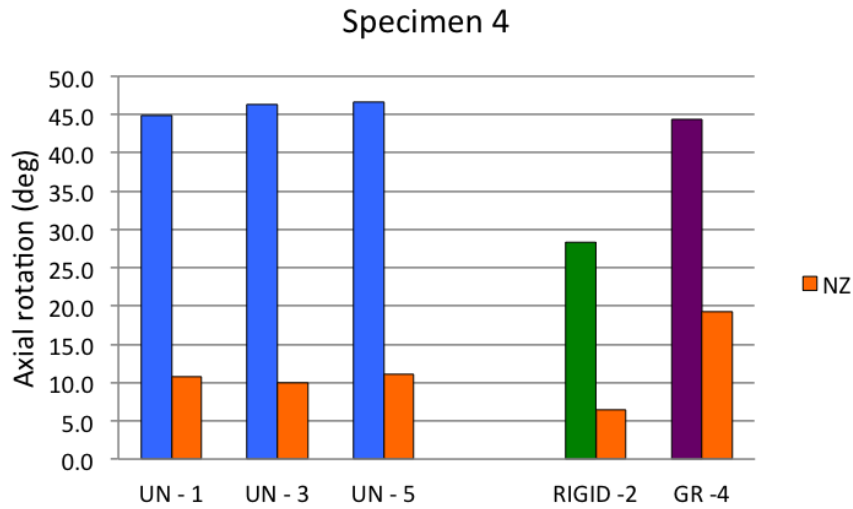
Specimen 3

(UN; un-instrumented, GR; dual semi-constrained & RIGID; dual rigid rods)

Figure 4.5. Total ROM (deg) for each of the 6 specimens tested in axial rotation with 5 minutes rest between tests to allow for relaxation of tissues. Testing protocol as per Table 3.2 and as per numbered labels along the x-axis of each graph. All tests were conducted at 8deg.s^{-1} except Specimen-6 which was tested at 4deg.s^{-1}.

Specimen 1
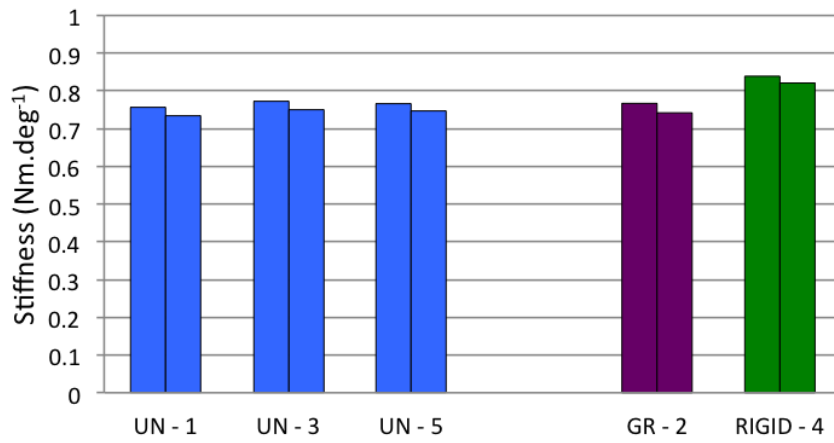
Specimen 2
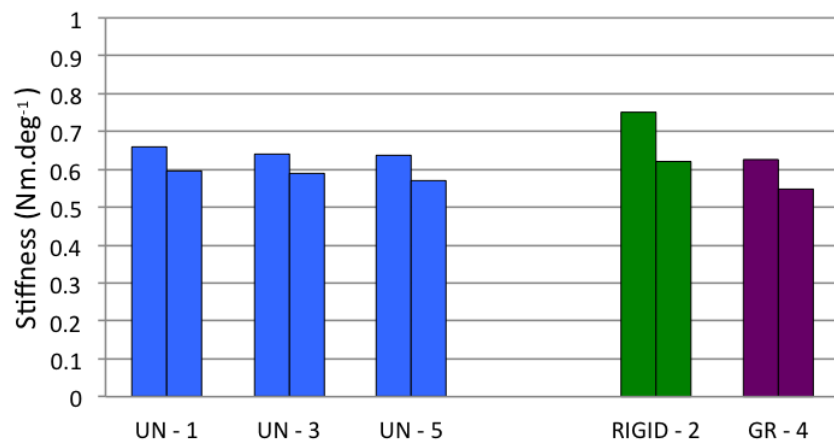
Spercimen 3
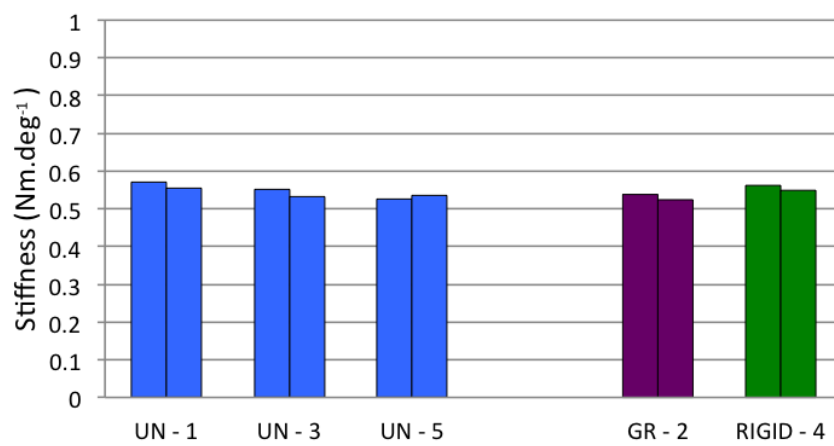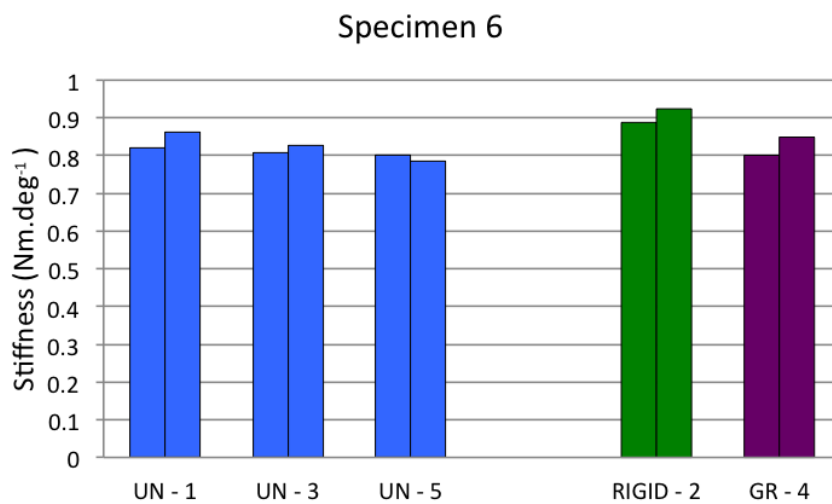
(UN; un-instrumented, GR; dual semi-constrained & RIGID; dual rigid rods)

Figure 4.6. Calculated Stiffness (Nm.deg^{-1}) for each of the 6 Specimens tested as per Table 3.2. Separate Stiffness values for loading to the left and right are displayed in paired columns. All tests were conducted at 8deg.s^{-1} except for Specimen-6, which was tested at 4deg.s^{-1}.
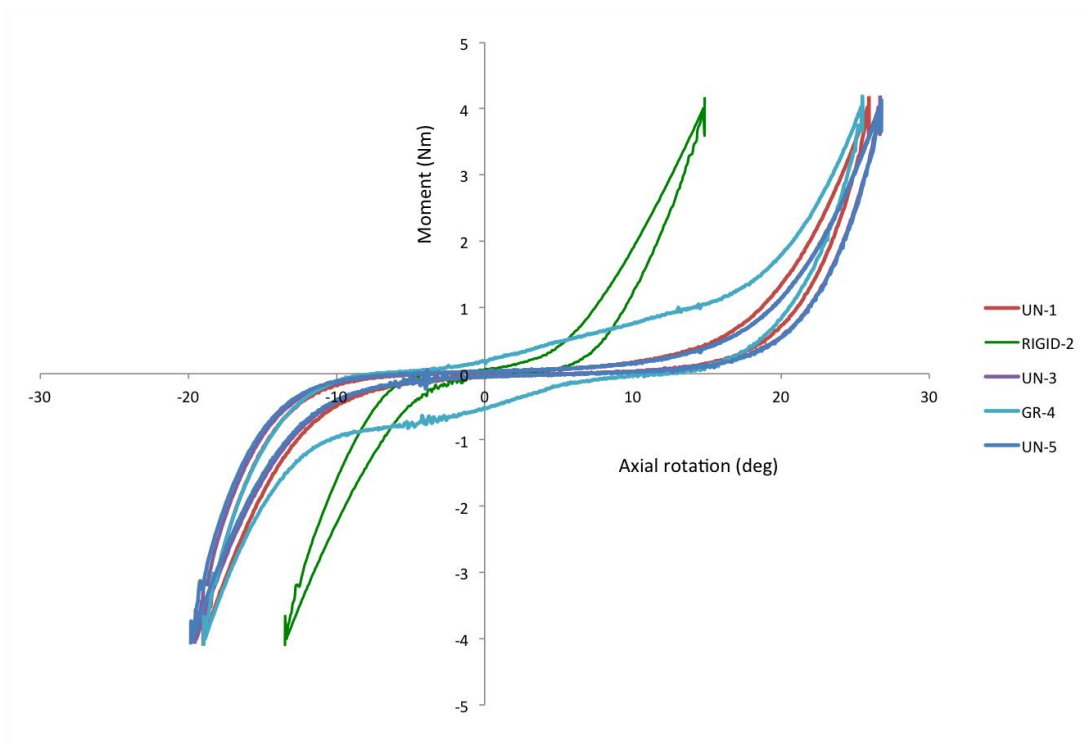
Figure 4.7. Moment versus axial rotation plot for Specimen 4. Dual rigid rods (RIGID) tested prior to dual semi-constrained growing rods (GR) at 8deg.s[st] to the set maximum moment of ±4Nm.
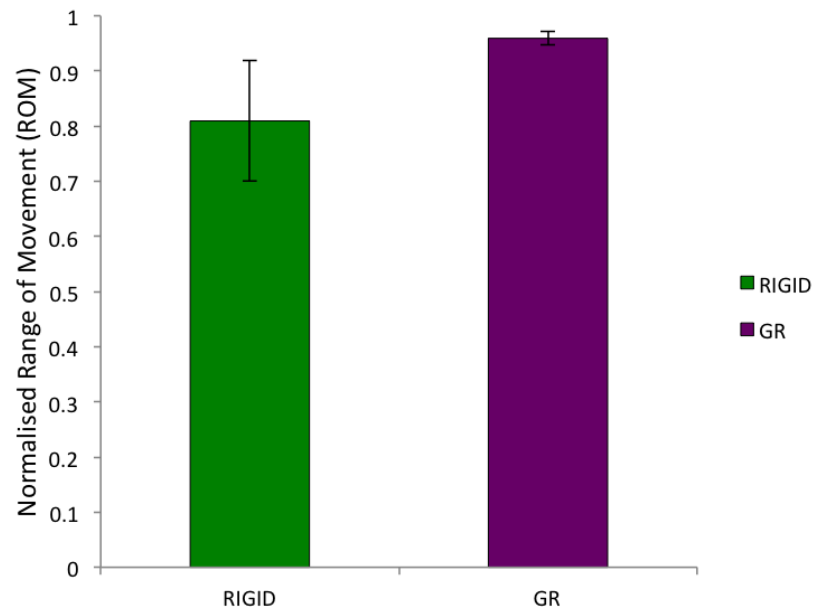
Figure 4.8. The average normalised total ROM for each of the six 7-level specimens during rod testing (±SD difference between specimens) with respect to the averaged un-instrumented ROM for each spine.
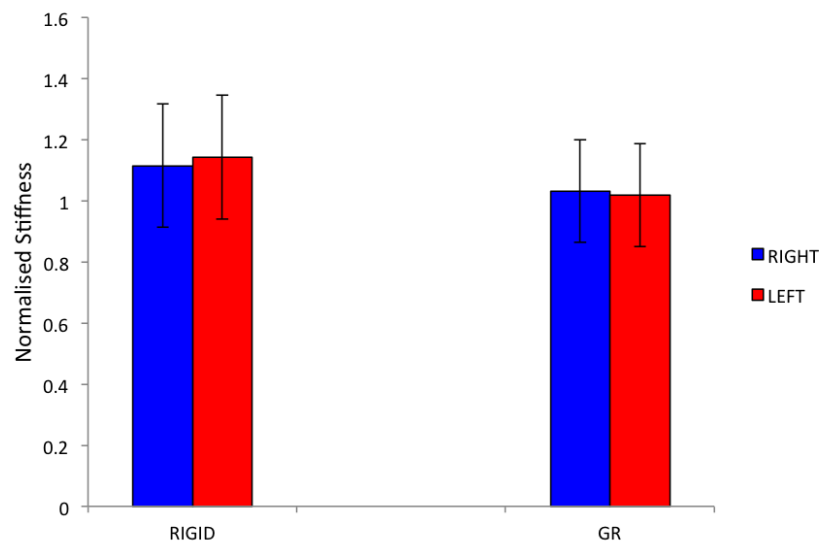

Figure 4.9. The average normalised stiffness for each of the six 7-level specimens with instrumented rods in paired columns during left and right axial rotation (±SD) with respect to the averaged un-instrumented stiffness for each spine.

4.2 Optotrak configuration and analysis of intervertebral rotations

The total ROM of each individual intervertebral joint derived from the Optotrak data is shown in Figure 4.10 below, for Specimen 2. The intervertebral ROMs for all specimens are given in Appendix 6. Between the fixation points (levels 2 and 6) of Specimen 2 displayed below, semi-constrained growing rods was comparable to the un-instrumented testing in the same specimen. Dual rigid rods however, showed reduced intervertebral ROM within the instrumented section compared to both un-instrumented and semi-constrianed growing rod tests.

The Total Intervertebral ROM for each instrumented test sequence was normalised (Appendix 7). As an example Figure 4.11 shows Specimen 2 with dual RIGID rods tested prior to GR rods. The application of RIGID rods compared to GR revealed a 30-50% difference in Total Intervertebral ROM through the instrumented levels of 2-3 through to 5-6. Normalising the Optotrak data from each rod test to the average of the un-instrumented tests is shown in Figure 4.12 with only –ve SD being displayed for clarity.

Within the instrumented levels, rigid rods showed reduced Total Intervertebral ROM compared to semi-constrained growing rods and the un-instrumented test sequences.
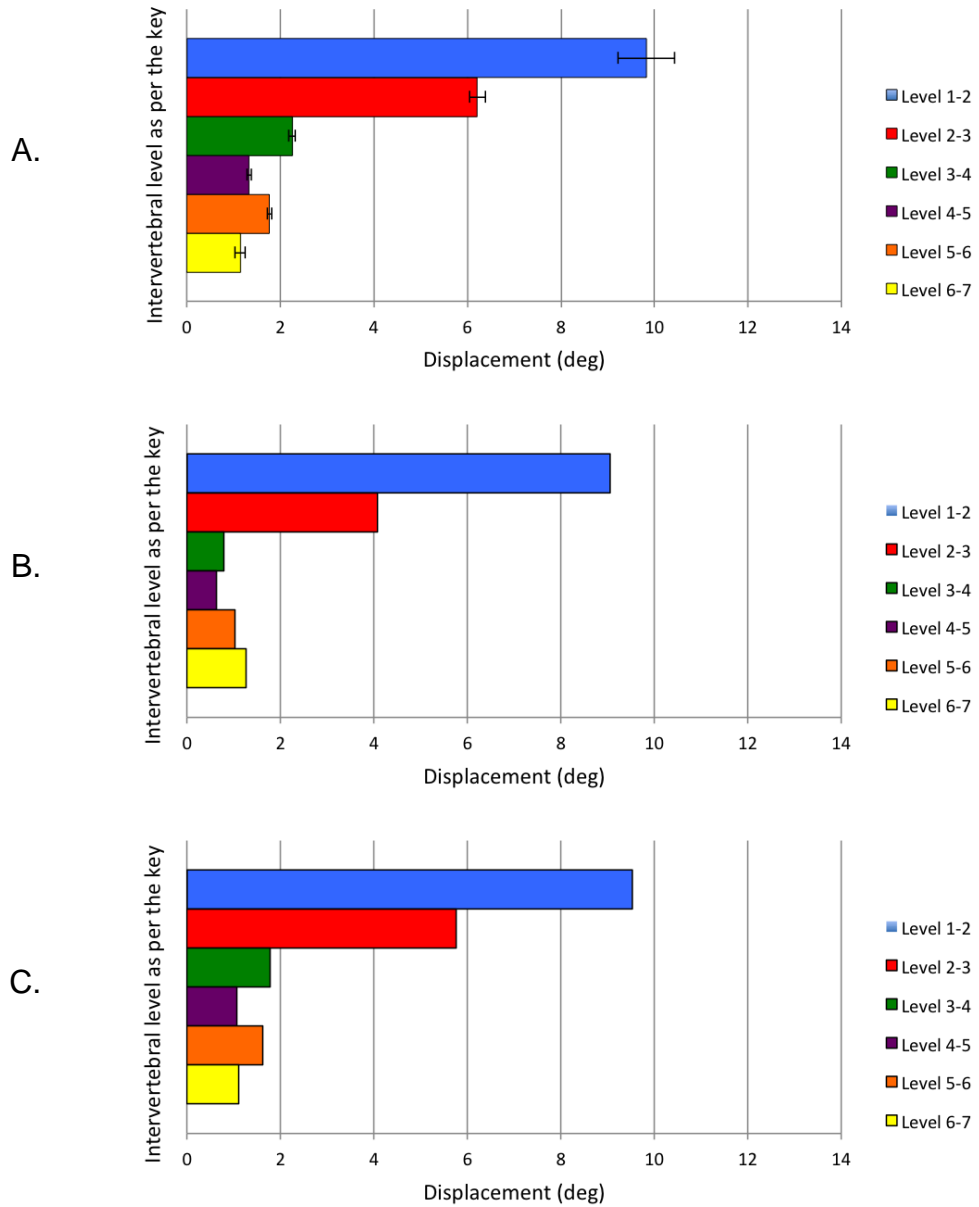
Figure 4.10. Intervertebral ROM from Optotrak data of Specimen 2 during un-instrumented testing A). Average of the three un-instrumented tests (±SD) as per Table 3.2 B). The dual rigid rod test with rods secured at levels 2 and 6 C). Dual semi-constrained rod testing with fixation at level 2 and 6 within the 7 level MSU spine model.
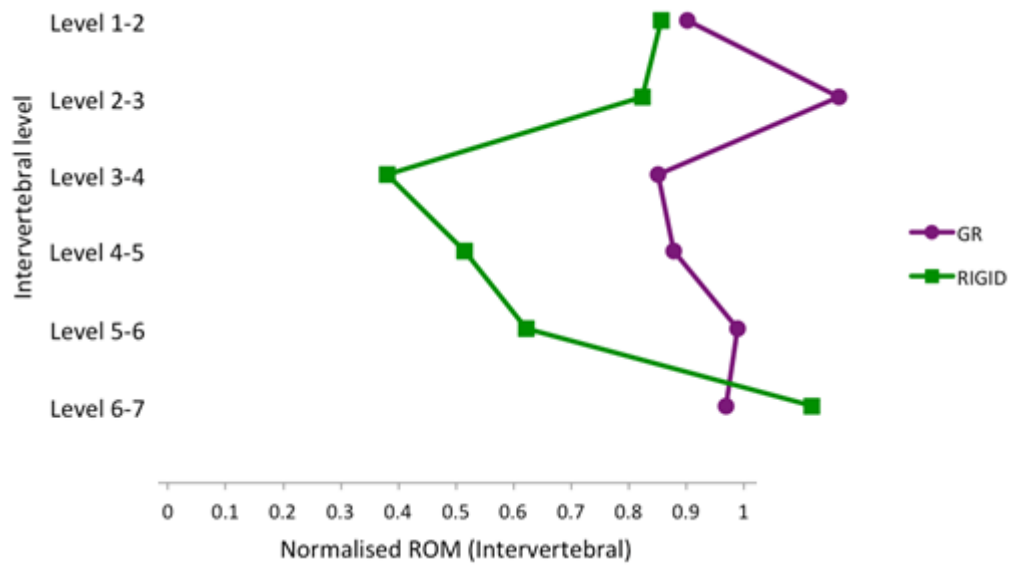
Figure 4.11. Specimen 2 as an example of normalised total intervertebral ROM for each joint for each dual rod test. Each joint was normalised to its un-instrumented response.
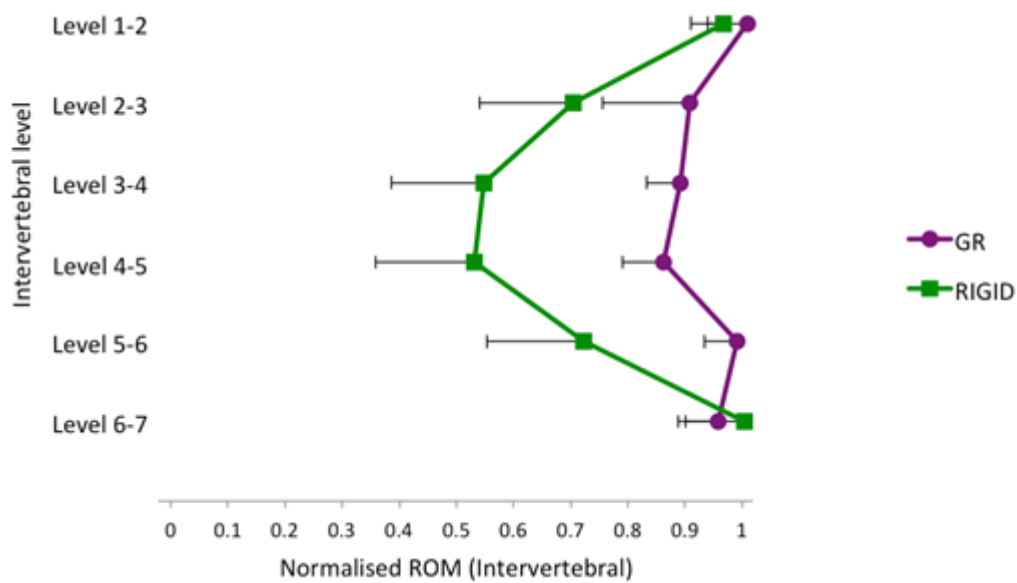

Figure 4.12. Average normalised total intervertebral ROM for each spinal joint for each dual rod. Each joint was normalised to its un-instrumented response. (-ve SD only expressed for clarity).

4.2.1 Differences in total ROM between the Instron and Optotrak data.

The total rotation measured for the Instron axis would be expected to be equal to the sum of the individual intervertebral rotations measured by the Optotrak system. Utilising specimen 2 as an example the averaged un-instrumented total ROM from the Instron data was 24.79 deg (range 23.80 to 25.17 deg), compared to 22.56 deg (range 20.56 to 23.60 deg) form Optotrak total intervertebral ROM (deg) data analysis. This discrepancy is discussed further below.

4.2.2 Relative ROM between semi-constrained growing rod components

The total relative ROM of the semi-constrained growing rod components for each specimen is displayed below in Table 4.1 and graphically in the appendix (Appendix 8). Spines instrumented with dual semi-constrained growing rods recorded within 0.5 degrees of the difference between each specimens level 2 and 6 (fixation levels) total ROM (deg).

Table 4.1. Each specimens Relative ROM (deg) for the growing rod components.

Specimen	Relative ROM (deg)
1	4.95
2	10.75
3	11.39
4	26.8
5	7.76
6	5.48

5 Discussion

The aim of this study was to understand the biomechanics of two different types of rods, which are already being used to manage early onset scoliosis (EOS). In particular this study examined the newer semi-constrained growing rods during axial rotation of the spine in relation to rigid rods.

This multi-segment porcine spine study has shown that semi-constrained growing rods do enable a similar degree of axial rotation to un-instrumented porcine spines under displacement controlled testing, at a constant rate to a set maximum moment of ±4Nm. By allowing almost similar physiological axial rotation to un-instrumented spines, semi-constrained growing rods have the potential to maintain optimal spinal function, aid growth through the telescopic sleeve and assist with improved capacity for curve correction prior to final spinal fusion at maturity. When compared to dual semi-constrained growing rods, rigid rods significantly reduced ROM across all spinal levels and also showed reduced ROM within the instrumented levels. Although correction may be achieved through rigid rod instrumentation, they have been shown in this study to limit function. The principle of distraction based fusionless techniques to manage EOS is to preserve motion and function, aspects that are achieved with the semi-constrained growing rod. The implications of these findings are significant since it is the first biomechanical study investigating semi-constrained growing rods.

Intervertebral rotations obtained through Optotrak analysis

Regardless of test sequence, applying a constant rate to a set maximum moment ensured every level of the seven level construct experienced the same ±4Nm. The study hypothesis was that, dual rigid rods would result in a decrease in ROM of the instrumented levels and therefore an overall decrease in ROM. This was shown to be the case irrespective of test sequence order. Dual rigid rods significantly reduced the total intervertebral ROM across every instrumented level (levels 2-3 down to levels 5-6) with a P < 0.05 compared with semi constrained growing rods. There was no significant difference between un-instrumented MSU testing compared to semi constrained growing rods (Appendix 6). It was hypothesised that dual semi-constrained growing rods would allow an even distribution of rotation across all instrumented levels similar to un-instrumented MSU spines and this was found in the third study. The smallest intervertebral joint ROM was recorded at levels 4-5, independent of test sequence or specimen.

The largest ROM in this study was shown to occur in the middle thoracic compared with the lower thoracolumbar porcine spine segments. This was a similar finding to the study by Busscher et al., [82] despite not testing under the same conditions. This difference however changed in the study by Busscher et al. following removal of posterior support structures with all levels having similar ROM. It highlights the anatomical differences and geometric restrictions that the zygapophysial joints cause to spinal motion in the lower thoracic porcine spine, which is orientated in a more sagittal plane. A vertebral region which has been shown in previous porcine anatomical

measurement studies, to occur in similar orientation to human lumbar vertebrae [78, 84, 85, 94]. Intervertebral rotations from Optotrak data in this study also showed significantly larger values in the superior levels of the MSU construct, which included middle thoracic vertebrae, compared to lower levels of the construct which recorded reduced ROM and included lower thoracic and upper lumbar vertebrae (Figure 5.1, copied from Figure 4.10 on page 83).
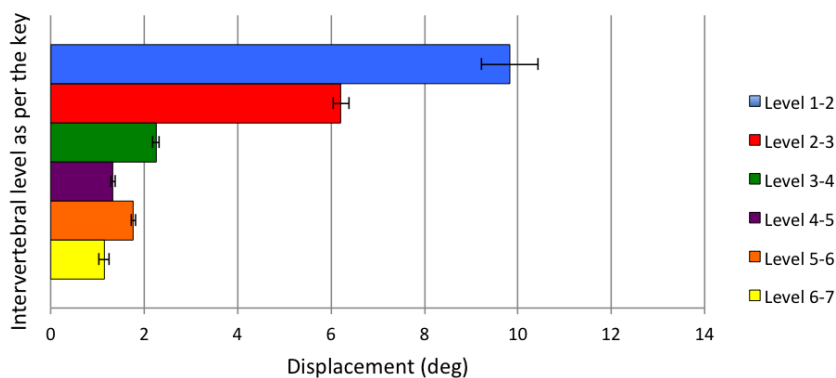

Figure 5.1. Intervertebral ROM from Optotrak data of Specimen 2 during un-instrumented testing A). Average of the three un-instrumented tests (±SD) as per Table 3.2.

Measurement of porcine facet (zygagpophysial) orientation was beyond the scope of this study however observational changes were noted when analysing CT scans of each MSU spine between the middle thoracic porcine vertebrae compared to the lower thoracic levels of the 7 level MSU. Such that middle thoracic vertebrae (upper levels in the chosen MSU spine) were orientated in a more coronal plane, which would account for increased intervertebral rotation calculated through Optotrak analysis.

Utilising Specimen 2 as an example a two and half degree (2.5°) difference between the recorded total ROM from the Instron and total intervertebral ROM from the Optotrak data was calculated across all test sequences. This difference or source of discrepancy could be attributed to cement movement within the mounting cups, loosening of the mounting plate bolts or cement deformation during testing. Although any test apparatus compliance would be very low in a 4Nm study with consistent test protocol as used here, future research could place Optotrak markers on the upper and lower specimen mounting cups so as to assess whether the measured relative rotation angle is equal to the Instron angle.

Biomechanical parameters of two different rod constructs

Comparative biomechanical analysis of the two types of growing rods in the third study indicated that during axial rotation, dual rigid rods consistently exhibited decreased ROM and increased stiffness as hypothesised, when compared to dual semi-constrained growing rods. A statistically significant decrease in total ROM and increase in both left and right axial rotation stiffness was found, when comparing all the tested spines using paired t-test analysis ($p<0.05$) (Figure 5.2, copied from Figure 4.8 and Figure 4.9 on page 81).

A.   B.
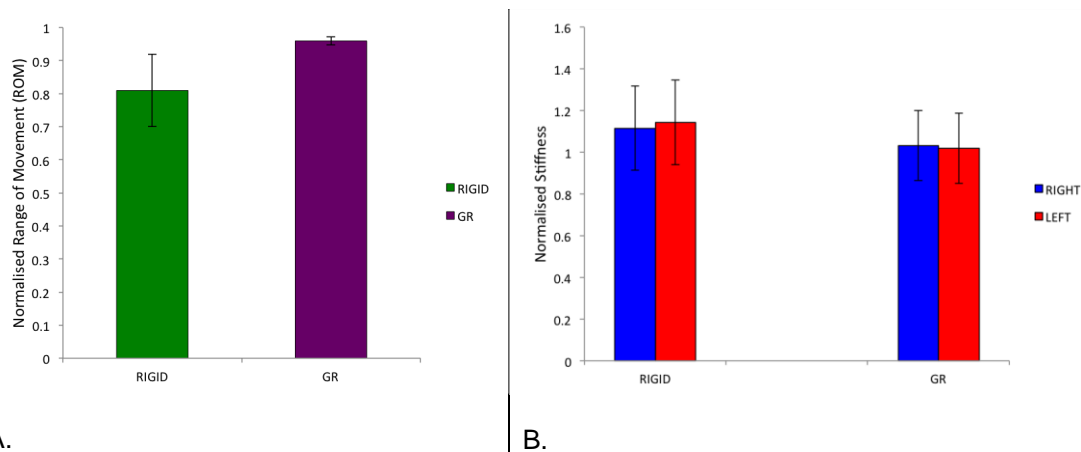
Figure 5.2. Reproduced for easy of reference. The average normalised ROM (A) and stiffness (B) for each of the six 7-level specimens with instrumented rods in paired columns during left and right axial rotation (±SD), with respect to the averaged un-instrumented stiffness for each spine.

Through repeated sequence testing the difference in total ROM from the last to the first un-instrumented test (refer to Table 3.2) averaged 4.5%, with the largest change being 6.7%. Although well within acceptable limits, this change was not shown in the first preliminary study for repeated un-instrumented spine testing. It is however similar to the specimen changes in the second preliminary study or repeated rigid rod study which showed a 5% increase in total ROM between the last and first tests (un-instrumented testing, Figure 4.3, test 7 compared to test 1), which could be attributable to repeated specimen cycling and tissue property changes, although this was not a statistically significant change.

An interesting moment versus axial rotation curve was plotted during the semi-constrained growing rod test from specimen 4 (Figure 4.7). This specimen recorded the largest ROM for all tests compared to the other five specimens and a significantly larger and abnormal NZ during GR testing, indicating that the spinal segments were more flexible. A larger NZ has been

a sensitive indicator for spinal instability and injury [108, 125]. However, because consistent results were recorded during un-instrumented testing of the same specimen, instability of the specimen is unlikely (Figure 5.3 copied from Figure 4.7 on page 80 and Figure 4.5 on page 77).
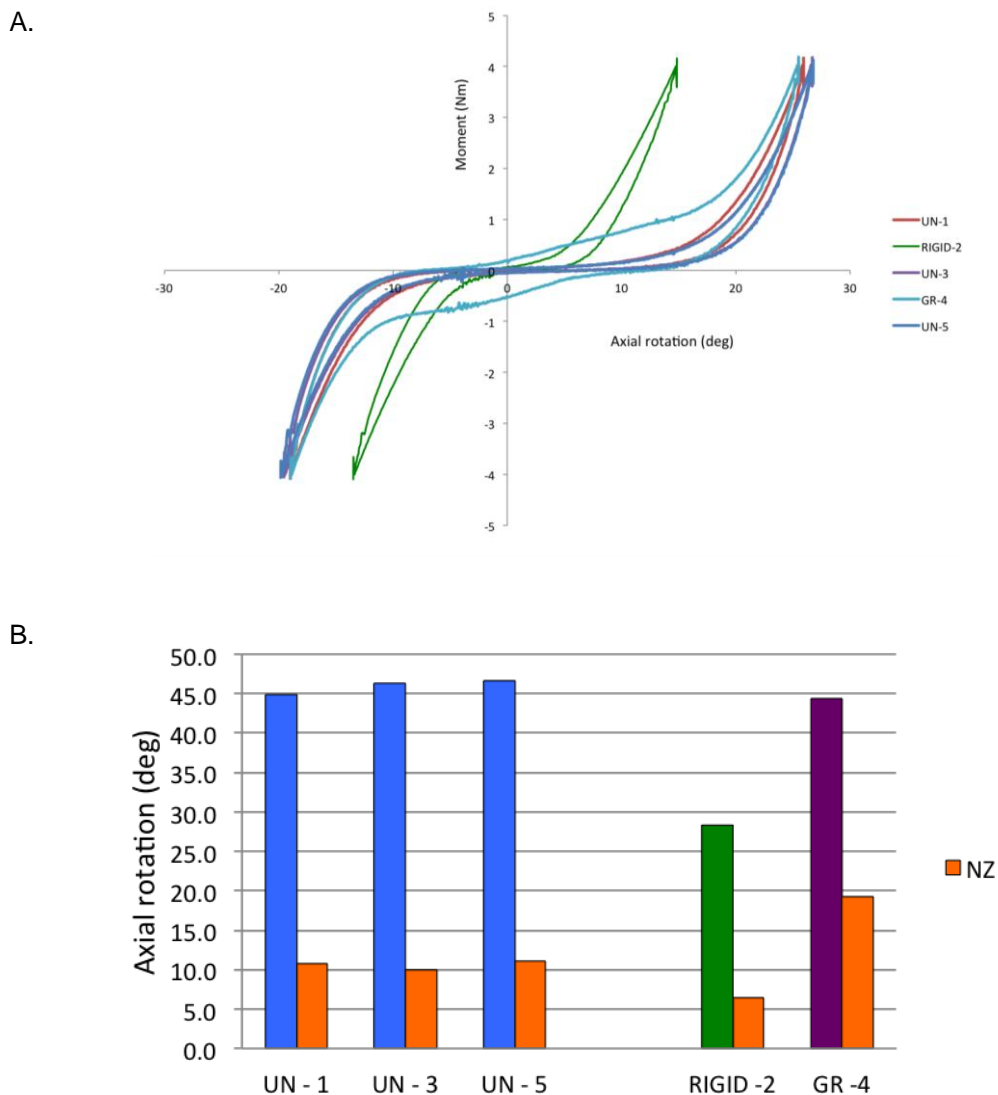
A.

B.

Figure 5.3. A) Moment versus axial rotation plot for Specimen 4. Abnormal semi-constrained growing rod curve with widened NZ. B) Total ROM (deg) and NZ size (deg) for Specimen 4. Tests were conducted at 8deg.sst to the set maximum moment of ±4Nm, in order as per Table 3.2 and x-axis labels/key.

One possible explanation is debris within the telescopic sleeve of the semi-constrained growing rod, causing friction. On inspection post testing there was no obvious wear debris within or on the sleeve component. However wear debris and metallosis from the titanium alloy components is commonly noted visually at growing rod lengthenings and final fusion surgeries. This finding has recently been addressed with changes to the rod coatings, which now contain a polymer sleeve instead of metal on metal bearing surfaces, as in the tested semi-constrained growing rods in this study.

Apparatus development for in-vitro spine testing

Previous animal studies have applied a range of set maximum moments of between 2 to 5Nm [82, 95, 126], in order to analyse porcine spinal biomechanics. A set maximum moment of ±4Nm was applied to the porcine model at a constant rate of axial rotation, as pilot studies showed this to be an appropriate moment to avoid damaging vertebral segments. Damage to higher thoracic segments of the MSU model was noted in early pilot studies when loaded with more than 5Nm over repeated cycles. This current thesis achieved similar physiological ranges of axial rotation, to that found by Busscher et al. [82], without damaging the porcine segment, in the mid to lower thoracic levels. Although double the set maximum moment to that of the work by Busscher et al., moments below 4Nm were found to not reach the same physiological ranges of motion.

Each specimen experienced a constant rate of rotation about the primary axis to a set maximum moment. The overall rotation rate was applied to a seven level construct, which was shared between all segments. This aspect of constrained (constant rotation rate) testing is not well documented in the published literature, with studies by Hongo et al., [95] and Lysack et al., [107] being the only two which clearly outline the strain rate used during spinal biomechanics testing. Unlike linearly ramped moment testing, constrained or constant rate testing, allows the consistent application of rotation to a set maximum moment. Whilst preventing changes in rotation speed during the test so as to avoid rate-induced discrepancies in stiffness measurements.

There are numerous studies, which have used spine models to investigate spinal biomechanics however, only a few studies were found which investigate thoracic levels specifically. They include human cadaveric [108, 127], calf [110], sheep [97], and porcine [82, 126, 128] studies. However research by Busscher et al. [82] was the only study found to investigate multi-segments utilising a porcine model. Through moment controlled testing of a four level MSU spine, Busscher et al. [82] drew conclusions that the mid to lower thoracic porcine spine is a representative model of the human thoracolumbar spine with regard to biomechanical spine testing. These findings directed the choice of using mid to lower thoracic porcine vertebrae, particularly since the thoracic region is commonly instrumented during EOS surgery. The choice of specimen length and number of vertebral levels depends on the experimental question being asked or implants being investigated. There is gathering consensus regarding the use of multi-segment spine units for

testing of implants which include at least one free functional spinal unit on either side of the construct length, enabling evaluation of spinal devices without apparatus constraint [76, 109]. In this study, a seven level MSU porcine spine model was found to be the most appropriate size for analysing the modified semi-constrained growing rods.

The initial two preliminary studies determined the consistency and repeatability of testing a multi-segment unit (MSU) porcine spine model under displacement controlled testing at a constant rotation rate. This was through commonly used biomechanical terms and parameters including; range of motion, neutral zone and stiffness. These properties were characteristically similar during test-retest for the three un-instrumented spines analysed in the first preliminary study as denoted by small SD's (Figure 4.1) for both the total ROM and NZ. Differences however, exist with all biological tissues and the first preliminary study displays this with inter-specimen variability (Figure 4.1). This is an aspect that can't be controlled for, but with similar intra-specimen results across several biomechanical parameters, support for test-retest of specimens is further substantiated. The second preliminary single MSU porcine study adds further weight to supporting the test-retest of specimens with highly reproducible characteristic moment versus axial rotation curves being obtained in (Appendix 4).

Lowering the constant rotational rate from 10 to $8deg.s^{-1}$ (a necessary requirement so that the Instron could capture data), did not alter the stiffness for the first un-instrumented specimen (Appendix 2), nor change the other

biomechanical parameters significantly. Despite re-thawing for a third time only a small 7.5% change in total ROM was recorded during repeated testing which was not statistically significant. This difference may be attributed to the time dependence of the tissues during axial rotation, although a 5-minute wait period between testing was used to allow for viscoelastic recovery. Single freeze-thaw tests of porcine spines have shown changes with intervertebral motion parameters [129, 130], particularly the neutral zone (NZ) and NZ slope, however all tests conducted in this study underwent two freeze-thaw procedures prior to testing. The small change in motion parameters in this study further supports the freeze-thaw research by Hongo et al., whereby stable biomechanical results were obtained following less than three but greater than one freeze-thaw cycle [95].

Holding the z-axis (position) during testing was decided during Instron protocol formulation. The largest average compressive z-axis load was during rigid rod testing, with a magnitude of 110N being recorded. The MSU spine specimen contracted under axial rotation testing, generating a tensile axial load (Appendix 5). With consistent repeatable results, throughout each of the three studies, it can be assumed that no recorded structural damage occurred during axial rotation testing with a fixed z-axis.

There is a lack of supporting literature in the reporting of error during biomechanical testing. A small calculated stiffness error (±0.002Nm.deg^{-1}) reflects consistency in the study results and allows closer interpretation of rod constructs. The Optotrak has previously been shown to have only a small

resolution error of ±0.1mm [131], delivering precise and repeatable results during real time acquisition.

Study limitations and future research -

The Instron and Optotrak data was not synchronised during testing because software was run on two separate computers. The data obtained was sufficient to answer the questions posed in the hypotheses of the study. Future research could analyse the moments at each vertebral level with respect to intervertebral rotations, by aligning the time delay in the Optotrak file with the peaks and troughs of loading in the Instron data, which is available and stored separately on the QUT database for data storage. Every test sequence initially started with a hold period at zero torque creating a reference for the two measurement files. Through linear regression in MATLAB the differing number of obtained data points could be interpolated and examined. This would enable the current data to be further analysed and lead to further understanding of spinal biomechanics particularly the effect of instrumenting across multiple segments.

This study focused on axial rotation as the plane of motion to be analysed. Future studies could investigate the other planes of motion, which was beyond the scope of this study.

6 Conclusion

This low cycle multi-segment porcine spine study has been the first biomechanical study to investigate the newer semi-constrained growing rod. The study showed that when instrumented with semi-constrained growing rods spines were shown to have a similar axial rotation response to that when un-instrumented. This is significant as it supports the concept of fusionless scoliosis surgery, where by spinal motion and function are maintained whilst correcting spinal deformity in EOS. The data shows that instrumentation with dual rigid rods significantly reduced ROM across all instrumented levels. This study has added to the already building literature regarding fusionless scoliosis surgery for managing EOS.

7 References

1.   Shaw M, Adam C, Izatt M, Licina P and Askin G. Use of iPhone for Cobb angle measurement in scoliosis. *European Spine Journal.* 2012; 21 (6): 1062-8.
2.   Mehta M. The Rib-Vertebra Angle in the early diagnosis between resolving and progressive Infantile Scoliosi. *Journal of Bone and Joint Surgery Br.* 1972; 2: 230-43.
3.   Roaf R. The basic anatomy of scoliosis. *The Journal of Bone and Joint Surgery.* 1966; 48: 786-92.
4.   Dickson R, Lawton J and Archer I. The pathogenesis of idiopathic scoliosis: biplanar spinal asymmetry. *The Journal of Bone and Joint Surgery.* 1984; 66: 1151-4.
5.   Deacon P, Archer I and Dickson R. The anatomy of spinal deformity: a biomechanical analysis. *Orthopaedics.* 1987; 10: 897-903.
6.   Ponseti I and Friedman B. Prognosis in Idiopathic Scoliosis. *The Journal of Bone and Joint Surgery.* 1950; 32: 381-95.
7.   Scoliosis Research Society Terminology Committee: A glossary of scoliosis terms. *Spine.* 1976; 1: 57-8.
8.   Dimeglio AMD. Growth in Pediatric Orthopaedics. *Journal of Pediatric Orthopaedics.* 2001; 21: 549-55.
9.   Dickson R. Conservative treatment for idiopathic scoliosis. *The Journal of Bone and Joint Surgery.* 1985; 67: 176-81.
10.   Moe J and Kettleson D. Idiopathic scoliosis. Analysis of curve patterns and preliminary results of Milwaukee-brace treatment in one hundred sixty-nine patients. *The Journal of Bone and Joint Surgery.* 1970; 52: 1509-33.
11.   Riseborough E and Wynne-Davies R. A genetic survey of idiopathic scoliosis in Boston, Massachusetts. *The Journal of Bone and Joint Surgery.* 1973; 55: 974-82.
12.   Robinson C and McMaster M. Juvenile idiopathic scoliosis. Curve patterns and prognosis in one hundred and nine patients. *The Journal of Bone and Joint Surgery Am.* 1996; 78: 1140-8.
13.   Sanders J, Khoury J, Kishan S, et al. Predicting scoliosis progression from skeletal maturity: a simplified classification during adolescence. *The Journal of Bone and Joint Surgery.* 2008; 90: 540-53.
14.   Brooks H, Azen S and Gerberg E. Scoliosis: A prospective epidemiological study. *The Journal of Bone and Joint Surgery.* 1975; 57: 968-72.
15.   Ascani E, Bartolozzi P, Logroscino C, et al. Natural history of untreated idiopathic scoliosis after skeletal maturity. *Spine.* 1986; 11: 784-9.
16.   Campbell R, Smith M, Mayers T, et al. The characteristics of thoracic insufficiency syndrome associated with fused ribs and congenital scoliosis. *The Journal of Bone and Joint Surgery.* 2003; 85-A: 399-408.
17.   Karol L, Johnston C and Mladenov K. Pulmonary function following early thoracic fusion in non-neuromuscular scoliosis *The Journal of Bone and Joint Surgery.* 2008; 90: 1272-81.
18.   Lonstein J, Bradford D and R W. *Moe's Textbook of Scoliosis and Other Spinal Deformities.* 3rd ed. Philadelphia: PA: Saunders, 1995.

19.   Klemme W, Denis F, Winter R, Lonstein J and Koop S. Spinal instrumentation without fusion for progressive scoliosis in young children. *Journal of Paediatric Orthopaedics*. 1997; 17: 734-42.

20.   Katsaris G, Loukos A and Valavanis J. The immediate effect of a Boston brace on lung volumes and pulmonary compliance in mild adolescent idiopathic scoliosis. *The European Spine Journal*. 1999; 8: 2-7.

21.   Figueriedo U and James I. Juvenile idiopathic scoliosis. *The Journal of Bone and Joint Surgery*. 1981; 63: 61-9.

22.   Allington N and Bowen J. Adolescent idiopathic scoliosis: treatment with the wilington brace. A comparison of full-time and part-time use. *The Journal of Bone and Joint Surgery*. 1996; 78: 1056-62.

23.   Rowe D, Bernstein S, Riddick M, Adler F, Emans J and Gardner-Bonneau D. A meta-analysis of ther efficacy of non-operative treatments for idiopathic scoliosis. *The Journal of Bone and Joint Surgery*. 1997; 79: 664-74.

24.   Karol L. Effectiveness of bracing in male patients with idiopathic scoliosis. *Spine*. 2001; 26: 2001-5.

25.   Jarvis J, Garbedian S and Swany G. Juvenile idiopathic scoliosis: The effectiveness of part time bracing. *Spine*. 2008; 33: 1074-8.

26.   Nonan K, Dolan L, Jacobson W and Weinstein S. Long-term psychosocial characteristics of patients treated for idiopathic scoliosis. *Journal of Paediatric Orthopaedics*. 1997; 17: 712-7.

27.   Matsunaga S, Hayashi K and Naruo T. Psychological management of brace therapy for patients wit hidiopathic scoliossis. *Spine*. 2005; 30: 547-50.

28.   Deceuninck J and Bernard J. Quality of life and idiopathic scoliosis treated by brace. Transversal study. *Scoliosis*. 2010; 5 (Suppl 1): O38.

29.   Acaroglu E, Yazici M, Alanay A and Surat A. Three-Dimensional Evolution of Scoliotic Curve During Instrumentation Without Fusion in Young Children. *Journal of Pediatric Orthopaedics*. 2002; 22: 492-6.

30.   Goldberg C, Moore D and EF F. Long-term results from in situ fusion for congenital vertebral defomrity. *Spine*. 2002; 27: 619-28.

31.   Akbarnia B and Emans J. Complicatioons of growth-sparing surgery in early onset scoliosis. *Spine*. 2010; 35: 2193-204.

32.   Yazici M and Olgun Z. Growing rod concpets: state of the art. *European Spine Journal*. 2012.

33.   Kesling K and Reinker K. Scoliosis in twins: A meta-analysis of literature and report of six cases. *Spine*. 1997; 22: 2009-15.

34.   Inoue M, Minami S and Kitahara H. Idiopathic scoliosis in twins stduied by DNA fingerprinting: The incidence and tyoe of scoliosis. *The Journal of Bone and Joint Surgery*. 1998; 80: 212-7.

35.   Machida M, Dubousset J and Y I. Role of melatonin deficiency in the development of scoliosis in pinealectomised chickens. *The Journal of bone and joint surgery American volume*. 1995; 77: 134-8.

36.   Machida M, Dubousset J and Imamura Y. A possible role in pathogenesis of adolescent idiopathic scoliosis. *Spine*. 1996; 21: 1147-52.

37.   Bagnall K, Raso V and Hill D. Melatonin levels in idiopathic scoliosis: Diurnal and nocturnal serum melatonin levels in girls with adolescent scoliosis. *Spine*. 1996; 21: 1974-8.

38.   Lonstein J and Carlson J. The prediction of curve progression in untreated idiopathic scoliosis during growth. *The Journal of Bone and Joint Surgery*. 1984; 66: 1061-71.

39.   Cheung C, Lee W, Kit Tse Y, et al. Abnormal peri-pubertal anthropometric measurements and growth pattersn in adolescent idiopathic scoliosis: A study of 598 patients. *Spine*. 2003; 28: 2152-7.

40.   Arkin A and Katz J. The effects of pressure on epiphyseal growth; the mechanism of plasticity of gorwing bone. *The Journal of Bone and Joint Surgery*. 1956; 38: 1056-76.

41.   Stokes I, Aronsson D and Urban J. Biomechanical factors influencing progression of angular skeletal deformities during growth. *European Journal of Experimental Muscuuloskeletal research*. 1994; 3: 51-60.

42.   Mente P, Stokes I and Spence H. Progression of vertebral wedging in an asymmetrical loaded rat tail model. *Spine*. 1997; 22: 1292-6.

43.   Stokes I and Labile J. Three-dimensional osseo-ligamentous model of the thorax representing initiation of scoliosis by asymmetric growth. *Journal of Biomechanics*. 1990; 23: 589-95.

44.   Millner P and Dickson R. Idiopathic scoliosis: Biomechanics and biology. *European Spine Journal*. 1996; 5: 362-73.

45.   Stokes I, Spence H, Aronsson D and Kilmer N. Mechanical modulation of vertebral body growth: Implications for scoliosis progression. *Spine*. 1996; 21: 1162-7.

46.   Maguire J, Madigan R and Wallace S. Intraoperative long latency reflex activity in idiopathic scoliosis demonstrates abnormal central processing. A possible cause of idiopathic scoliosis. *Spine*. 1993; 18: 1621-6.

47.   Samuelsson L and Lindell D. Scoliosis as the first sign of a cystic spinal cord lesion. *European Spine Journal*. 1995; 4: 284-90.

48.   Barrack R, Wyatt M and Whitecloud T. Vibratory hypersensitivity in idiopathic scoliosis. *Journal of Paediatric Orthopaedics*. 1988; 8: 389-95.

49.   Beaulieu M, Toulotte C and Gatto L. Postural imbalance in non-treated adolescent idiopathic scoliosis at different periods of progression. *European Spine Journal*. 2008; 18: 38-44.

50.   Lao M, Chow D, Guo X, Cheng J and Holmes A. Impaired dynamic balance control in adolescents with idiopathic scoliosis and abnormal somatosensory evoked potentials. *Journal of Paediatric Orthopaedics*. 2008; 28: 846-9.

51.   Sahlstrand T and Petruson B. Vestibulospinal reflex activity in patients with adolescent idiopathic scoliosis: Postural effects during caloric labyrinthine stimulation recorded by stabilometry. *Acta orthopaedica Scandinavica*. 1979; 50.

52.   Harrington PR. Treatment of scoliosis. Correct and internal fixation by spine instrumentation. *Journal of Bone and Joint Surgery Am*. 1962; 44: 591-610.

53.   Marchetti P and Faldini A. "End fusion" in the treatment of some progressing or severe scoliosis in childhood or early adolescence. *Orthopaedic Transactions*. 1978; 2: 271.

54.   Moe J, Kharrat K, Winter R and Cummine J. Harrington Instrumentation Without Fusion Plus External Orthotic Support for the treatment of Difficult Curvature Problems in Young Children. *Clinical Orthopaedics & Related Research May*. 1984; 185: 35-45.

55.   Mineiro J and Weinstein S. Subcutaneous rodding for progressive spinal curvatures: early results. *Journal of Paediatric Orthopaedics*. 2002; 22: 290-5.

56.   Bess S, Akbarnia BA, Thompson AG, et al. Complications of growing rod treatment for early onset scoliosis. *The Journal of Bone and Joint Surgery*. 2010; 92: 2533-43.

57.   Akbarnia B, Marks D, Boachie-Adjei O, Thompson A and Asher M. Dual Growing Rod Technique for the Treatment of Progressive Early-Onset Scoliosis: A Multicenter Study. *Spine*. 2005; 30(17S): S46-S57.

58.   Akbarnia BA, Breakwell LM, Marks DS, et al. Dual Growing Rod Technique Followed for Three to Eleven Years Until Final Fusion: The Effect of Frequency of Lengthening. *Spine April*. 2008; 33: 984-90.

59.   Thompson G, Akbarnia B, Kostial P, et al. Comparison of single and dual growing rod techniques followed through definitive surgery. *Spine*. 2005; 30: 2039-44.

60.   Wattenbarger J, Richards B and Herring J. A comparison of single-rod instrumentation with double-rod instrumentation in adolescent idiopathic scoliosis. *Spine*. 2000; 25: 1680-8.

61.   McCarthy RE, Sucato D, Turner JL, Zhang H, Henson MA and McCarthy K. Shillla Growing Rods in a Carpine Animal Model. A Pilot study. *Clinical orthopaedics and related research*. 2010; 468: 705-10.

62.   Luque E and Cardoso A. Treatment of scoliosis without arthrodesis or external support, preliminary report. *Orthopaedic Transactions*. 1977; 1: 37-8.

63.   Mardjetko S, Hammerberg K, Lubicky J and Fister J. The Luque trolley revisted. Review of nine cases requiring revision. *Spine*. 1992; 17: 582-9.

64.   Pratt R, Webb J, Burwell R and Cummings S. Luque trolley and convex epiphysiodesis in the management of infantile and juvenile idiopathic scoliosis. *Spine*. 1999; 24: 1538-47.

65.   Ouellet J. Surgical technique. Modern Luque trolley, a self guiding rod technique. *Clinical Orthopaedics & Related Research*. 2011; 469: 1356-67.

66.   Wilke H, Kluger P, Naumann T, Kron T, Lase L and Puhl W. In Situ Rigidity of a New Sliding Rod for Management of Growing Spine in Duchenne Muscular Dystrophy. *Spine*. 1996; 21: 1957-61.

67.   Sankar WNM, Skaggs DLM, Yazici MM, et al. Lengthening of Dual Growing Rods and the Law of Diminishing Returns. *Spine May*. 2011; 36: 806-9.

68.   Noordeen H, Shah SA, Elsebaie H, Garrido E, Farooq N and Al Mukhtar M. In vivo distraction force and length measurements of growing rods. *Spine*. 2011; 36: 2299-303.

69.   Zarzycki D, Tesiorowski M, Zarzycka M, Kacki W and Jasiewicz B. Long-Term Results of Lower Limb Lengthening by Physeal Distraction. *Journal of Pediatric Orthopaedics May/June*. 2002; 22: 367-70.

70.   Letts R and Meadows L. Epiphysiolysis as a method of limb lengthening. *Clinical Orthopaedics & Related Research*. 1978: 230-7.

71.   Alberty A. Effects of physeal distraction on the vascular supply of the growth area: a microangiographical study in rabbits. *Journal of Paediatric Orthopaedics*. 1993; 13: 373-7.

72.   Gorman T, Vanderwerff R and Pond M. Mechanical axis following staple epiphysiodesis for limb-length inequality. *The Journal of Bone and Joint Surgery*. 2009; 91: 2430-9.

73.   Braun J, Hoffman M, Akyuz E, Ogilvie J, Brodke D and Bachus K. Mechanical modulation of vertebral body growth in the fusionless treatment of progressive scoliosis in an experimental model. *Spine*. 2006; 31: 1314-20.

74.   Olgun Z, Ahmadiadli H, Alanay A and Yazici M. Vertebral body growth during growing rod instrumentation: Growth preservation of stimulation? *Journal of Paediatric Orthopaedics*. 2012; 32: 184-89.

75.   Panjabi MM, Brand RA, Jr. and White AA. Three-dimensional flexibility and stiffness properties of the human spine. *Journal of Biomechanics*. 1976; 9: 185-92.

76.   Goel V, Panjabi M, Patwardhan A, Dooris A and Serhan H. Test Protocols For Evaluation Of Spinal Implants. *Journal of Bone and Joint Surgery*. 2006; Supplementary 2: 103-9.

77.   Akbarnia BA, Mundis GM, Salari P, Yaszay B and Pawelek JB. Innovation in Growing Rod Technique: A Study of Safety and Efficacy of a Magnetically Controlled Growing Rod in a Porcine Model. *Spine*. 2012; 37: 1109-14.

78.   Busscher I, Ploegmakers J, Verkerke G and Veldhuizen A. Comparative anatomical dimensions of the complete human and procine spine. *European Spine Journal*. 2010; 19: 1104-14.

79.   Wilke H, Jungkunz B, Wenger K and Claes L. Spinal segment range of motion as a function of invitro test conditions: Effects of exposure period accumulated cycles, angular-defomrity rate and moisture condition. *The Anatomical Record*. 1998; 251: 15-9.

80.   Wilke H-J, Jungkunz B, Wenger K and Claes LE. Spinal segment range of motion as a function of in vitro test conditions: Effects of exposure period, accumulated cycles, angular-deformation rate, and moisture condition. *The Anatomical Record*. 1998; 251: 15-9.

81.   Wilke HJ, Wenger K and Claes L. Testing criteria for spinal implants: Recommendations for the standardization of in vitro stability testing of spinal implants. *European Spine Journal*. 1998; 7: 148-54.

82.   Busscher I, van der Veen AJ, van Dieen JH, Kingma I, Verkerke GJ and Veldhuizen AG. In Vitro Biomechanical Characteristics of the Spine: A Comparison Between Human and Porcine Spinal Segments. *Spine*. 2010; 35: E35-E42.

83.   Berge S. Genetical researches on the number of vertebrae in the pig. *Journal of Animal Science*. 1948; 7: 233-8.

84.   McLain R, Yerby S and Moseley T. Comparative Morphology of L4 Vertebrae: Comparison of large animal models for the human lumbar spine. *Spine*. 2002; 27: E200-6.

85.   Dath R, Ebinesan A, Porter K and Miles A. Anatomical measurements of procine lumbar vertebrae. *Clinical Biomechanics*. 2007; 22: 607-13.

86.   Berry JL, Moran JM, Berg WS and Steffee AD. A morphometric study of human lumbar and selected thoracic vertevrae. *Spine*. 1987; 12: 362-7.

87.   Mosekilde L, Kragstrup J and Richards A. Compressive strength, ash weight and volume of vertebral trabecular bone in experimental flurosis in pigs. *Calcif Tissue Int*. 1987; 40: 318-22.

88.   Aerssens J, Boonen S, Lowet G and Dequeker J. Interspecies differences in bone composition, density and quality: potential implications for in vivo bone research. *Endocrinology.* 1998; 139: 663-70.

89.   Smit T. The use of quadruped as an in vivo model for the study of the spine - biomechanical considerations. *The European Spine Journal.* 2002; 11: 137-44.

90.   Yazici M, Pekmezci M, Cil A, Alanay A, Acaroglu E and Oner F. The Effect of Pedicle Expansion on Pedicle Morphology and Biomechanical Stability in the Immature Porcine Spine. *Spine October.* 2006; 31: E826-E9.

91.   Kettler A, Liakos L and Hammerberg K. Are the spines of calf, pig and sheep suitable models for pre-clinical implant tests? *The European Spine Journal.* 2007; 16: 2186-92.

92.   Panjabi M, Goel V, Oxland T, et al. Human lumbar vertebrae: Quantitaive three-dimensional anatomy. *Spine.* 1992; 17: 299-306.

93.   Panjabi M, Takata K, Goel V, et al. Thoracic human vertebrae quantitative three-dimensional anatomy. *Spine.* 1991; 16: 888-901.

94.   Bozkus H, Crawford N, Chamberlain R, et al. Comparative anatomy of the porcine and human thoracic spines with reference to thoracoscopic surgical techniques. *Surgical Endoscopy.* 2005; 19: 1652-65.

95.   Hongo M, DGay R, Hsu J-T, et al. Effect of multiple freeze-thaw cycles on intervertebral dynamic motion characteristics in the procine lumbar spine. *Journal of Biomechanics.* 2008; 41: 916-20.

96.   Costi JJ, Hearn TC and Fazzalari NL. The effect of hydration on the stiffness of intervertebral discs in an ovine model. *Clinical Biomechanics.* 2002; 17: 446-55.

97.   Clarke E, Appleyard R and Bilston L. Immature sheep spines are more flexible than mature spines. *Spine.* 2007; 32: 2970-9.

98.   Thompson R, Barker T and Pearcy M. Defining the neutral zone of sheep intervertebral joints during dynamic motions: An in vitro study. *Clinical Biomechanics.* 2003; 18: 89-98.

99.   Panjabi M. Biomechanical Evaluation of Spinal Fixation Devices: I. A Conceptual Framework. *Spine.* 1988; 13: 1129=34.

100.   Panjabi M, Oxland T, Yamamoto I and Crisco J. Mechanical Behavior of the Human Lumbar and Lumbosacral Spine as Shown by Three-Dimensional Load-Displacement Curves. [Article]. *Spine.* 1994; 76: 413-24.

101.   de Visser H, Rowe C and Pearcy M. A robotic testing facility for the measurement of the mechanics of spinal joints. *Proceedings of the Institution of Mechanical Engineers, Part H: Journal of Engineering in Medicine.* 2007; 221: 221-7.

102.   Panjabi M. Biomechanical Evaluation of Spinal Fixation Devices: I. A Conceptual Framework. *Spine.* 1988; 13: 1129-34.

103.   Wilke H, Rohlmann A, Neller S, et al. Is it possible to stimulate physiologi loading conditions by applying pure moments? A comparison of invo and in vitro load components in an internal fixator. *Spine.* 2001; 26: 636-42.

104.   Crawford N, Brantley A, Dickman C and Koneman E. An apparatus for applying pure nonconstarining moments to spine segments in vitro. *Spine.* 1995; 20: 2097-100.

105.   Eguizabal J, Tufaga M, Scheer J, Ames C, Lotz JC and Buckley J. Pure moment testing for spinal biomechanics applications: Fixed versus

sliding ring cbale-driven test designs. *Journal of Biomechanics*. 2010; 43: 1422-5.
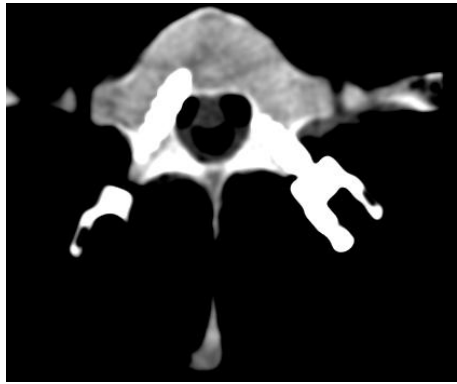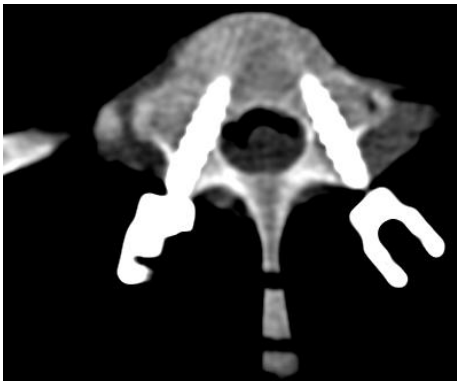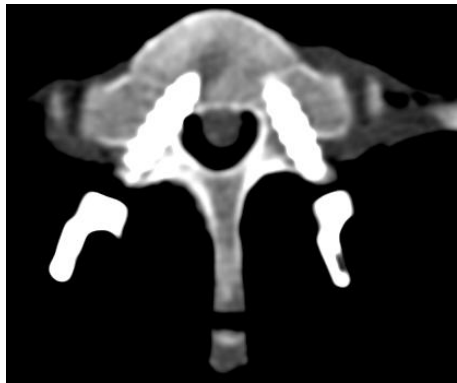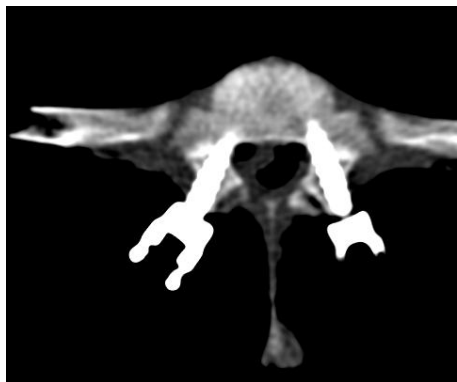
106. Tang J, Scheer J, Ames C and Buckley J. Pure moment testing for spinal biomechanics applications: Fixed versus 3D floating cable-driven test designs. *Journal of biomechanics*. 2012; 45: 706-10.

107. Lysack J, Dickey J, Genevieve A and Yen D. A continuous pure moment loading apparatus for biomechanical testing of multi-segment spine specimens. *Journal of Biomechanics*. 2000; 33: 765-70.

108. Oxland T, Lin R and Panjabi M. Three-dimensional mechanical properties of the thoracolumbar junction. *Journal of Orthopaedic Research*. 1992; 10: 573-80.

109. Goel V, Wilder D, Pope M and Edwards W. Controversy Biomechanical Testing of the Spine: Load-Controlled Versus Displacement-Controlled Analysis. *Spine*. 1995; 20: 2354-7.

110. Wilke H, Krischak S, Wegner K and Claes L. Load displacement properties of the thorcolumbar calf spine: Experimental results and comaprison to known human data. *European Spine Journal*. 1997; 6: 129-37.

111. Blakemore L, Scoles P, Poe-Kochert C and Thompson G. Submuscular Isola rod with or without limited apical fusion in the management of severe spinal defomrities in young children: preliminary report. *Spine*. 2001; 26: 2044-8.

112. Thompson G, Akbarnia B and Campbell R. Growing Rod Techniques in Early-Onset Scoliosis. *Journal of Pediatric Orthopaedics April/May*. 2007; 27: 354-61.

113. Yang JSM, Sponseller PDM, Thompson GHM, et al. Growing Rod Fractures: Risk Factors and Opportunities for Prevention. *Spine*. 2011; 36: 1639-44.

114. Mahar AT, Bagheri R, Oka R, Kostial P and Akbarnia BA. Biomechanical comparison of different anchors (foundations) for the paediatric dual growing rod technqiue. *The Spine Journal*. 2008; 8: 933-9.

115. Skaggs DL, Myung K, Johnston C, Akbarina B and GSS G. Pedicle screws have fewer complications than hooks in children with growing rods. *International congress on early onset scoliosis and growing spine*. Toronto2010.

116. Baghdadi Y, Larson AN, McIntosh A, Shaughnessy W, Dekutoski M and Stans A. Complications of Pedicle Screws in Children 10 Years or Younger: A Case Control Study. *Spine*. 2013; 38: E386-E93.

117. Kim Y, Lenke L, Cho S, Bridwell K, Sides B and Blanke K. Comparative Analysis of Pedicle Screw Versus Hook Instrumentation in Posterior Spinal Fusion of Adolescent Idiopathic Scoliosis. *Spine*. 2004; 29: 2040-8.

118. Wang X, Aubin C-E, Crandall D, Parent S and Labelle H. Biomechanical Analysis of 4 Types of Pedicle Screws for Scoliotic Spine Instrumentation. *Spine*. 2012; 37: E823-E35.

119. Kuklo T, Potter B, Polly D and Lenke L. Monaxial Versus Multiaxial Thoracic Pedicle Screws in the Correction of Adolescent Idiopathic Scoliosis. *Spine*. 2005; 30: 2113-20.

120. Harimaya KMDP, Lenke LGMD, Son-Hing JPMDF, et al. Safety and Accuracy of Pedicle Screws and Constructs Placed in Infantile and Juvenile Patients. *Spine*. 2011; 36: 1645-51.

121.   Oda I, Abumi K and DS L. Biomechanical role of the posterior elements, costovertebral joints, and rib cage in the stability of the thoracic spine. *Spine*. 1996; 21: 1423-9.

122.   Crawford N and Dickman C. Construction of local vertebral coordinate systems using a digitizing probe: Technical note. *Spine*. 1995; 22: 559-63.

123.   Goel V and Winterbottom J. Experimental investigation of three-dimensional spine kinetics. *Spine*. 1991; 16: 1000 - 2.

124.   Fast Track 8800 Controller Technical Data Book. *Electronic Technical Specifications*. Canton, MA: Inston, Corporate headquaters, 2003.

125.   Panjabi MM. The stabilizing system of the spine. Part II. Neutral zone and instability hypothesis. *Journal of Spinal Disorders*. 1992; 5: 390-7.

126.   Busscher I, van Dieen J, Kingma I, van der Veen A, Verkerke G and Veldhuizen A. Biomechanical Characteristics of Different Regions of the Human Spine; An In Vitro Study on Multilevel Spinal Segments. *Spine*. 2009; 34: 2858-64.

127.   Oda I, Abumi K, Cunningham B, Kaneda K and McAfee P. An in vitro human cadaveric study investigating the biomechanical properties of the thoracic spine. *Spine*. 2002; 27: E64-70.

128.   Busscher I, van Dieen J, van der Veen A, et al. The effects of creep and recovery on the in vitro biomechanical characteristics of human multi-level thoracolumbar spinal segments. *Clinical Biomechanics*. 2011; 26: 438-44.

129.   Bass EC, Duncan NA, Hariharan JS, Dusick J, Ulrich Bueff H and Lotz JC. Frozen storage affects the compressive creep behaviour of the porcine intervertebral disc. *Spine*. 1997; 22: 2867-76.

130.   Dhillon N, Bass EC and Lotz JC. Effect of frozen storage on the creep behavior of human intervertebral discs. *Spine*. 2001; 26: 883-8.

131.   Grant C. Mechanical testing and modelling of a bone-implant construct. *School of Chemistry, Physics and Mechanical Engineering*. Queensland University of Technology, 2012.

8 Appendices

Appendix 1. Axial slices from post-testing CT scan of the MSU porcine spine specimens showing superior and inferior multi-axial Medtronic screw orientation

Spec.	Superior multi-axial screw fixation	Inferior multi-axial screw fixation
Dual RIGID rods		
1		
2		
3		

4

5

6
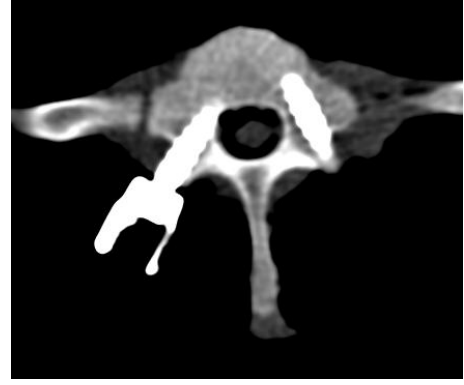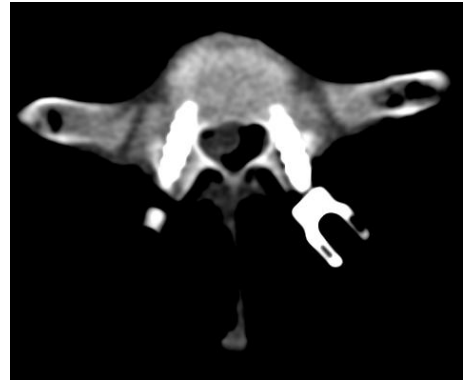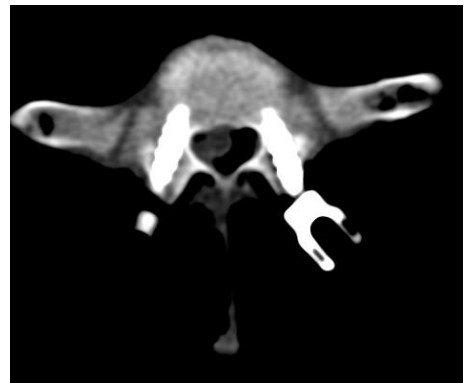
As previously mentioned the Instron has independently reported accuracies for each channel includes forces and displacements. Accuracies are noted as the larger of either ±0.5% of the measured value or ±0.005% of the actual cell (channel) capacity. Additionally noise in the signal occurs at ±0.005% of the full scale. As these two error sources are random in nature, they have an additive effect on the error of the recorded value.

The Instron machine has a full-scale load cell capacity of 25kN, full-scale torque of 100Nm and rotational full-scale value of 270 degrees. Adding the additional noise to each of these values changes the accuracies to;

Load full scale value   =25000N*(0.005%+0.005%)= 2.5N=3N (rounded)

Torque full scale value   = 100 * (0.005%+0.005%) = 0.01Nm

Position full scale value   = 270 * (0.005% of actual channel+0.005% noise)

= 0.027deg

= ±0.01deg

Position accuracy in rotational travel is reported as being ±0.005% of the total travel.

With the moment controlled testing in this thesis set at ±4Nm the most extreme rotation recorded in either left or right rotation was 25deg such that measured accuracies are:

Torque measured error = (tested torque x 0.5%) + (additional noise)

= (4 * 0.5%) + (100 * 0.005%)

= ±0.03Nm

Position measured error = (tested torque x 0.5%) + (additional noise)

= (25 * 0.5%) + (270 * 0.005%)

= 0.125 + 0.0135

= ±0.1 deg (un-instrumented - left or right ROM)

Since the error was larger in the measured value this was taken as the documented error and used to calculate total error by adding the individual error measurements. This converts them back to a % form. Stiffness was then calculated from the data.

Total error = (0.03/4) + (0.1/25) = 0.0115 = (1.15%)

Stiffness = 4/25 = 0.16 $Nm.deg^{-1}$

Stiffness error = 0.16 * 0.0115

= ±0.002 $Nm.deg^{-1}$

Throughout the results section based on the errors obtained in the Instron data analysis displacement (axial rotation) in degrees was rounded to 1 decimal place, torque to 2 decimal places and stiffness to 3 decimal places.

Calculated average stiffness (Nm/deg) from the 5th test of 5 cycles of un-instrumented MSU porcine spines tested to a maximum moment of +/-4Nm in axial rotation.

Pre-liminary specimen	Strain rate (deg.s^{-1})	Total ROM (deg) (±SD)	NZ size (deg) (±SD)	Stiffness (Nm.deg^{-1}) . (r)^2	
				Loading to the Left	Loading to the Right
i	10	30.2 (0.07)	10.83 (0.35)	0.49 (0.99)	0.47 (0.99)
i	8	32.4 (0.04)	10.16 (0.39)	0.51 (0.99)	0.49 (0.99)
ii	8	20.4 (0.13)	3.42 (0.24)	0.62 (0.99)	0.61 (0.99)
iii	8	21.8 (0.03)	2.25 (0.64)	0.58 (0.99)	0.58 (0.99)
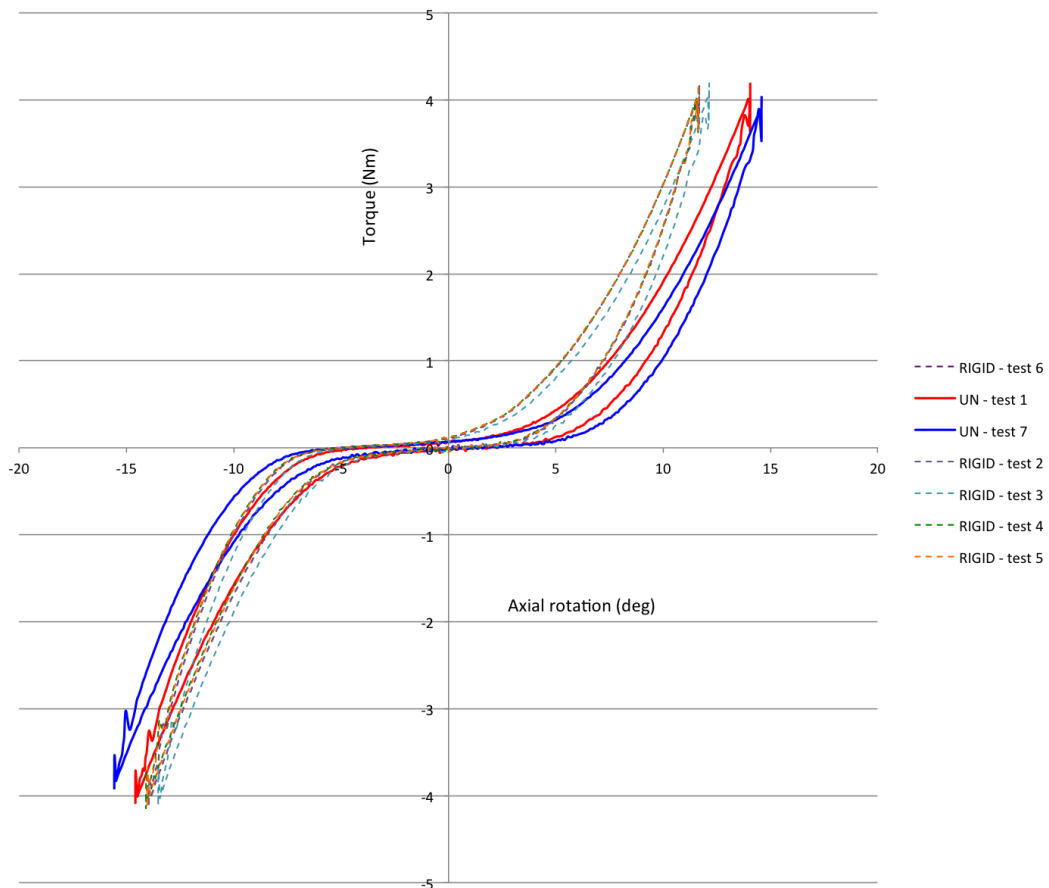
The overlying moment versus axial rotation plots shown above in Appendix 4 show overlapping dual rigid rod tests (from test 2 to test 6) displayed as dotted lines in the repeatability analysis.

**Appendix 5. The induced z-axis loads (kN) of Specimen 1 during the first un-instrumented test at 8deg.s^{-1} to a set maximum moment of ±4Nm.**
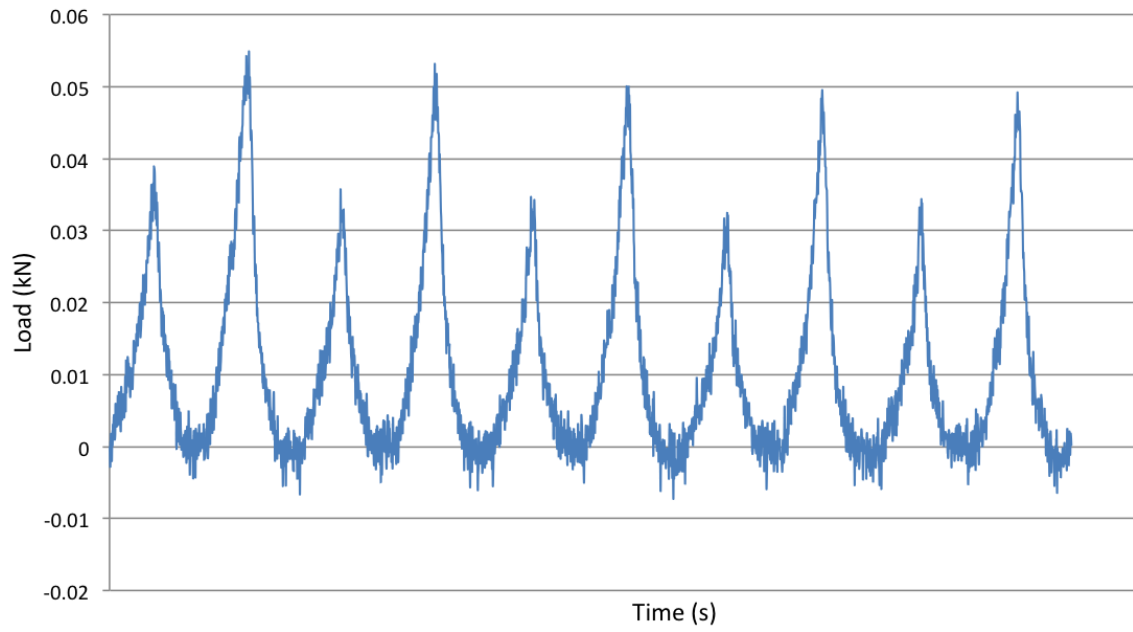
Total Intervertebral ROM (deg) Specimen 1 - UN (test 1)
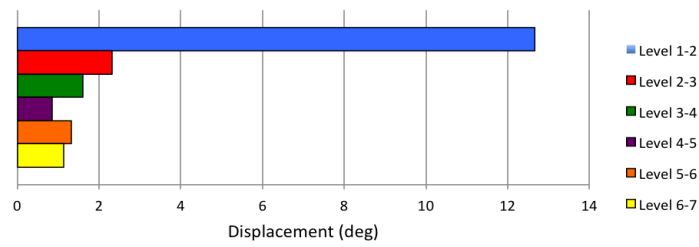
Total Intervertebral ROM (deg) Specimen 1 - UN (test 3)
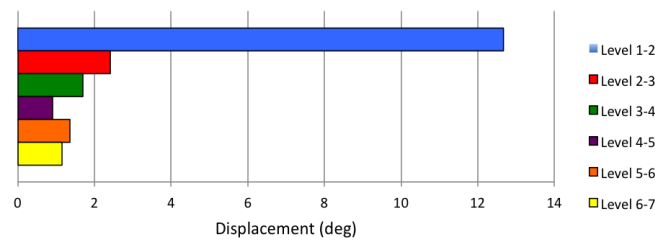
Total Intervertebral ROM (deg) Specimen 1 - UN (test 5)
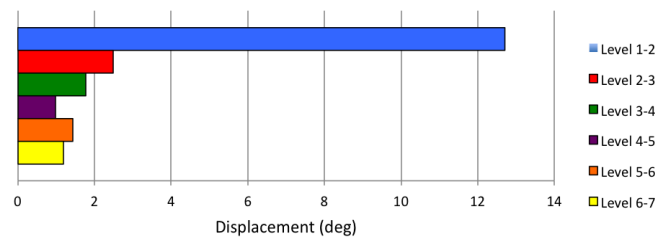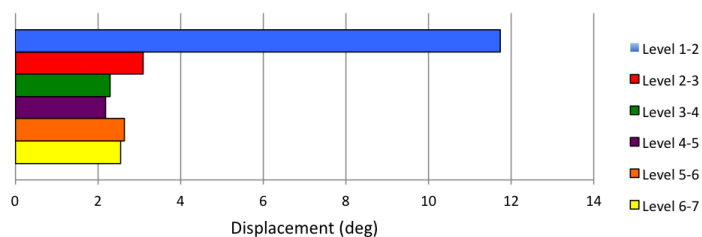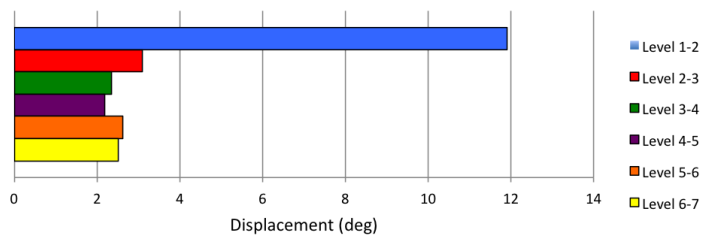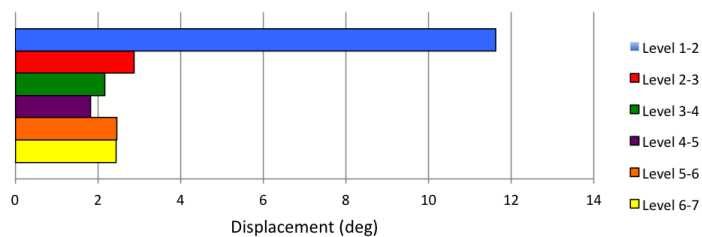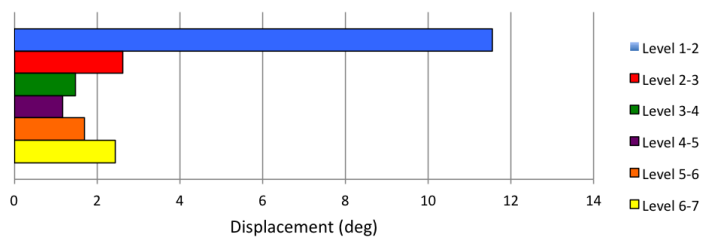

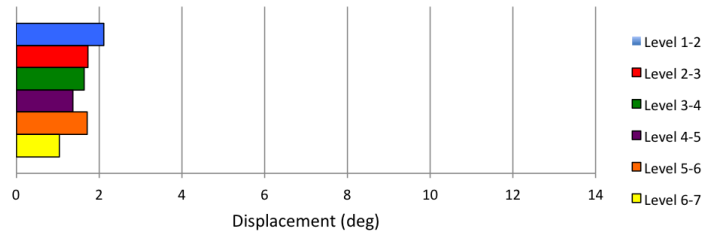Total Intervertebral ROM (deg) Specimen 1 - GR (test 2)
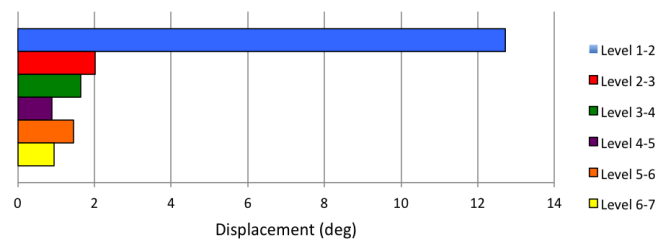
Total Intervertebral ROM (deg) Specimen 1 - RIGID (test 4)
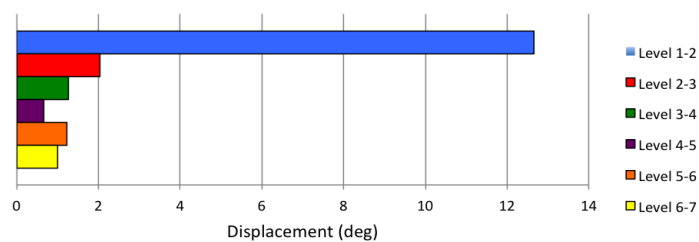
Total Intervertebral ROM (deg) Specimen 2 - UN (test 1)
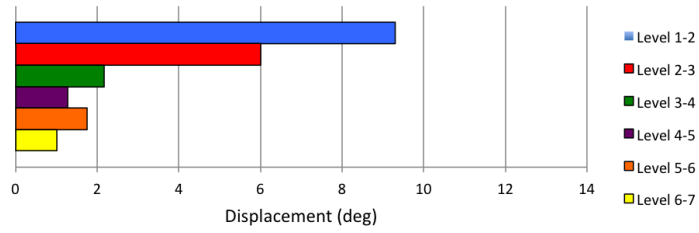
Displacement (deg)

Level 1-2
Level 2-3
Level 3-4
Level 4-5
Level 5-6
Level 6-7

Total Intervertebral ROM (deg) Specimen 2 - UN (test 3)

Displacement (deg)

Level 1-2
Level 2-3
Level 3-4
Level 4-5
Level 5-6
Level 6-7

Total Intervertebral ROM (deg) Specimen 2 - UN (test 5)

Displacement (deg)

Level 1-2
Level 2-3
Level 3-4
Level 4-5
Level 5-6
Level 6-7
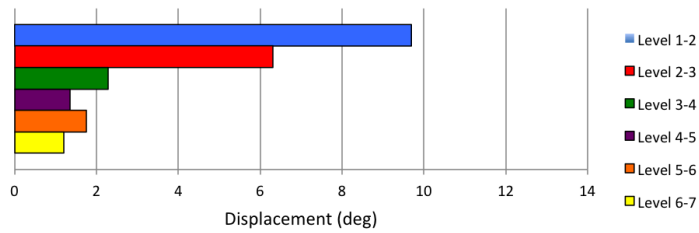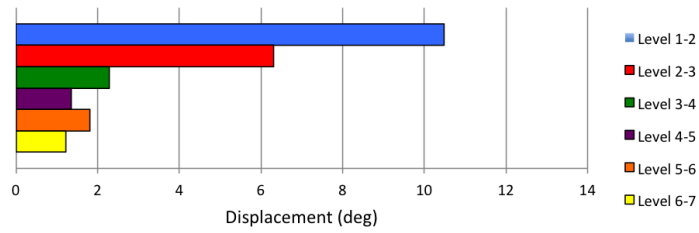
Total Intervertebral ROM (deg) Specimen 2 - RIGID (test 2)

Displacement (deg)

Level 1-2
Level 2-3
Level 3-4
Level 4-5
Level 5-6
Level 6-7
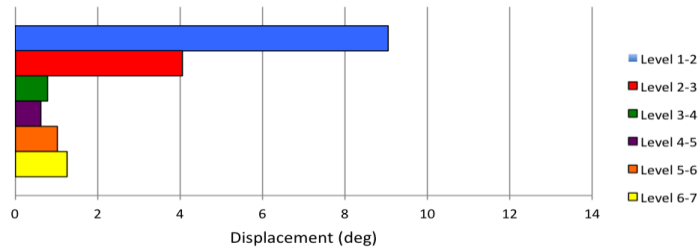
Total Intervertebral ROM (deg) Specimen 2 - GR (test 4)

Displacement (deg)

Level 1-2
Level 2-3
Level 3-4
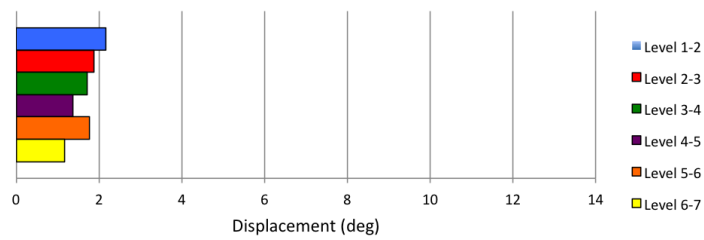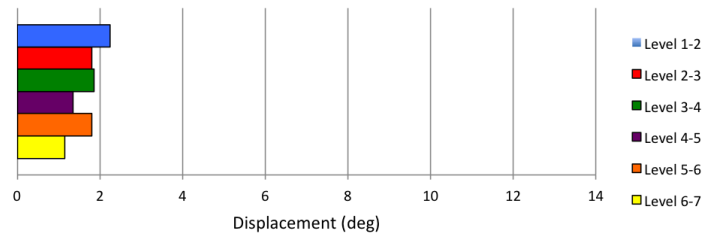Level 4-5
Level 5-6
Level 6-7
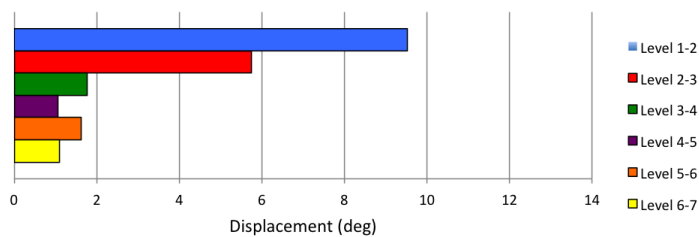
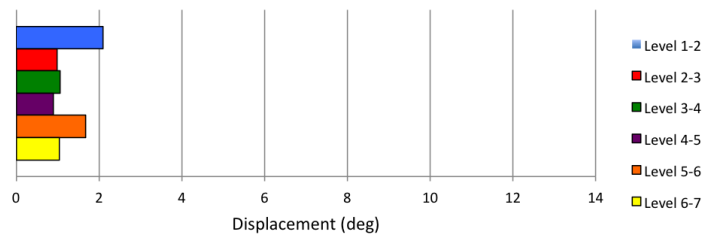Total Intervertebral ROM (deg) Specimen 3 - UN (test 1)
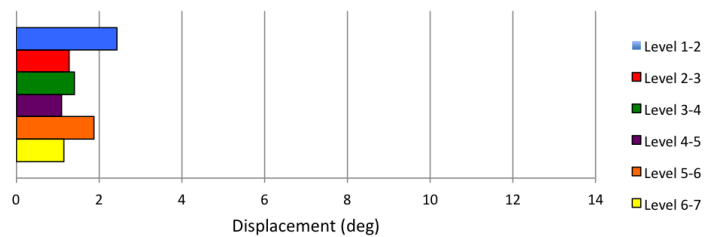

Total Intervertebral ROM (deg) Specimen 3 - UN (test 3)
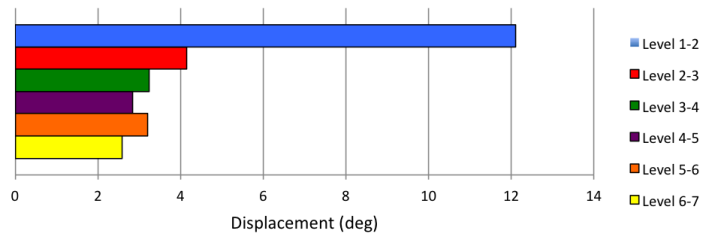
Total Intervertebral ROM (deg) Specimen 3 - UN (test 5)
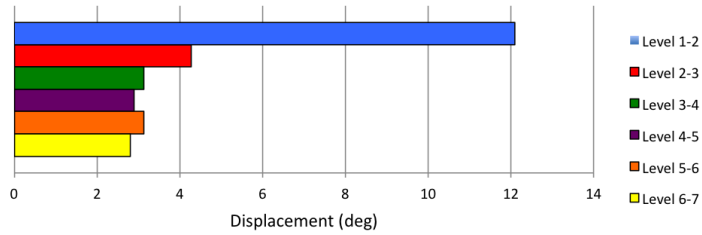
Total Intervertebral ROM (deg) Specimen 3 - GR (test 2)
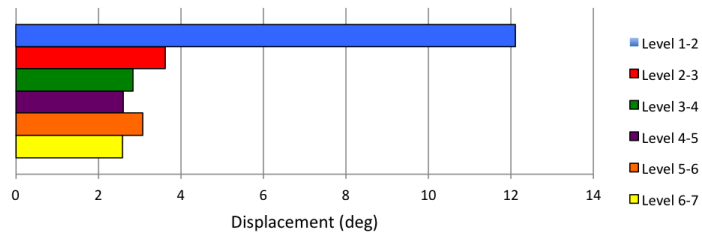
Total Intervertebral ROM (deg) Specimen 3 - RIGID (test 4)
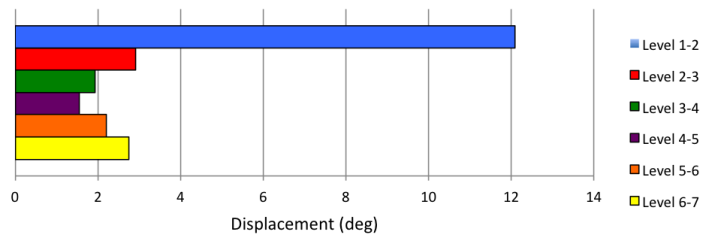
Total Intervertebral ROM (deg) Specimen 4 - UN (test 1)
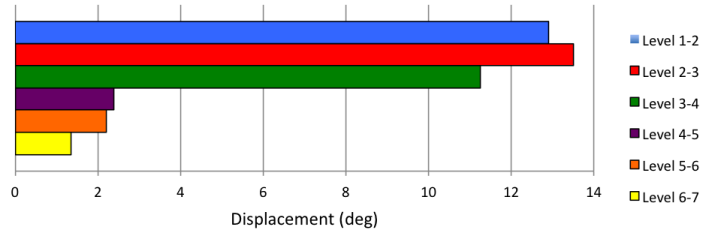
Total Intervertebral ROM (deg) Specimen 4 - UN (test 3)
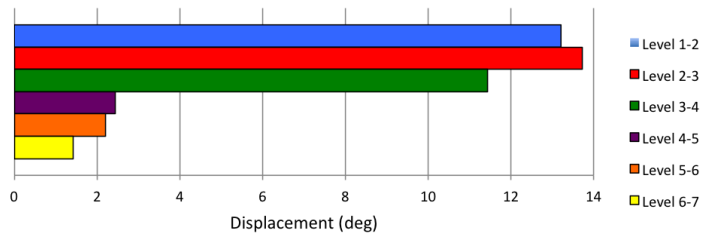
## Total Intervertebral ROM (deg) Specimen 4 - UN (test 5)
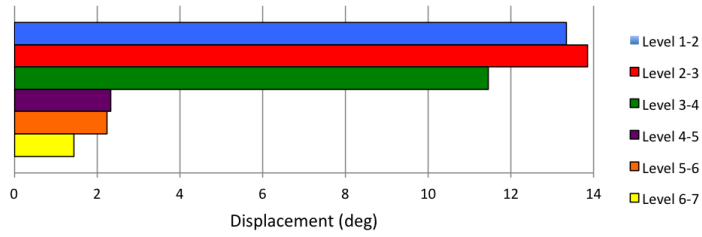
## Total Intervertebral ROM (deg) Specimen 4 - RIGID (test 2)
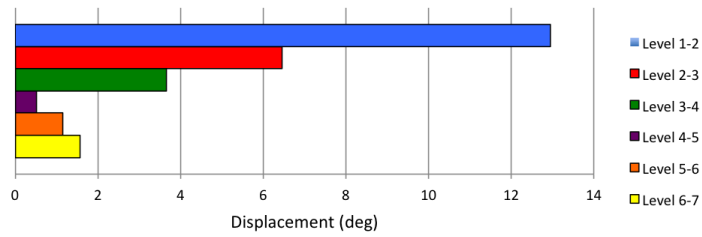
Total Intervertebral ROM (deg) Specimen 4 - GR (test 4)
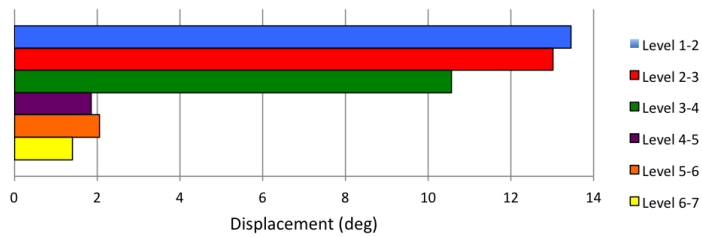
Total Intervertebral ROM (deg) Specimen 5 - UN (test 1)
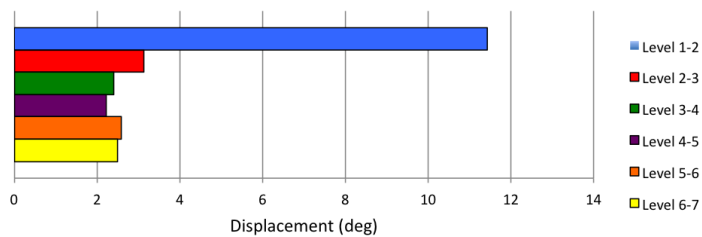
Displacement (deg)

Level 1-2
Level 2-3
Level 3-4
Level 4-5
Level 5-6
Level 6-7

Total Intervertebral ROM (deg) Specimen 5 - UN (test 3)

Displacement (deg)

Level 1-2
Level 2-3
Level 3-4
Level 4-5
Level 5-6
Level 6-7

Total Intervertebral ROM (deg) Specimen 5 - UN (test 5)

Displacement (deg)

Level 1-2
Level 2-3
Level 3-4
Level 4-5
Level 5-6
Level 6-7

Total Intervertebral ROM (deg) Specimen 5 - GR (test 2)

Displacement (deg)

Level 1-2
Level 2-3
Level 3-4
Level 4-5
Level 5-6
Level 6-7

## Total Intervertebral ROM (deg) Specimen 5 - RIGID (test 4)

Displacement (deg)

Level 1-2
Level 2-3
Level 3-4
Level 4-5
Level 5-6
Level 6-7

Total Intervertebral ROM (deg) Specimen 6 - UN (test 1)

Displacement (deg)

Level 1-2
Level 2-3
Level 3-4
Level 4-5
Level 5-6
Level 6-7

Total Intervertebral ROM (deg) Specimen 6 - UN (test 3)

Displacement (deg)

Level 1-2
Level 2-3
Level 3-4
Level 4-5
Level 5-6
Level 6-7

Total Intervertebral ROM (deg) Specimen 6 - UN (test 5)

Displacement (deg)

Level 1-2
Level 2-3
Level 3-4
Level 4-5
Level 5-6
Level 6-7

Total Intervertebral ROM (deg) Specimen 6 - RIGID (test 2)

Displacement (deg)

Level 1-2
Level 2-3
Level 3-4
Level 4-5
Level 5-6
Level 6-7

Total Intervertebral ROM (deg) Specimen 6 - GR (test 4)

Displacement (deg)

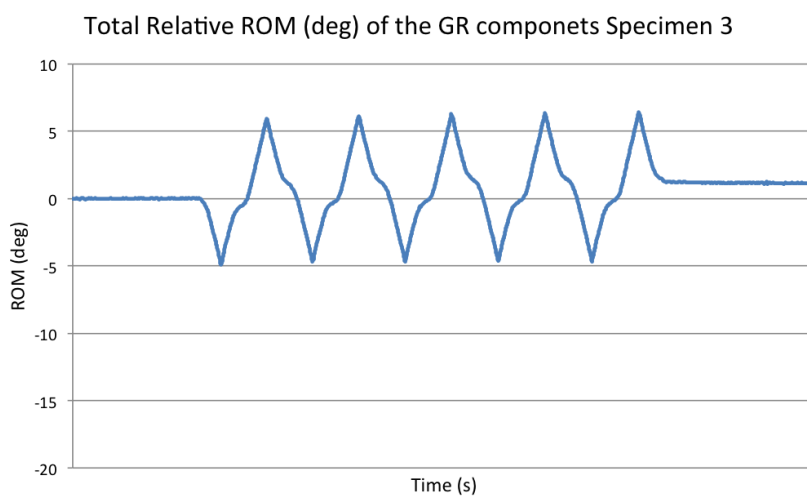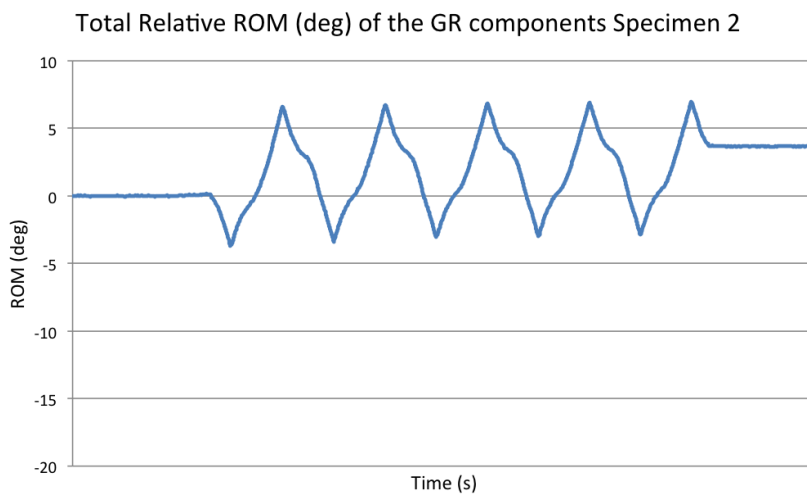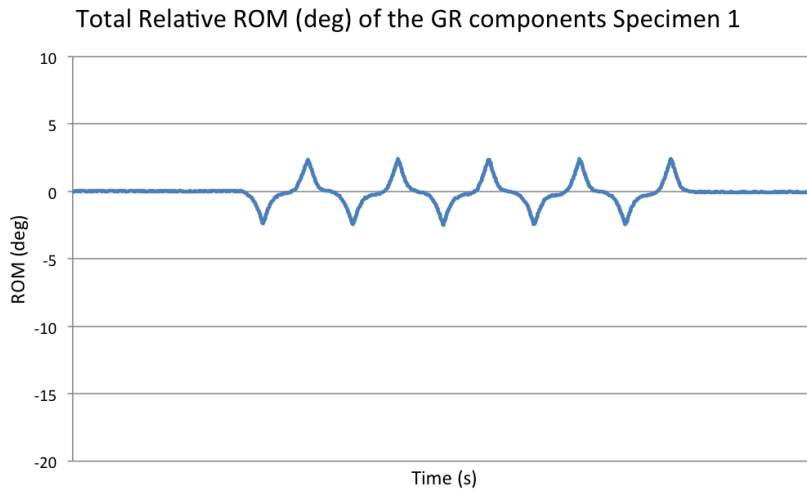Level 1-2
Level 2-3
Level 3-4
Level 4-5
Level 5-6
Level 6-7

Appendix 7. Normalised Total Intervertebral ROM (deg) for each dual rod tested across each intervertebral level normalised to its averaged UN state of 1 (with sequence testing as per (Table 2.3).
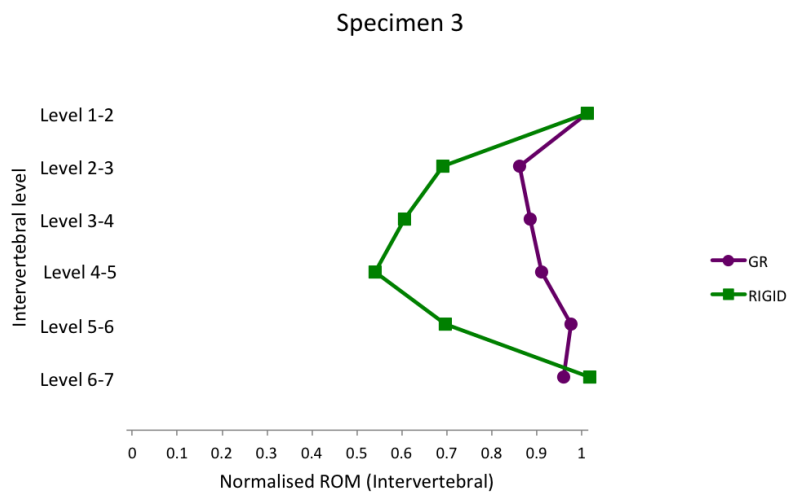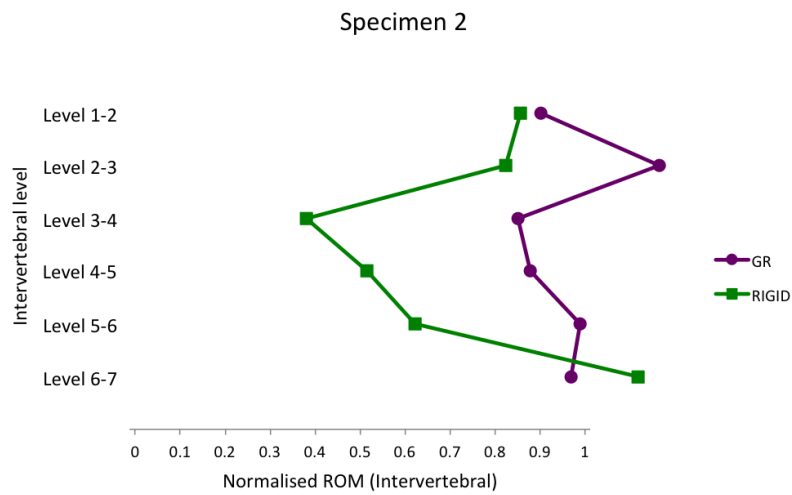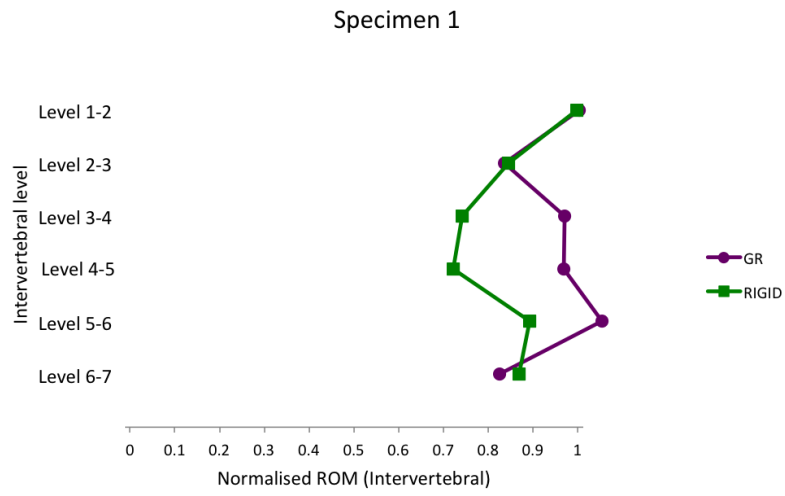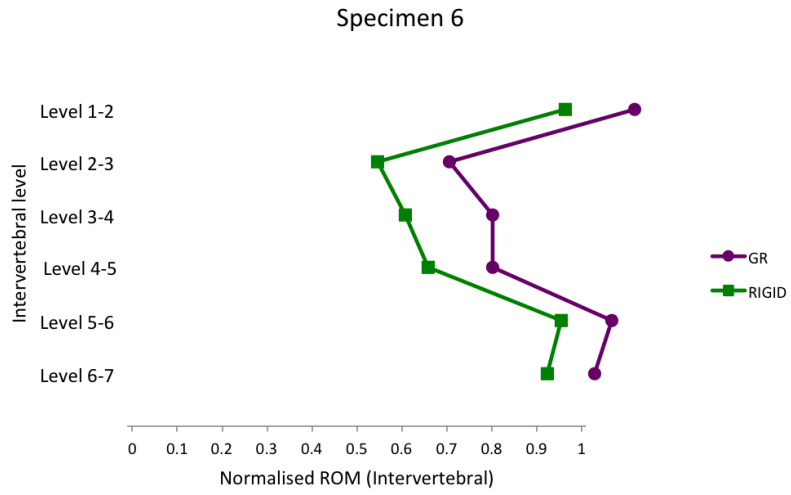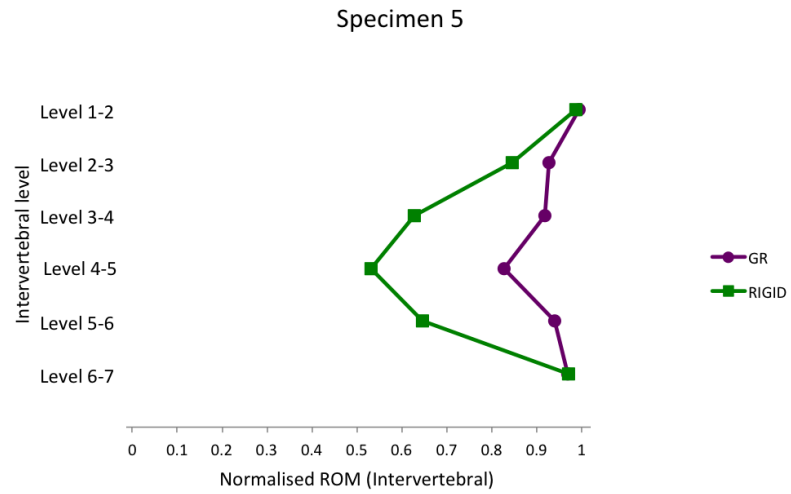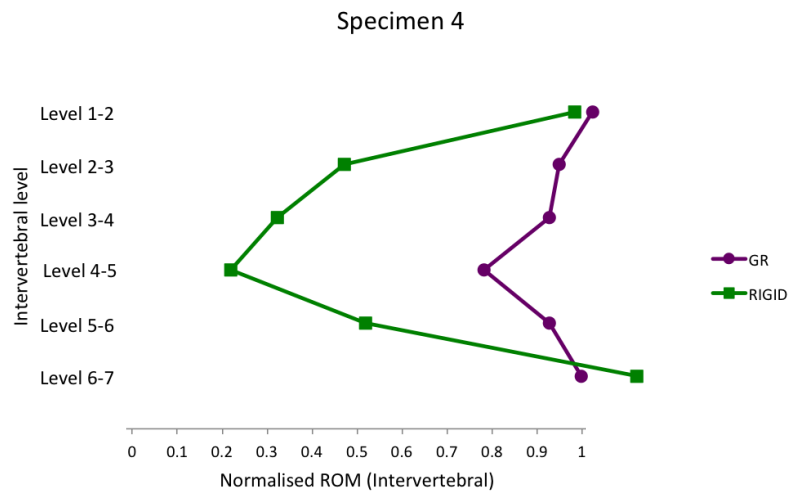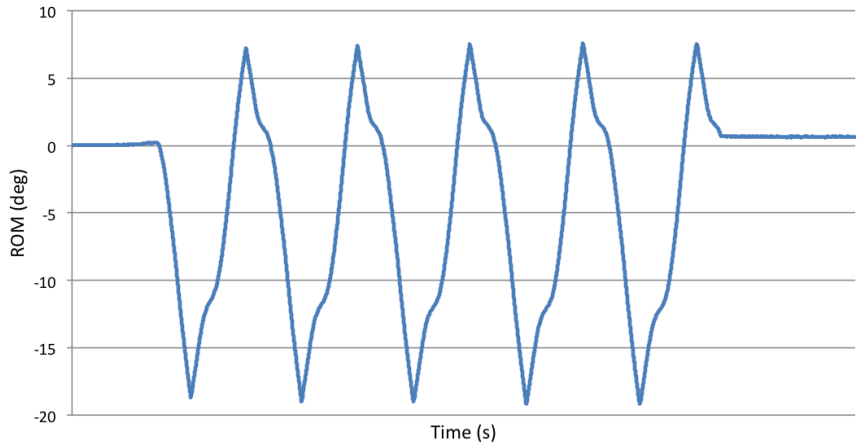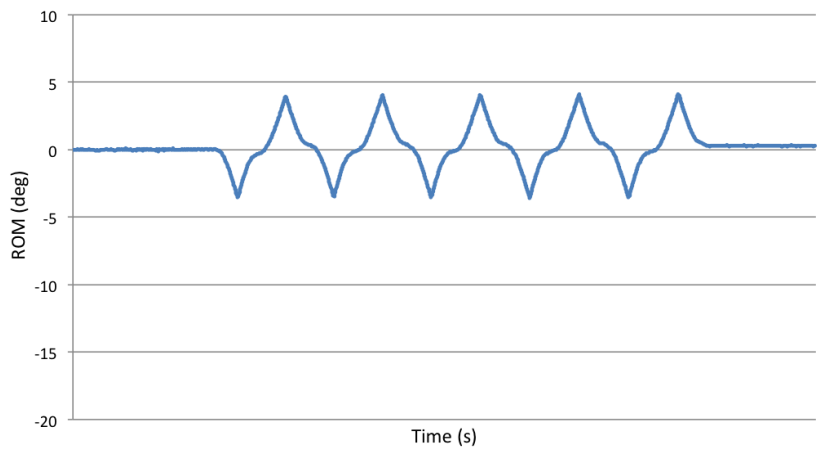
Specimen 1

Specimen 2

Specimen 3

Specimen 4

Specimen 5

Specimen 6

Total Relative ROM (deg) of the GR components Specimen 1

Total Relative ROM (deg) of the GR components Specimen 2

Total Relative ROM (deg) of the GR componets Specimen 3

Total Relative ROM (deg) of the GR components Specimen 4

Total Relative ROM (deg) of the GR components Specimen 5

Total Relative ROM (deg) of the GR components Specimen 6